OPTIMAL DESIGN OF TRUSS STRUCTURE WITH ACTUATORS

A THESIS SUBMITTED TO
THE GRADUATE SCHOOL OF NATURAL AND APPLIED SCIENCES
OF
MIDDLE EAST TECHNICAL UNIVERSITY

BY

ASLI AKGÖZ

IN PARTIAL FULFILLMENT OF THE REQUIREMENTS
FOR
THE DEGREE OF MASTER OF SCIENCE

IN

MECHANICAL ENGINEERING

NOVEMBER 2004

Approval of the Graduate School of Natural and Applied Sciences

Prof. Dr. Canan Özgen
Director

I certify that this thesis satisfies all the requirements as a thesis for the degree of Master of Science.

Prof. Dr. Kemal İder
Head of Department

This is to certify that we have read this thesis and that in our opinion it is fully adequate, in scope and quality, as a thesis for the degree of Master of Science.

Prof. Dr. E. Bülent Platin
Co-Supervisor

Prof. Dr. Tuna Balkan
Supervisor

Examining Committee Members

Prof. Dr. Mehmet Çalışkan	(METU, ME)	
Prof. Dr. Tuna Balkan	(METU, ME)	
Prof. Dr. E. Bülent Platin	(METU, ME)	
Prof. Dr. Levend Parnas	(METU, ME)	
Prof. Dr. Yavuz Yaman	(METU, AEE)	

I hereby declare that all information in this document has been obtained and presented in accordance with academic rules and ethical conduct. I also declare that, as required by these rules and conduct, I have fully cited and referenced all material and results that are not original to this work.

Name, Last name: Aslı Akgöz

Signature :

ABSTRACT

OPTIMAL DESIGN OF TRUSS STRUCTURE WITH ACTUATORS

Akgöz, Aslı

M. Sc., Department of Mechanical Engineering Department

Supervisor : Prof. Dr. Tuna Balkan

Co-Supervisor: Prof. Dr. E. Bülent Platin

November 2004, 157 pages

Smart structures become highly popular with the developing technology. The aim of this study is to develop a basic model, which can be also used in the design of more complex systems by performing simultaneous optimization of a structure and associated controller with respect to some design parameters and feedback gains.

In this thesis work, two smart structures are used as case studies and their results are compared with the available results in the literature. The first case study is simple two-bar truss problem controlled by either one or two actuators. This problem is solved both numerically and analytically. The latter is a twenty-element parabolic truss, which is controlled by four actuators. This problem is solved numerically only.

In the optimization process, the design parameters are taken as the cross sectional areas of bar elements, positions and/or number of actuators, and the elements of

closed loop gain matrix. In the second case study, in addition to these parameters, shape design parameters are also optimized.

A coordinate transformation is applied in both cases from the displacement space to the modal space. The modal model reduction method is used in the design of second problem.

The optimization goal in both cases studies is to minimize the system energy while satisfying some frequency and mass constraints. In the second case study, in addition to the original objective function, system controllability and stability robustness are also maximized.

In the solution of design problem, two optimization algorithms are used one embedded within the other. In the outer loop, a hide and seek simulated annealing algorithm optimizes structural design parameters, and positions and/or number of actuators. In order to generate a candidate design family for this level, optimal closed loop gain matrices are calculated by using MATLAB®.

Keywords: Simultaneous structure/controller optimization, hide and seek simulated annealing algorithm, quadratic optimal controller.

ÖZ

EYLEYİCİLİ ÇUBUK-KAFES YAPININ ENİYİLENEREK TASARIMI

Akgöz, Aslı
Yüksek Lisans, Makina Mühendisliği Bölümü
Tez Yöneticisi : Prof. Dr. Tuna Balkan
Ortak Tez Yöneticisi: Prof. Dr. E. Bülent Platin

Kasım 2004, 157 sayfa

Akıllı yapıların kullanımı gelişen teknoloji ile birlikte oldukça yaygınlaşmıştır. Bu tezin amacı bu tür bir problemin eniyilenmiş yapısal ve denetleyici tasarımını gerçekleştirerek daha karmaşık sistemlerin çözümüne temel oluşturacak bir yöntem geliştirmektir.

Bu çalışmada, eyleyici ile denetlenen iki farklı çubuk-kafes yapının hem yapısal hem de denetleyici tasarım değişkenlerinin beraber eniyilenmesi yapılmıştır. Çözülen bu problemler daha önce yapılan çalışmalardaki çözümlerle karşılaştırılmıştır. İlk problemde, tek eyleyici ile denetlenen, iki elemanlı düzlemsel bir çubuk-kafes yapı analitik ve sayısal yöntemler kullanılarak çözülmüştür. Diğer problemde ise, dört eyleyici ile denetlenen yirmi elemanlı parabolik şekilli bir düzlemsel çubuk-kafes yapı sayısal yöntemler kullanılarak çözülmüştür.

Tasarım parametreleri olarak, çubuk elemanların kesit alanları, eyleyicilerin yerleri ve/veya eyleyici sayısı ile durum değişkenlerinin geri besleme kazanç katsayıları alınmıştır. İkinci problemde, bunların yanısıra şekil tasarım değişkenleri de kullanılmıştır. Her iki çalışmada da modele, yerdeğiştirme uzayından modal uzaya, koordinat dönüşümü uygulanmıştır. İkinci problemde yüksek mertebedeki doğal frekanslar gözardı edilerek modal model düşürme yöntemi uygulanmıştır.

Her iki problemde eniyilemenin amacı hem frekans hem kütle sınırlamasını sağlarken sistem enerjisini en az seviye getirmektir. İkinci problemde, bunların yanında, sistemin denetlenebilirliğinin ve kararlılık gürbüzlüğünün artırılmaya çalışıldığı bir durum incelenmiştir.

Problemin çözümünde iç içe iki eniyileme yöntemi kullanılmıştır. Dış döngüde yapısal tasarım değişkenleri ile eyleyicinin yeri ve/veya eyleyici sayısını belirleyen araştır ve sakla tavlama benzetimi yöntemi kullanılmıştır. İç döngüde ise, yaratılan bu tasarım değişkenleri kullanılarak oluşturulmuş modelin eniyi denetleyici kazanç katsayıları MATLAB® kullanılarak hesaplanmaktadır.

Anahtar Kelimeler: Yapı ve Denetleyici Beraber Eniyilemesi, Araştır ve Sakla Tavlama Benzetimi Yöntemi, İkinci Dereceden Eniyilenmiş Denetleyici

To my Family,

ACKNOWLEDGMENTS

I would like to express my sincere thanks and appreciation to my supervisor Prof. Dr. Tuna Balkan and co-supervisor Prof. Dr. E. Bülent Platin for being a continuous source of support and encouragement while this work was being completed. I am deeply grateful for the time and effort they have taken to teach me and provide direction for my research.

The greatest thanks go to my family for their love, support, and thrust. Their role in this study is inestimable.

Thanks to Gülnihal Odabaşı, Cengiz Tendürüs, Anıl Ünal, and the other friends in Roketsan Inc. for creating me a good environment to love my job and sharing their talents and experiences during this thesis work.

Very special thanks to my special friends Gizem Karslı, Danish Ahmed and A. Özgür Vural for giving me strength to complete this work.

Finally, I would like to thanks to Ç. Görkem Bingöl for being part of my life.

TABLE OF CONTENTS

LIST OF TABLES

TABLE

LIST OF FIGURES

FIGURE

NOMENCLATURE

$[A]$	system matrix
$[A^c]$	closed loop system matrix
a	cross sectional area of a bar element
$[B]$	actuator distribution matrix
$\{D\}$	design parameter vector
$[C]$	structural damping matrix
E	Young modulus of elasticity
$\{e\}$	closed loop eigenvalue vector of controller
$\{F\}$	general force vector
$[F_a]$	directional global actuator force matrix
$\{F_e\}$	external force vector
$\{f_a\}$	directional elemental actuator force vector
f_c	constraint function
$[G]$	closed loop gain matrixr
$[I]$	identity matrix
J	objective function
$[K]$	structural stiffness matrix
$[k]$	elemental stiffness matrix
L	length of a bar element
$[M]$	structural mass matrix
M_t	mass of truss structure
$[M_e]$	external mass matrix

$[m]$	elemental mass matrix
$[m_a]$	elemental actuator mass matrix
m_{act}	actuator mass
m_e	point mass
m_t	mass of a bar element
N	cross penalty weight of states and inputs
n	total number of state variables
n_b	total number of bar elements
n_c	total number of constraints
n_d	total number of design parameters
n_o	total number of objective function
$[O]$	observation matrix
$[P]$	penalty weight of control inputs
pw^o	penalty weight of objective functions
pw^c	penalty weight of constraints
$[Q]$	penalty weight matrix of states
$\{q\}$	vector of nodal displacements
$\{\dot{q}\}$	vector of nodal velocities
$\{\ddot{q}\}$	vector of nodal accelerations
$[R]$	Riccati matrix
r	number of control inputs
$[S]$	modal matrix
$[S_A]$	eigenvectors of system matrix
$\{Sd\}$	search direction vector
$[Svd_c]$	singular value decomposition of actuator distribution matrix
$\{s\}$	vector of principal (modal) coordinates
T	dimensionless time

t_1	direction cosine with respect to x-axis
t_2	direction cosine with respect to y-axis
t_3	direction cosine with respect to z-axis
u	displacement in x-direction
$\{U\}$	control input vector
$[V]$	normalized mode shape matrix
v	displacement in y direction
w	displacement in z direction
X	dimensionless spatial coordinate
$\{x\}$	state variable vector
$\{\dot{x}\}$	vector of first derivatives of state variables
Y	dimensionless spatial coordinate
Z	dimensionless spatial coordinate
Greek	
α	stiffness proportional damping
β	mass proportional damping
δ	Kronecker delta
ρ	material density of bar element
Ω	square of structural natural frequency
ω	structural natural frequency
ζ	modal damping coefficient
Subscript	
i	number of bar element
j	number of nodes
l	lowest/lower
0	initial condition
o	required constraint value
Superscript	
*	optimum values
T	transpose

ABBREVIATIONS

dof	degree of freedom
EA	Evolutionary algortihm
FEM	Finite Element Model
HSSA	Hide and seek Simulated Annealing
LQR	Linear quadratic regulator
MIMO	Multi-Input-Multi-Output
mdof	multi degree of freedom
PZT	lead zirconate titanate
QPI	Quadratic Performance Index
SA	Simulated Annealing

CHAPTER 1

INTRODUCTION

The function of a structure usually determines the general features of its geometry. The enviroment and the current technology determine its material. The past experience with the enviroment and the structure's function define the loads. Considering the loads with worst case scenarios, a structural engineer designs the structure by determining the free geometrical parameters of the structure's material volume such that the structural response never exceeds the limits set to ensure the structure's functionality and integrity. The structure is constructed according to its design, and let unattended to complete its design life. In a modern manner of speaking, this is called as the passive design. Historically, this has been the only design paradigm avaliable to the structural engineers.

The experience with space structures since early Sixties has shown that a passively designed space structure can be monitored continuously, and its response can be controlled actively if some means of to do so are provided during its construction. With the advances in sensor, actuator, and microprocessor technologies, it became economically feasible to actively control some of the responses of a passively designed space structure in real time. Initially, the telemetry data obtained from spacecrafts was evaluated by human operators on the earth's surface, and corrective actions were relayed to the spacecrafts through radio signals. Later, using reliable excitation-response relations of spacecrafts and various feedback control algorithms, on-board microprocessors took over the job of human operator. In order to keep the structure at the close proximity of its nominal state, computers continuously evaluate the outputs of sensors which monitor deviations from the nominal state, and issue commands to the actuators when required to eliminate these deviations. This modern

approach may be called as the design by incorporating intelligence into the system. It is very likely that this design by incorporating intelligence into the engineering products will be the new design paradigm for all engineering branches in this millenium.

The new design paradigm of incorporating intelligence into engineering products is basically the result of the availability of extremely capable microprocessors at a minute fraction of the total cost of many engineering products, and the result of advances in sensor and actuator technologies. This situation encourages the engineers to use active means in controlling the response of their products in addition to the passive means. Modern passive design techniques rely heavily on digital simulations of products' behavior under speculated loading conditions. By incorporating the microprocessors into engineering products for inteligent and user-friendly behavior, a new area opens for microprocessors beyond their current use in numerical simulations [1].

Intelligent structures are those which incorparate actuators and sensors that are highly integrated into the structure and have structural functionality, as well as highly integrated control logic, signal conditioning, and power amplification electronics. Such actuating, sensing, and signal processing elements are incorporated into a structure for the purpose of influencing its states or characteristics, which can be mechanical, termal, optical, chemical, electrical, or magnetic. For example, a mechanically intelligent structure is capable of alternating both its mechanical states (its position or velocity) or its mechanical characteristics (its stiffness or damping).

Because of difficulties in lifting and deploying heavy objects such as space stations, which can contain large solar arrays, antennas, precision lasers, and optical systems, the spacecraft structures must be highly flexible. Moreover, stringent performance requirements for pointing accuracy, vibration suppression, shape control, etc., demand active controls to augment any passive damping. The goal of integrated design is to take advantage of any synergistic interaction between the flexible structure and its active control system.

When disturbed, a large structure is likely to continue vibrating for some time because of its low frequencies and possibly small damping. Therefore, the objective of vibration control is to design the structure and its control to reduce dynamic responses in the structure. An effective way to achieve this goal is using damping augmentation that can be obtained by active or passive means.

In addition to the space technology with a recent increases in demand for machines having an integrated control system, a mutual interaction of the structure and control system has become an essential factor and plays important role in the design of machines and mechanical systems. Especially in vibration control, simultaneous optimum design of structures and their control systems has attracted the attention of researchers in recent decades.

An adaptive structure may be considered as an intelligent variant of its passively designed counterpart. It is passively designed considering most of the loading scenerios, but some active means are considered and incorporated into the design in order to control random loading effects.

A wide variety of applications exist for intelligent structure technologies. Despite the fact that truly intelligent structures (i.e., those with embedded controllers as well as actuators and sensors) have not yet been built, a number of experimental implementations of active structures (i.e., those with distributed actuators and sensors) were successfully demonstrated [2]. Notable experimental implementations include aeroelastic control and maneuver enhancement, reduction of vibrations and structure borne noise and acoustic transmission, jitter reduction in precision pointing systems, shape control of plates and mirrors, trusses, and lifting surfaces, isolation of offending machinery and sensitive instruments, and robotic control [3], [4].

Onada, Sano, and Kamiyama [5] made some experiments and analyses to show the effectiveness of active systems with respect to passive ones in terms of vibration suppression. Furthermore, they proposed a new semiactive vibration suppression technique to overcome the disadvantages of the passive system. Finally, they concluded that, active system was the best one in the damping augementation while

the semiactive vibration technique gave quite satisfactory results, although it was primitive.

Structural modeling and optimization algorithms are the two main challenging issues of this subject. A review of the work that is carried out is given in next section. It will be logical to define the optimization problem first and then explain the mathematical modeling of structural part.

1.1 OPTIMIZATION PROBLEM

Integrated structure/controller design problems are handled in three different methodologies in the literature up to now. These methods can be classified as simultaneous, sequential, and multilevel optimization.

In the simultaneous methods, the control law design and the structural design are directly combined into a single problem. Both the control and structural design parameters are then selected to satisfy an integrated design objective, which is usually some combination of structural and controller design objectives. With this approach, the design problem may be high order since the mathematical model must include not only the dynamics of both the control system and the structure, but also the combined constraint and design parameter sets. Examples of simultaneous methods were given by Haftka et. al [6] and Liu and Begg [7].

The sequential methods solve the integrated controller/structural design problem by first structural (or controller) design followed sequentially by a control (or structural) design. The process is then repeated iteratively until a satisfactory integrated solution is found. Although these methods retain the original sizing of the structure and control law design problems, their main drawback is that the integrated solution is dependent on the sequential ordering of the control and structure design solutions.

Gilbert and Schmidt [8] designed both the structure and controller independently. Integration of the independently obtained control and structural designs was achieved

by formulation and solution of a higher-level design coordination problem using the multilevel optimization methods.

An optimization problem begins with a set of independent parameters which, are design parameters, and often includes conditions or restrictions that define acceptable values of the parameters. Such restictions are termed the constraints of the problem. The other essential component of an optimization problem is a single measure of “goodness”, termed as the objective function, which depends in some way on the design parameters.

Final part of the optimization and computationally the most challenging part is the solution of the problem. Many optimization algorithms are available in the literature. In this thesis work, the hide and seek simulated annealing algorithm is used.

Optimization problem can be summarized under four main topics: design parameters, objective fuction, constraints and solution algorithm .

1.1.1 Design Parameters

Design parameters are the physical characteristics of a system that can be changed to improve its design. It will be adequate to categorize design parameters under two groups as follows:

- Structural design parameters
- Controller design parameters

The structural design parameters typically characterize the material distribution and/or geometry of the structure. For the past 30 years, an optimization using sizing parameters such as cross sectional areas or thicknesses has been the most popular form of structural design optimization. This type of optimization is called as the “size optimization“ in the literature.

The shape and topology optimizations are more complex types of structural optimizations, which end up with changes in the layout of structures. In the shape optimization, nodal coordinates, support positions, or shape parameters are taken as design parameters while connections of nodes or number of elements are the design parameters in the topology optimization.

The aim of controlling of elastic modes in a structure is to increase its damping and/or stiffness to achieve a desired time response. This behavior depends on the number and position(s) of sensor(s) and actuator(s) as well as on the structural dynamics of the controller. Therefore, controller design parameters may be taken as feedback gain matrix and/or position(s)/number of actuator(s)/sensor(s). Schulz and Heimbold [9] worked on dislocated actuator/sensor positioning and many other researches worked on actuator positioning and sizing [5], [10]-[16].

Structural and controller parameter linking schemes are used in order to avoid a prohibitively large increase in the total number of independent design parameters. Cross sectional areas, actuator and sensor positions or controller gain matrix may be linked with an engineering intuition such that the optimal system will not be affected much. This is applied in structural design when symmetrical systems are available [17]. The tendency to subordinate gains to a dependent parameter status can be attributed to the fact that for system models with a large number of degrees of freedom, the feedback gain matrix contains prohibitively large numbers of independent design parameters. The main ideas underlying the creation of alternative control design parameter linking schemes are 1) separation of velocity and position parts of gain matrix, 2) various row and column schemes corresponding to actuator and degree of freedom linking, and 3) linking schemes based on only allowing changes in various sets of velocity gains [18], [19].

1.1.2 Constraints

Constraints are the conditions that must be satisfied for the design to be acceptable (inequality-one sided, equality-precisely, side bounds on the design parameters) which can also be grouped as:

- Structural constraints
- Controller constraints

Any quantity characterizing the response of the structure, such as stress, displacement, or frequency, may be constrained to preclude a structural failure. Weight, structural natural frequency, tensile/compresive stresses, buckling loads and displacement are the most common type of constraints in structural optimization problems [20].

Weight can be used as either equality or inequality constraint in the optimization problems. It can be also used as an objective in the optimization problem according to definition of the design problem. In structural analysis, weight is used as an objective function since its minimization without losing the structural integrity means money. However, in smart structures it is commonly used as a constraint.

The design optimization of structures with fundamental or multiple-frequency constraints is extremely useful when improving the dynamic performance of structures. Modifying a particular frequency can significantly improve its overall performance under dynamic external force excitations. Generally, the control of the critical ranges of the natural frequencies is equivalent to the control of the dynamic response in most narrowband forced excitation problems. A structural optimization under some frequency constraints gives the ability to a designer to control the selected frequencies in a desired fashion in order to improve the dynamic characteristics of the structure [21]-[24].

In the linear quadratic regulator (LQR) theory, control gains relating actuator forces to sensor outputs by means of a linear transformation are taken as typical control design parameters. The control input, location of closed loop poles, number of actuators and sensors are some common design constraints used by control engineers. Closed loop poles of system effect transient and frequency response of the optimized system [14], [25]. They can be applied as either equality or inequality constraints. Limits on a

control input are directly related to the available actuator. It usually has a maximum limit, in other words, it is used in optimization problems as an inequality constraint [25].

Some design parameters may have bounds; i.e., cross sectional areas of bar elements must be greater than zero or applied actuator force must be smaller than actuator maximum force capacity. These upper and lower bounds may be entered to the problem as inequality constraints. These type constraints are called side or bound constraints in the optimization terminology. Defining bounds is useful for the search algorithm performace; in terms of reduced evaluation steps .

1.1.3 Objective function

In the structural optimization, the objective function is often related to the cost of the structure, and it may involve the mass of the structure or the volume of the material.

The structural response may be static or dynamic, although time usually plays no particular role in the formulation of the structural optimization problems. In contrast, in modern optimal control, optimizing some performance index over a given time interval is synthesized. The performance index is rendered independent of time by integrating over the control time.

Quadratic performance index (QPI) is used frequently as the simplest, positively defined objective function of the intelligent structure optimum design. It minimizes magnitude of controller input, nodal displacements and velocities or outputs of the system.

By solving reduced matrix Riccati equation, one can determine a control law that minimizes QPI for a given positive definite or semidefinite state weighting matrix $[Q]$ and a positive definite control-weighting matrix $[P]$. The choice of weighting matrices is at the discretion of controller designer. Each choice produces a different optimal control. In practice, the designer alters $[Q]$ and $[P]$ to balance system performance

and control effort. As an example, one particular choice might result in saturation of an actuator in some simulations. Then, the designer might increase the weighting factor(s) associated with that particular actuator. In this sense, the performance index is not used to compare candidate control laws. Canfield and Merovitch [26] used an independent modal space control, Sunar and Rao [27] worked on the optimal selection of weighting matrices due to these reasons.

Cheng and Liu [28] summarized most popular objective functions that are used in integrated structure/control design as follows:

- To better utilize materials and reduce costs of a structure, structural mass can be chosen as the objective function:

$$f_1 = W_t = \sum_{i=1}^{n_b} \rho_i a_i L_i \tag{1-1}$$

  where ρ_i, A_i, L_i, and n_b are density, cross sectional area, length of member i, and total number of bar elements respectively.

- In a given structure, when the internal work (strain energy) done by stresses and strains has a minimum value, the structure has an optimal shape. For example, minimizing the strain energy of a truss structure produces a natural structural shape. Strain energy is given by

$$f_2 = E_s = \sum_{i=1}^{n_b} \sigma_i \varepsilon_i VI_i \tag{1-2}$$

  where σ_i, ε_i and VI_i are stress, strain, and volume of member i respectively.

- Minimizing potential structural energy can reduce the effects of external forces and increase the safety level of a structure. If given loads

are $\{P\}^T = \{p_1, p_2, ..., p_{noel}\}$, and the coressponding displacements are $\{\Delta\}^T = \{\delta_1, \delta_2, ..., \delta_{noel}\}$, the potential energy of the structure is written as

$$f_3 = E_p = \{P\}^T \{\Delta\} = \sum_{i=1}^{noel} p_i.\delta_i \tag{1-3}$$

- To minimize changes in the shape of a structure under the action of different loading conditions, displacement(s) at a selected point(s) on a region of the structure are taken as the objective function(s) as follows.

$$f_{4,i} = \delta_i \tag{1-4}$$

- To design a controller using a linear quadratic regulator over a finite time interval $t \in (0, t_f)$, an objective function (J) can be defined as

$$f_5 = \int_0^{t_f} \left(\{x\}^T [Q] \{x\} + \{U\}^T [P] \{U\} \right) dt \tag{1-5}$$

where $[Q]$ is a positive semidefinite state weighting matrix, $[P]$ is the positive definite control weighting matrix, $\{x\}$ is the state vector, and $\{U\}$ is the control input vector. Minimizing the quadratic performance index and satisfying the structural system state equation gives an optimal linaer state feedback control law

$$\{U\} = -[P]^{-1} [B]^T [R] \{x\} = -[G] \{x\} \tag{1-6}$$

where $[G]$ is the closed loop gain matrix and $[R]$ satisfies the algerabic matrix Riccati equation. The optimized objective function for a structure to minimize the control effort supplied by the actuators as a response to a set of arbitrary initial conditions can be taken as

$$f_5^* = \{x_o\}^T [R] \{x_o\} \tag{1-7}$$

Here $\{x_0\}$ is the initial state vector (disturbance vector).

Obviously, a designer has to deal with more than one objective functions to meet the design requirements of a structure or a structure/control system in most real world optimization problems. Therefore, when an optimization is concerned with real structures, a multiobjective optimization problem is formulated.

Slater and Mc Laren [29] used both weight and quadratic performance index as objective functions of their optimization problem. However, their solution algorithm does not need any engineering judgment on weighting of objective functions.

Optimum quadratic performance index depends on initial condition of the system as given in Eq. (1-7). This result is not very useful since the initial state is not always known or it changes. To compare performance indeces for each candidate structure trace of Riccati matrix is used. By this way two level optimization is carried out. In the inner loop closed loop gain matrix is optimized by solving reduced matrix Riccati equation and in the outer loop other design variables are optimized by using trace of Ricatti matrix. Many of researches in the literature used this approximation as their optimization criteria, i.e. [7], [16], [26], [27], [30].

1.1.4 Solution Algorithm

Structural/controller optimization problems can be formulated as an integer programming problem. When the number of bar members is large, it is almost impossible to obtain the global optimal placement because of the discrete nature of available actuator positions and the resulting huge number of possible configurations. Therefore, many approaches have been proposed to obtain a nearly optimal solution with a reasonable amount of calculation.

Heuristic optimization algorithms, especially evolutionary algorithms(EA) and simulated annealing (SA), are the most preferred techniques for the multi-objective optimization. The main reason behind the popularity of the EAs as a multi-objective optimization technique is their population-based nature. This idea gives the opportunity of finding the trade-offs within the problem in a single run. Their working procedure is built on the operators such as, mutation, and crossover. The parameters that define how to use these operators affect the convergence of the algorithm and shall be selected according to the problem. This is the main drawback of the EAs. In addition, the quality of the results that are generated by evolutionary algorithms usually depends on the initial population. If the population is initialized with some known good solutions, then the results are often also good. But, if the initial population has a poor fitness then the quality of the results may be quite poor or it may converge rather slowly [31].

The Simulated Annealing technique simulates the physical annealing process. It generates new points in search space by applying operators to current points and statistically moving toward more optimal positions in the search space. It does not require the derivatives of the cost function and can thus deal with discrete parameters as well as discontinuous cost functions. Bélisle et. al developed a SA algorithm for continuous optimization, called hide and seek [32]. This method was used by Karslı [33] in the optimization of a multi-objective satellite optimization problem. They showed that hide and seek simulated annealing (HSSA) algorithm works efficently independent from initial design family.

Onada and Hanawa [34] used genetic and improved SA algorithms and compare these with SA, worst out best in, and exhaustive single-point substitution based on a realistic example. The improved SA algorithm gave the best results.

Liu and Begg [7], [17] studied five different solution algorithms and compared these algorithms with each other. These algorithms were namely guided random search techniques, sequential mathematical programming and their mixtures. They described multiobjective, constraint simultaneous optimization problem which included both structural and controller design parameters. They showed that, all of these algorithms

work efficiently in the integrated structure/controller design even where there are conflicting design requirements.

The sensitivity of the structural response to changes in the design parameters is frequently the major computational cost in an optimization process. From the control theory viewpoint, the sensitivity is concerned with the variations in the controller objective function caused by variations in the plant and control influence matrices. A systematic sensitivity analysis is essential for the development of well-behaved algorithms in the solution of integrated structural/controller design problems [15], [17], [35], [36].

1.2 MATHEMATICAL MODELING

Mathematical modeling may be explained under three main subjects: structural modeling, controller modeling and modal state space transformation.

1.2.1 Structural Modeling

Finite element modeling (FEM) is used for modeling the dynamics of the structure. Stiffness, mass and force matrices of the structure are derived by using finite element method.

A typical strategy for the solution of an optimization problem is to use an iterative approach where the optimum is found by calculating the performance index repetitively until it cannot be improved any further [17]. Depending on the number of variables, such an iterative technique may require a large number of structural analyses that are generally costly and time consuming. The cost of a structural analysis depends on the type of analysis required to determine the constraints and/or the objective function. For example, the non-linear structural analysis of complex structural shapes using finite element method procedures is a real handicap for the structural optimization process. For those cases in which the analysis becomes complex and computationally expensive, displacement based optimization methods were used to improve the efficiency of the process. This optimization process

searches for the optimal structure in the displacement space only. Then corresponding set of sizing variables are found for this optimum displacement field [37].

Finite element force method is another type of solution used in literature. Sedagathati, Suleman, and Tabarrok [21] were used this method in the optimization of a truss structure with multiple frequency constraints. This method is not so popular due to its computational difficulties. They showed that the structural optimization based on finite element force method gives lighter structures. They showed that this method should be preffered when optimization goal based on element forces; e.g., adaptive geometry optimization.

1.2.2 Controller Modeling

Most researches have focused on linear control laws, based on output or state feedback. In the case of output feedback, several studies have been made, where the structural dimensions and the control gains are treated as strictly independent design parameters in optimization. On the other hand, in the case of full-state feedback control, a sequential approach is usually adopted in which the control gains are determined by solving Riccati equations corresponding to the changing structural system during design iterations.

Actuators and sensors are the heart of control systems. With increasing technology on materials and electronics very efficient actuator and sensors have become available in the market today.

Actuators for intelligent structures must be capable of being highly distributed and influencing the mechanical states of the structure. An ideal mechanical actuator would directly convert electrical inputs into strain or displacement in the host structure. Its primary performance parameters include its maximum achievable stroke or strain, stiffness, and bandwith. Secondary performance parameters include linearity, temperature sensitivity, strength, density, and efficiency [3]. The actuators, located at

specified structural elements can be sized so that they produce control forces or torques in order to suppress vibration levels of selected nodes.

Onada and Watanabe [10] used variable-stiffness members, Darby and Pellegrino [11] used inertial slip-stick actuators, Sun and Wang [12] used a bar element consisting extension-contraction device, Hyde and Anderson [13] used active D-strut and Matanuga, Yu, and Ohkami [14] used proof-mass actuators in their vibration suppression studies.

Sensory elements of intelligent structures must be sensitive to the mechanical states of a structure and also capable of being highly distributed. An ideal sensor for an intelligent structure converts the strain or displacement (or their temporal derivatives) at a point directly into electrical outputs. The primary functional requirements for such sensors are their sensitivity to the strain or displacement (or their time derivatives), spatial resolution, and bandwidth. Secondary requirements include the transverse and temperature sensitivity, linearity and hysteresis, electromagnetic compatibility, and size of sensor packaging. It is desirable to make sensors small enough to placed unobtrusive positions [3].

Piezoelectric devices (actuator/sensor pairs) seem to be more suitable for controling precision structures, where very small displacement requirements are to be satisfied. These materials have added new dimensions to the control problem, which comes from the fact that not only positioning but also sizing of the distributed actuator/sensor should be considered in the optimal design [15], [16].

There exists several studies in which the state feedback control is used [7], [8], [11]. Most of these studies assume a perfect knowledge about the states, even though these states have to be reconstructed from the sensor signals by an observer in the actual situation. Onada and Watanabe [38] included observer design to the integrated structure/controller design of a large flexible spacecraft.

Robust optimization is a very essential subject in a smart structure design because of plant uncertainties. The control system is said to be robust if it can maintain its

stability and performance in the presence of plant uncertainties. The plant model of a smart structure is a function of structural frequencies, damping, and vibration modes. The uncertainties can be generally characterized into two groups: structured and unstructured. A structured uncertainty is defined as the variation of the real parameters in the plant. This may be due to the inaccuracies in the calculation of the frequencies and damping due to approximations in the structural model, material properties, mass, damping, etc. Neglecting the actuator and sensor dynamics and higher-order structural modes are the reasons of the unstructured uncertainties. Khot and Heise [39] designed a minimum weight integrated structure/control system, which is robust under both structured and unstructured plant uncertainties. Several new ideas in the definition and optimization of robustness for structures and structural controllers were presented in Lim and Junkin's work [40]. They showed that maximizing stability robustness measure produces more robust designs than minimizing eigenvalue sensitivity directly. Rao, Pan, and Venkayya [41] worked on effect of structural modifications on robustness of controller and showed that stability and performance robustness indexes can be used to decide structural design parameters effectively.

A complex issue in the control of large flexible space structures is that there may exist repeated or closely spaced modes clumping together in the lower range of the natural frequency spectrum. In practice, only a few modes can be selected for control because of the limited capacity of the hardware. One of the criteria for mode selection is the modal controllability and observability, quantitatively. Liu, Wang, Hu and Yu [42] used the singular value decomposition of the input matrix to define a measure for controllability of the structure. Similar treatment can be done for observability measure for sensor positioning [17].

1.2.3 Modal State Transformation and Model Reduction

Optimization can be carried on original spatial model of the structure which is constructed from large degree of freedom (dof). However, a modern complex system may have many inputs and many outputs, and these may be interrelated in a complicated manner. To analyze such a system, it is essential to reduce the

complexity of the mathematical expressions as well as to resort to computers for most of the tedious computations necessary in the analysis. The modal state-space approach is the best suited from this viewpoint.

While the conventional control theory is based on the input-output relationship, or transfer function, the modern control theory is based on the description of system equations in terms of n first-order differential equations. The use of vector-matrix notation greatly simplifies the mathematical representation of systems of equations. The increase in the number of state variables, the number of inputs, or the number of outputs does not increase the complexity of the equations. In fact, the analysis of a complicated multiple-input-multiple-output systems can be carried out by the procedures that are only slightly more complicated than those required for the analysis of systems of first-order scalar differential equations.

A modal transformation can be performed by using all dof's of the system. Since engineering problems are often set from large number of dof, using all dofs would not be practical. A reduced modal model is used frequently in the literature which includes only low-order natural frequencies in designing the control system [43].

Kajiwara, Tsujioka, and Nagamatsu [25] include the effects of higher order natural modes of structure on the stability check of the system. They used reduced modal model with small dof of which the control system is composed. All design parameters are optimized by using this model. Original modal model of medium dof used for judging stability of the higher order poles which have been ignored in composing the control system.

The model reduction methods directly use a set of physical coordinates as the states of a reduced order model to be constructed such that it will provide the same frequency response characteristics as the original full model within the frequency range of interest. Frequency characteristics of a reduced order model constructed using these methods are independent of the selection of the physical dofs used for construction a reduced order model [44].

It was shown that the number of modes that have to be taken into account depends very much on the type of actuator and sensor pair considered. The number of modes needed to reach the same accuracy in damping prediction was much higher for bending actuator pairs like lead zirconate titanate (PZT) plates than for transverse actuator-sensors pairs like proof-mass actuators and accelerometers. The error caused by modal reduction could be compensated taking into account a feed through element in the state space representation of the controlled system. Physically, this is due to the collocation of actuator and sensor and it represents a direct proportionality between input and output. This feed through or static correction of the transfer function allows using a much lower number of modes to calculate modal damping accurately [45].

1.3 DEFINITION OF THE CURRENT PROBLEM

In this study, both structural and controller optimizations will conducted simultaneously. The main goal of the optimization problem is suppressing vibration levels in large truss structures using active damping.

Design optimization can be defined as follows:

- *Design parameters*: Cross sectional areas of bar elements are chosen as structural design parameters; controller gain matrix, positions and/or number of actuators are chosen as controller design parameters.

- *Constraints*: Structural lowest natural frequency (inequality and equality) and mass of truss structure (equality) are used as structural constraints; controller constraint is not set.

- *Objective function:* Trace of Riccati matrix is minimized. Full state feedback controller is used. Multi objective design is also carried out by using weighting sum method. Other objective functions are controllability and stability robusttness of the system which are maximized.

- *Solution algorithm*; HSSA algorithm is used in the determination of cross sectional areas of bar elements and positions and/or number of actuators. LQR theory is used for the calculation of optimal closed loop gain matrix of actuators for the candidate design family. Penalty weights are chosen positive definite in order to assure the system stability after controller design.

- States of system matrix are chosen as displacements and velocities of active nodes of structure.

- Proportional damping is assumed for modal transformation and same modal damping ratio is used for all controlled modes.

- Modal reduction is used in the controller design. Number of actuators is equated to number of modes that are desired to be controlled; i.e., truncation order of modal transformation. Effects of higher order modes are neglected.

- Design parameter linking scheme is used for both cross sectional areas of bar elements and actuator positions.

- A mathematical model is established for every candidate design family and performance index is calculated for this structure.

- Actuators are modeled such that their masses are lumped into respective junction nodes of the bar element on which actuator is inserted. Actuator force is applied as an external force to a system whose direction is parallel to connected bar element's centerline. In the second case study, optimization problem is solved only for optimal placement of the actuators.

- Full state feedback is applied. Therefore, positions and/or number of sensors are not optimized.

CHAPTER 2

MATHEMATICAL MODELING

In integrated structural/controller optimization problems, the system should be modeled in terms of optimization design parameters to be able to calculate performance indices, which are mainly related with the system energy, dynamic and static characteristics of the system. A mathematical model of a dynamic system is defined as a set of equations that represents the dynamics of the system accurately or, at least, fairly well [46]. The dynamics of physical systems can be described in terms of differential equations, which are obtained from basic physical laws governing them. In this thesis work, the finite element method is used for arranging this set of equations for representing the dynamics of a truss system.

Mathematical models may set in many different forms. Depending on the application one mathematical model may be better suited than other models. Since a controller optimization will be done in this thesis work, a modal state space representation is the best one in terms of analyzing system performance.

Bars and actuators are the elements of structure of which, physical parameters will be optimized. Finite element method is used for the mathematical modeling of the structure, which requires the calculation of the structural stiffness, mass, and force matrices. The stiffness and mass matrices include both mass and stiffness values of bars and actuators. Since the optimization problem involves the positioning of the actuators and the sizing of the truss members, structural mass and stiffness matrices change in every iteration step. The force matrix has two components, which are actuator and external forces. The actuator forces are also dynamic due to reason stated for mass and stiffness matrices.

In this chapter, firstly a brief introduction will be done about FEM and then the modal state space transformation and modal model reduction methods will be explained.

2.1 FINITE ELEMENT MODEL

The finite element method is a numerical procedure for analyzing structures and continua. The finite element method is probably the most widely used form of computer-based engineering analysis. Most engineers, from all disciplines, will touch on the method at some point in their careers. The method can be used for analysis of a broad range of engineering problems.

Finite element methods are predominantly used to perform analysis of structural, thermal, and fluid flow situations. They are used mainly when hand calculations cannot provide accurate results. This is often the case when the geometry or process in question is very complex.

The solution techniques differ between FEM computer programs, but much of the fundamental mathematics behind structural finite element analysis is common. In Appendix A definitions of terms used in FEM are given.

In the modeling equilibrium equation, the sum of the forces is equal to the contributions of the stiffness $[K]$ and deflection $\{q\}$, damping $[C]$ and velocity $\{\dot{q}\}$, and mass $[M]$ and acceleration $\{\ddot{q}\}$, is used as given in Eq. (2-1). Total force $\{F\}$ is summation of external forces $\{F_e\}$ and actuator force matrix.

$$[M]\{\ddot{q}\}+[C]\{\dot{q}\}+[K]\{q\}=\{F\}=[F_a]\{U\}+\{F_e\} \tag{2-1}$$

where $\{F_a\}$ is directional global actuator force matrix and $\{U\}$ is the control input vector.

In a dynamic analysis, inertia becomes important. The mass matrix, written as $[m]$ for an element and $[M]$ for a structure, accounts for inertia and is a discrete representation of the continuous distribution of mass in a structure. The effects of damping, if important, are accounted for damping matrices $[c]$ and $[C]$ similarly.

Dynamic problems can be categorized as wave propagation problems and structural dynamics problem. In wave propagation problems the loading is often impact or an explosive blast. The excitation and the structural response are rich in high frequencies. A problem that is not a wave propagation problem, but for which inertia is important, is called structural dynamics problem. In this category, the frequency of excitation is usually of the same order as the structure's lowest natural frequencies of vibration.

Problems of structural dynamics can be subdivided into two broad classifications. In one, it is tried to find structural natural frequencies of vibration and the corresponding mode shapes. Usually, it is desirable to compare natural frequencies of the structure with frequencies of excitation. In design, these frequencies usually should be well separated. In the other classification, it is tried to found how a structure moves with time under prescribed loads and/or motions of its supports, which is called as time history analysis.

In this study, structural dynamic analysis will be carried on and a structural constraint is applied on the lowest natural frequency. If a natural frequency of the structure is close to an excitation frequency, then a severe vibration and "beating" are likely. This usually necessitates alteration of the structure's natural frequencies by resizing or by adding members or dampers. If frequencies of the structure and the excitation are well separated, the structure still vibrates, but the amplitude of the response is likely to be tolerable.

The damping in structures is not viscous; rather, it is due to mechanisms such as hysterics in the material and slip in connections. These mechanisms are not well understood. Moreover, they are improper to incorporate into the equations of

structural dynamics, or they make the equations computationally difficult. Therefore, the actual damping mechanism is usually approximated by viscous damping.

The treatment of damping in computational analyses can be categorized as phenomenological damping methods, in which the actual physical dissipative mechanisms such as elastic-plastic hysterics loss, structural joint friction, or material microcracking are modeled, or spectral damping methods, in which viscous damping is introduced by means of specified fractions of critical damping. Phenomenological methods require detailed models for the dissipative mechanisms and usually result in nonlinear analyses; hence, they are seldom used. With spectral damping approaches, experimental observations of the vibratory response of structures are used to assign a fraction of critical damping as a g-function of frequency, or more commonly, a single damping fraction for the entire frequency range of a structure. The damping ratio ζ depends on the material and stress level. In steel piping, ζ ranges from 0.5% at low stress levels to about 5% at high stress levels. In bolted or riveted steel structures, and in reinforced or prestressed concrete, ζ has the approximate range 2% to 15% [47].

A popular spectral damping scheme, called Rayleigh or proportional damping, is to form damping matrix $[C]$ as a linear combination of stiffness and mass matrices, that is,

$$[C] = \alpha[K] + \beta[M] \tag{2-2}$$

Matrix $[C]$ given in Eq. (2-2) is an orthogonal damping matrix because it permits modes to be uncoupled by eigenvectors associated with the undamped eigen problem.

In the first case study, damping is neglected while in the second one proportional structural damping is assumed for all modes. Therefore, damped natural frequencies

are the same as undamped natural frequencies and damped mode shapes are the same as undamped mode shapes.

In static analysis, symmetry can be exploited for example, by analyzing half of the entire structure. In vibration analysis, symmetry of structure and supports does not imply symmetry of all vibration modes. By imposing symmetry, one would exclude all anti-symmetric modes, which are probably as important as symmetric modes.

Finite element model sets firstly calculating elemental mass stiffness and force matrices. Than, these elemental matrices are assembled to form structural mass, stiffness, damping, and force matrices. Therefore, it will be logical to define elements that are used in this thesis firstly.

2.1.1 Bar Element

The simplest structure type planar truss is examined which does not have any complicated formulation. Any pin-connected structure made of bar elements carrying axial loads is referred to as a truss. Unquestionably, this is the most thoroughly investigated structure in relation to design optimization. There are three principal reasons for this. First, many practical structures are trusses or can be approximated as trusses, including many bridge supports, transmission towers, ship masts, and roof supports. Second, a finite-element code for truss analysis is easily written, so the researcher in automated design does not have to spend a major effort on writing the analysis portion of the design program. Finally, truss structures can be created which span the range of complexity from very simple to highly nonlinear and indeterminate. Thus, these structures provide excellent test cases for the study of optimization techniques.

Figure 2-1 shows a uniaxial bar element, which has two nodes at the ends. Bar elements can carry only axial loads. It cannot carry moments in both ends. In addition, it is assumed that it does not buckle. Therefore, the entire length of the modeled component can be modeled as a single element. This member will transmit only axial loads and can be defined simply by its material, cross sectional area, and its length.

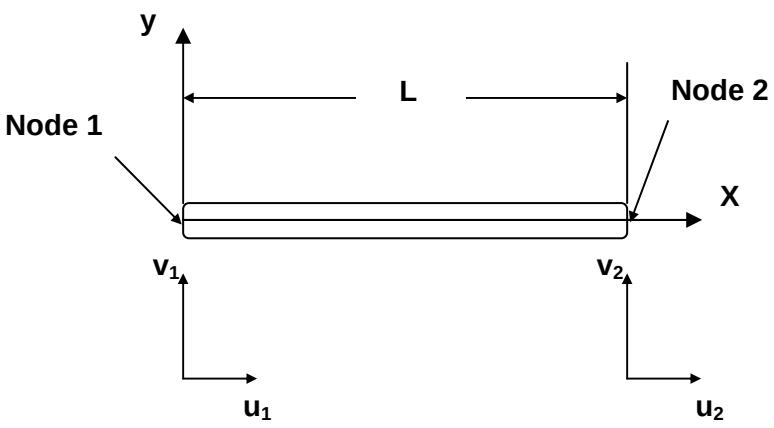

Figure 2-1 Bar element

Each node can move in two directions, x and y. Therefore, it can be said that each node has two dof (one in the x, and one in the y direction). The element has four dofs. For the case of a planar bar element, in static analysis the equilibrium equation would be written as:

$$\begin{Bmatrix} F_{x_1} \\ F_{y_1} \\ F_{x_2} \\ F_{y_2} \end{Bmatrix} = \begin{bmatrix} k_{11} & k_{12} & k_{13} & k_{14} \\ k_{12} & k_{22} & k_{23} & k_{24} \\ k_{13} & k_{23} & k_{33} & k_{34} \\ k_{14} & k_{24} & k_{34} & k_{44} \end{bmatrix} \begin{Bmatrix} u_1 \\ v_1 \\ u_2 \\ v_2 \end{Bmatrix} = \left[k_{ij} \right] \begin{Bmatrix} u_1 \\ v_1 \\ u_2 \\ v_2 \end{Bmatrix} \tag{2-3}$$

where $\left[k_{ij} \right]$ is the element of elemental stiffness matrix, u is displacement in x-direction, and v is displacement in y-direction

Eq. (2-3) represents a set of four linear simultaneous equations. The number of equations is equal to the number of dof in the problem.

Let the left end of the bar element is pinned to the ground. It is known that, there will be no displacement at this node, so u_1 and v_1 can be set to zero. Then equation Eq. (2-3) reduces to:

$$\begin{Bmatrix} F_{x_2} \\ F_{y_2} \end{Bmatrix} = \begin{bmatrix} k_{33} & k_{34} \\ k_{34} & k_{44} \end{bmatrix} . \begin{Bmatrix} u_2 \\ v_2 \end{Bmatrix} \tag{2-4}$$

The matrix $[k]$ is called the stiffness matrix, which defines the geometric and material properties of the bar. These matrices always define inherent properties of the system being studied. For the system at hand, stiffness matrix can be derived as

$$[k] = \frac{aE}{L} \begin{bmatrix} 1 & 0 & -1 & 0 \\ 0 & 0 & 0 & 0 \\ -1 & 0 & 1 & 0 \\ 0 & 0 & 0 & 0 \end{bmatrix} \tag{2-5}$$

where a is the cross sectional area, E is the Young modulus of elasticity, and L is the length of the bar element.

Deriving the stiffness matrix was easy in this case, partly because the bar is oriented parallel to the x-axis. If the bar were placed at an angle to the axis, then the equations would involve trigonometric terms. Through a similar derivation, it can be shown that the stiffness matrix for any bar oriented at an angle is given in Eq. (2-6)

$$[k] = \frac{a.E}{L} \begin{bmatrix} t_1^2 & t_1.t_2 & -t_1^2 & -t_1.t_2 \\ -t_1.t_2 & -t_2^2 & -t_1.t_2 & -t_2^2 \\ -t_1^2 & -t_1.t_2 & t_1^2 & t_1.t_2 \\ t_1.t_2 & t_2^2 & t_1.t_2 & t_2^2 \end{bmatrix} \tag{2-6}$$

where t_i are the direction cosines of bar element with respect to global axis of the structure. These are calculated as follows:

$$t_1 = \frac{X_2 - X_1}{L} \tag{2-7}$$

$$t_1 = \frac{Y_2 - Y_1}{L} \tag{2-8}$$

where X and Y are the nodal coordinates of bar element.

Once the stiffness matrix is calculated, the solution may be performed via matrix solution techniques. After the displacements $\{q\}$ are calculated, the stresses can be found. Above explanations are done for planar trusses but it can be extended to space trusses by adding z coordinates to formulation easily. In this study, all programs are written for space trusses, but it can be dealt with the planar trusses, simply by equating z coordinates of nodes to zero.

A mass matrix is a discrete representation of a continuous distribution of mass. A consistent mass matrix is used in finite element model. It is called consistent since the same shape function is used in the derivation of both mass and stiffness matrices. Elemental mass matrix is given in Eq. (2-9) has no transformation terms since mass matrix of bar element independent from element positions.

$$[m] = \rho a L \begin{bmatrix} 2 & 0 & 1 & 0 \\ 0 & 2 & 0 & 1 \\ 1 & 0 & 2 & 0 \\ 0 & 1 & 0 & 2 \end{bmatrix} \tag{2-9}$$

where ρ is the density of the bar element.

2.1.2 Actuator element

The actuator element is used in the model to control structure. It exerts force into the system when necessary at an appropriate level and fashion. The actuator force, which is assumed to be generated by a full state feedback control, will be calculated

optimally in this study. Therefore, the force matrix is established from direction cosines rather than the value of actuator force. Actuators are placed parallel to bar elements. Therefore, they have same nodal coordinates and direction cosines with these elements. Actuator force matrix is calculated as follows for each element

$$[f_a] = [T]^T \begin{bmatrix} -1 \\ 1 \end{bmatrix} U \tag{2-10}$$

where

$$[T] = \begin{bmatrix} t_1 & t_2 & 0 & 0 \\ 0 & 0 & t_1 & t_2 \end{bmatrix} \tag{2-11}$$

and U is the magnitude of the actuator force.

Only the mass of the actuator is added to system as a physical property of it. Mass of the actuator is modeled as lumped mass as follows

$$[m_a] = \frac{m_{act}}{2} . \begin{bmatrix} 1 & 0 & 0 & 0 \\ 0 & 1 & 0 & 0 \\ 0 & 0 & 1 & 0 \\ 0 & 0 & 0 & 1 \end{bmatrix} \tag{2-12}$$

where m_{act} is the unit mass of the actuator element.

2.1.3 Mass element

The primary use of mass elements is to idealize the mass of a component that provides a contribution to the loading of the part being studied, which is much more rigid and/or too complex to include as a mesh. Mass elements are used to represent engines in cars or motorcycles, display tubes in televisions or monitors, and pumps

and motors on models of machinery. Mass elements are typically single node elements and they cannot affect rigidity.

External masses are added to system mass matrix at the corresponding nodal dofs as shown at (2-13).

$$\left[M_e\right] = m_e \begin{bmatrix} 1 & 0 \\ 0 & 1 \end{bmatrix} \tag{2-13}$$

where m_e is the unit mass of the mass element.

2.2 CONTROLLER MODELLING

An automatic controller compares the actual value of the plant output with the reference input (desired value), determines the deviation, and produces a control signal that will reduce this deviation. The manner in which the controller produces the control signal is called the control action [46].

Industrial controllers may be classified according to their control actions as:

- Two-position or on-off controllers
- Proportional controllers
- Integral controllers
- Proportional-plus-integral controllers
- Proportional-plus-derivative controllers
- Proportional-plus-integral-plus-derivative controllers
- Compensators

Controllers may also be classified according to the kind of power employed in the operation, such as pneumatic controllers, hydraulic controllers, or electronic controllers. In this study, actuator modeling is not considered in detail. It is assumed

that, there is an actuator, which can provide an axial force and modeled by only its mass property while controller gain consists of stiffness and damping characteristics.

Figure 2-2 is a state space model of an industrial control system, which consists of a error detector, a controller, a plant, and a sensor. The controller detects the actuating error signal, which is usually at a very low power level, and amplifies it to a sufficiently high level. The output of an automatic controller is fed to an actuator. The actuator is a power device that produces the input to the plant according to the control signal so that the output signal will approach the reference input signal. The sensor is a device that converts the output variable into another suitable variable, such as a displacement, pressure, or voltage, that can be used to compare the output to the reference input signal.

Plant model is drawn by using finite element method as mentioned before. Full state feedback proportional controller is used to generate control force while reference input is set to zero. In fact, in the case studies, control system consists of a plant, a proportional controller, and the unity feedback sensors.

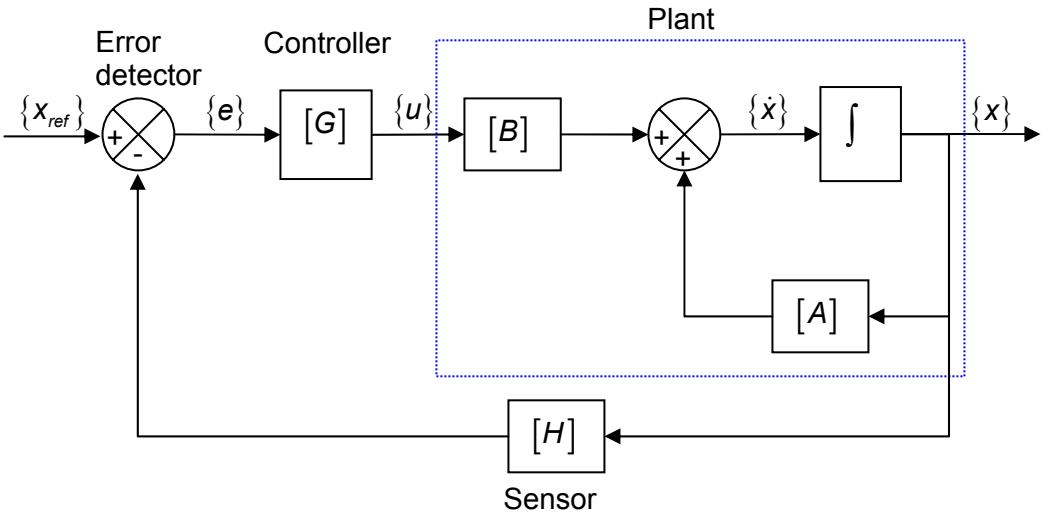

Figure 2-2 State space model of basic control system

2.2.1 Proportional Control Action

For a controller with proportional control action, the relationship between the output of the controller $\{U(t)\}$ and the actuating error signal $\{e(t)\}$ is

$$\{U(t)\} = [G]\{e(t)\} \tag{2-14}$$

where $[G]$ is the closed loop gain matrix.

Whatever the actual mechanism may be and whatever the form of the operating power, the proportional controller is essentially an amplifier with an adjustable gain.

Since reference input is set to zero, which is equilibrium condition for states for truss structure, $e(t)$ reduces to $-x(t)$ and Eq. 2-21 becomes

$$\{U(t)\} = -[G]\{x(t)\} \tag{2-15}$$

$\{U(t)\}$ is the actuators force vector in the direction of parallel truss.

2.3 MODAL STATE SPACE TRANSFORMATION

A complex system may have many inputs and many outputs, and these may be interrelated in a complicated manner. To analyze such a system, it is essential to reduce the complexity of the mathematical expressions as well as to resort to computers for most of the tedious computations necessary in the analysis. The modal state-space approach to system analysis is best suited from this viewpoint.

While conventional control theory is based on the input-output relationship in Laplace domain, or transfer function, modern control theory is based on the description of system in the time domain in terms of n first-order differential equations, which may

be combined into a first order vector-matrix differential equation. The use of vector-matrix notation greatly simplifies the mathematical representation of systems of equations. The increase in the number of state variables, the number of inputs, or the number of outputs does not increase the complexity of the equations. In fact, the analysis of complicated multiple-input-multiple-output systems (MIMO) can be carried out by the procedures that are only slightly more complicated than those required for the analysis of systems of first-order scalar differential equations [46].

The most useful method for determining the forced-vibration response of a linear multi-degree-of-freedom (mdof) system is modal analysis. The orthogonally conditions between the mode shapes determined from the free-vibration analysis are used to define a transformation between the generalized and a new set of coordinates, called the principal coordinates. When the principal (modal) coordinates are used as the dependent variables, the differential equations are uncoupled. The resulting uncoupled differential equations are solved by standard techniques.

2.3.1 Principal Coordinates: Decoupled Equations

The principal coordinates for an mdof system are a set of coordinates related to the chosen generalized coordinates a linear transformation as

$$\{q\} = [S]\{s\} \tag{2-16}$$

where $[S]$ is the modal matrix and $\{s\}$ is the vector of principal (modal) coordinates.

The general matrix form of the differential equation for forced vibrations of an undamped mdof linear system is given in Eq. (2-1). These differential equations are written using the principal coordinates as dependent variables by substituting first equation into above equation, leading to

$$[M][S]\{\ddot{s}\} + [C][S]\{\dot{s}\} + [K][S]\{s\} = \{F\} \tag{2-17}$$

Premultiplying above equation by $[S]^T$ yields

$$[S]^T[M][S]\{\ddot{s}\}+[S]^T[C][S]\{\dot{s}\}+[S]^T[K][S]\{s\}=[S]^T\{F\} \tag{2-18}$$

By using a energy scalar product, above equation can be reduced to Eq. (2-19). Derivation of this equation is given in Appendix B.

$$\{\ddot{s}\}+[\Lambda]\{\dot{s}\}+[\Omega]\{s\}=[S]^T\{F\} \tag{2-19}$$

where $[\Lambda]$ and $[\Omega]$ are the diagonal matrices which elements are $2\xi_i\omega_i$ and ω_i^2, respectively.

2.3.2 State Space Transformation

Eq. (2-19) can be transformed to state space by defining states as displacement and velocity of nodes for all dofs such that,

$$\begin{aligned} s_i &= x_i \\ \dot{s}_i &= s_{n+i} \end{aligned} \tag{2-20}$$

where $i=1\ldots n$.

By using these states, the system $[A]$, actuator distribution $[B]$ and external force $\{F_e\}$ matrices are found as shown in Eq. (2-22)-(2-25) for following state equation,

$$\{\dot{x}\}=[A]\{x\}+[B]\{U\}+\{F_e\} \tag{2-21}$$

where

$$[A]=\begin{bmatrix} 0 & 0 & \cdots & 0 & | & 1 & 0 & \cdots & 0 \\ 0 & 0 & \cdots & 0 & | & 0 & 1 & \cdots & 0 \\ \vdots & \vdots & \ddots & \vdots & | & \vdots & \vdots & \ddots & \vdots \\ 0 & 0 & \cdots & 0 & | & 0 & 0 & \cdots & 1 \\ -- & -- & -- & -- & -- & -- & -- & -- & -- \\ \omega_1^2 & 0 & \cdots & 0 & | & 2\zeta_1\omega_1 & 0 & \cdots & 0 \\ 0 & \omega_2^2 & \cdots & 0 & | & 0 & 2\zeta_2\omega_2 & \cdots & 0 \\ \vdots & \vdots & \ddots & \vdots & | & \vdots & \vdots & \ddots & \vdots \\ 0 & 0 & \cdots & \omega_n^2 & | & 0 & 0 & \cdots & 2\zeta_n\omega_n \end{bmatrix}_{2nx2n} \tag{2-22}$$

$$[B]=\begin{bmatrix} 0 & 0 & \cdots & 0 \\ 0 & 0 & \cdots & 0 \\ \vdots & \vdots & \ddots & \vdots \\ 0 & 0 & \cdots & 0 \\ -- & -- & -- & -- \\ s_{1i}f_{ai1} & s_{1i}f_{ai2} & \cdots & s_{1i}f_{air} \\ s_{2i}f_{ai1} & s_{2i}f_{ai2} & \cdots & s_{1i}f_{air} \\ \vdots & \vdots & \ddots & \vdots \\ s_{ni}f_{ai1} & s_{ni}f_{ai2} & \cdots & s_{ni}f_{air} \end{bmatrix}_{2nxr} \tag{2-23}$$

$$\{F_e\}=\begin{bmatrix} 0 \\ 0 \\ \vdots \\ 0 \\ -- \\ s_{1i}f_{ei1} \\ s_{2i}f_{ei2} \\ \vdots \\ s_{ni}f_{ein} \end{bmatrix}_{2nx1} \tag{2-24}$$

where $i = 1\ldots n$. Derivation of these terms is given in Appendix B.

In this thesis work the gravitational force is taken as the external force. Let

$$[B]\{U\}^T = [B]\{U\} + \{F_e\} \tag{2-25}$$

by assuming that the system is controllable Eq. (2-21) reduces to

$$\{\dot{x}\} = [A]\{x\} + [B]\{U\}^T \tag{2-26}$$

where ^{T} is the transpose of corresponding matrix.

From LQR theory, the observed $\{x\}$ is fed back to generate the control forces as necessary

$$\{U\}^T = -[G][O]\{x\} \tag{2-27}$$

in which $[O]$ is the observation matrix. In this thesis work regulator design is not carried out. It is assumed that all states are measured. Therefore observation matrix is equal to identity matrix.

The solution to a set of initial conditions x_0 of the structure under this control is given by

$$\{x(t)\} = \exp([A_c]t)\{x_0\} \tag{2-28}$$

where

$$[A_c] = [A] - [B][G] \tag{2-29}$$

2.3.3 Modal Model Reduction

The modal model reduction is applied to large dof systems. Since, the size of system matrices increases with increasing dof's, computational times become too long, and even sometimes impossible to handle.

The logic behind the modal model reduction is the modeling system only with low order natural frequencies. Neglecting high order natural frequencies does not change the response of the system so much. Depending on the application, the size of the reduced model may be changed. Whatever the system is, it would not be meaningful to solve a system with thousands dof's using the full size matrices.

The modal model reduction is applied such that modal matrix, $[S]$, consists of the eigenvalues of desired number of low order natural frequencies. Then, the modal space transformations is applied by using this truncated modal matrix.

CHAPTER 3

OPTIMIZATION ALGORITHM

Optimization gives designers an ordered approach to make a design decision instead of relying on intuition and experience. Much of the design task in engineering is quantifiable, and so it is possible to use a computer to analyze alternative designs rapidly. The purpose of numerical optimization is to aid engineers in rationally searching for the best design to meet system needs.

Optimization in design can be defined as the process of finding the minimum or maximum of some parameter, which maybe called as the “objective function”. For a design to be acceptable, it must also satisfy a certain set of specified requirements called “constraints”.

Numerical optimization techniques offer a systematic approach to design automation, and many algorithms have been proposed. Some of these techniques, such as linear, quadratic, dynamic, and geometric programming algorithms, have been developed to deal with specific classes of optimization problems. A more general category of algorithms referred to as nonlinear programming has evolved for the solution of general optimization problems. Methods for numerical optimization are referred to collectively as mathematical programming techniques.

3.1 GENERAL PROBLEM STATEMENT

A nonlinear constrained optimization problem can be expressed as follows:

Minimize a scalar objective function (3-1)

$$F(D)$$

subject to

$$h_j(D) \le 0 \qquad j = 1 \cdots m \qquad \text{inequality constraints} \tag{3-2}$$

$$h_k(D) = 0 \qquad k = 1 \cdots t \qquad \text{equality constraints} \tag{3-3}$$

$$d_i^l \le d_i \le d_i^u \qquad i = 1 \cdots r \qquad \text{side constraints} \tag{3-4}$$

where

$$\{D\} = \begin{Bmatrix} d_1 \\ d_2 \\ d_3 \\ \vdots \\ d_{n_d} \end{Bmatrix} \qquad \text{design parameters} \tag{3-5}$$

The vector $\{D\}$ is referred to as the vector of design parameters. The objective function $F(D)$ is given by (3-1), as well as the constraint functions defined by (3-2) and (3-3) may be linear or nonlinear functions of the design parameters $\{D\}$. These functions may be explicit or implicit in $\{D\}$ and may be evaluated by any analytical or numerical techniques. However, except for special classes of optimization problems, it is important that these functions be continuous and has continuous first derivatives in $\{D\}$. Equation (3-4) defines bounds on the design parameters $\{D\}$ and so is referred to as a side constraint. Although side constraints could be included in the equality constraint set given by (3-2), it is usually convenient to treat them separately because they define the region of search for the optimum, which minimize the computational burden.

3.2 THE ITERATIVE OPTIMIZATION PROCEDURE

Most optimization algorithms require that an initial set of design parameters, $\{D^0\}$, be specified. Beginning from this starting point, the design is updated iteratively. The most common form of this iterative procedure is given by

$$\{D\}^q = \{D\}^{q-1} + \alpha \{Sd\}^q \tag{3-6}$$

where q is the iteration number and $\{Sd\}$ is a vector search direction in the design space. The scalar quantity α defines the distance that we wish to move in direction $\{Sd\}$. The choice of $\{Sd\}$ is somewhat arbitrary as long as a small move in this direction will reduce the objective function without violating any constraints. By searching in a specified direction, the problem is actually converted from n_d parameters $\{D\}$ to one parameter α. New search direction must be found when entered to infeasible region until objective function is no more reduced without violating constraints.

Nonlinear optimization algorithms based on (3-1) can be separated into two basic parts. The first is determination of a direction of search $\{Sd\}$, which will improve the objective function subject to constraints. The second is determination of the scalar parameter α^* defining the distance of travel in the direction $\{Sd\}$. Each of these components plays a vital role in the efficiency and reliability of a given optimization algorithm. There are other considerations in developing the actual optimization program. The most important of these is deciding when to stop the iteration process.

Computationally, it is desirable to normalize the vector $\{Sd\}$. The simplest approach is to find the maximum absolute component $|Sd_i|$, $i = 1 \cdots n_d$, then normalize $\{Sd\}$ by dividing all components of $\{Sd\}$ by the scaling factor. This will aid to find the scalar α_q^* because a unit value of α_q will always make roughly the same change in $\{D\}$. This normalization has the further attribute to see which design parameter is being changed most rapidly. Therefore, the normalization provides a simple means of identifying the important parameters in the design.

3.3 SEARCH METHODS

It is convenient to categorize algorithms according to the type of information that must be provided in searching for the minimum of the function.

The simplest approach to minimizing $F(D)$ is to select randomly a large number of candidate $\{D\}$ vectors and evaluate the objective fuction for each of them. The $\{D\}$ corresponding to the minimum $F(D)$ obtained from this set is called the optimum, $\{D^*\}$. Obviously, if a precise solution to the problem is to be found, great many $\{D\}$ vectors may have to be considered. Methods such as this, which require only function values in searching for the optimum, are referred to as zero-order methods.

A more difficult but usually more efficient approach to the minimization problem is to use the gradient information in seeking the optimum. For example, the gradient of objective function, $\nabla F(D)$, can be calculated and then a search can be done in the negative $\nabla F(D)$ direction. Using this information to choose a new $\{D\}$ vector leads to a more rapid solution of the problem. By this way, the search area can be limited next to randomly searching the entire design space. If $F(D)$ is highly nonlinear then a new gradient should be calculated at every new $\{D\}$ vector and this process would be repeated up to no more reduction is encountered. Methods, which use gradient or first-derivative information, are called first-order methods.

The last class of algorithms is called second-order methods, which use second-derivatives of the objective function $F(D)$. Second-order methods are more efficient with respect to zero and first order methods since they use second order information, which shows type of the point such as minimum, maximum, or saddle. However, calculation of second order derivative of objective function is seldom available analytically and numerical methods are usually too costly to be useful in most cases.

3.3.1 Zero Order Methods

Optimization techniques, which require function values, only have enjoyed a long history of usefulness. These methods are usually reliable and easy to program, often can deal effectively with nonconvex and discontinuous functions, and in many cases can work with discrete values of the design parameters. The price paid for this generality is that these methods often require thousands of function evaluations to achieve the optimum, even for the simplest of problems. Therefore, these methods are considered most useful for problems in which the function evaluation is not computationally expensive.

Most commonly used zero order methods are random search and Powell's method. Many additional these type methods have been proposed which are conceptually similar to these methods. In this work, the random search method is used as an optimization algorithm.

3.3.2 Random Search

Random search methods are considered to be the most inefficient but are the most easily implemented of the zero order methods. These methods are very useful due to its ease of implementation.

The simplest of these methods is to select $\{D\}$ vectors randomly throughout the design space. To avoid searching longer than necessary, some reasonable side bounds such that $\{D\}^l \le \{D\} \le \{D\}^u$ should be provided. To produce a value for the i^{th} parameter between d_i^l and d_i^u, the following equation is used:

$$d_i^q = d_i^l + r\,(d_i^u - d_i^l) \tag{3-7}$$

where r is the random number between zero and one.

This method is effective also for problems where relative minima may exist, because every point in the design space has an equal likelihood of being selected as a candidate design.

If some tighter bounds can be imposed to parameters, the efficiency of the program is improved. Thus, the more the designer knows about the problem the better able he or she is to solve it.

Random search methods have an additional advantage that they can deal with integer or discrete parameters contained in a table. The only modification needed is that a random number generator must provide integer numbers in the feasible region (also, α must be an integer). The resulting designs are then used directly or as pointers to positions in a table, where any design outside the table is automatically rejected.

In the random search methods, a sequence of points in the feasible region following some prespecified probability distribution (which can change during the course of the algorithm) is generated. Pure random search, pure adaptive search and methods based on SA are the examples of random search methods.

SA is a sequential search technique that avoids being trapped in local maxima by accepting, in addition to transitions corresponding to an increase in function value, transitions corresponding to a decrease in function value. The later is done in a limited way by means of a probabilistic acceptance criterion. In the course of maximization process, the probability of accepting deteriorations descends slowly towards zero. These deteriorations make it possible to move away from local optima and explore the feasible region S in its entirely.

SA is originated from an analogy with the physical annealing process of finding low energy states of solid in a heat bath. One of the principal problems in the practical implementation of simulated annealing is the choice of a cooling schedule for the temperature parameter (which parameterizes the decrease of the acceptance probabilities for deteriorations). For discrete SA necessary and sufficient conditions for a cooling schedule that guarantee convergence to the global optimum provided for

the case of a deterministic cooling schedule; i.e., when the sequence of temperature is known in advance. In the HSSA method, adaptive cooling schedule for continuous optimization is used where the temperature employed depends upon the real time progress of the algorithm.

3.3.2.1 Hide and Seek Simulating Annealing

Hide and seek is a powerful yet simple and easily implemented continuous simulated annealing algorithm for finding the maximum of a continuous function over a compact body. The algorithm begins with any feasible interior point. At each iteration, program generates a candidate successor point by generating a uniformly distributed point along a direction chosen randomly at the current iteration point. The candidate point is then accepted as the next iteration point according to the Metropolis criterion parameterized by an adaptive cooling schedule. The temperature changes as the process progress, depending on the closeness of the solution to the global optimum. It is the only algorithm with a statistical proof of convergence of the algorithm to the global optimum. Theory of the algorithm can be found in Appendix C. The flowchart given in Figure 3-1, summarizes the general structure of HSSA algorithm.

Relative accuracy and temperature are decision criteria of HSSA algorithm, as if it finds global optimum or not. One of them can be used as convergence criterion. Maximum iteration number should also used to avoid program crash. Decision of the relative accuracy is not so straight forward. Since it may be to small that numerically it cannot be satisfied. Although, solution may be near the global solution. If similar results are achieved after certain number of run it will be convenient to say result is a global optimum.

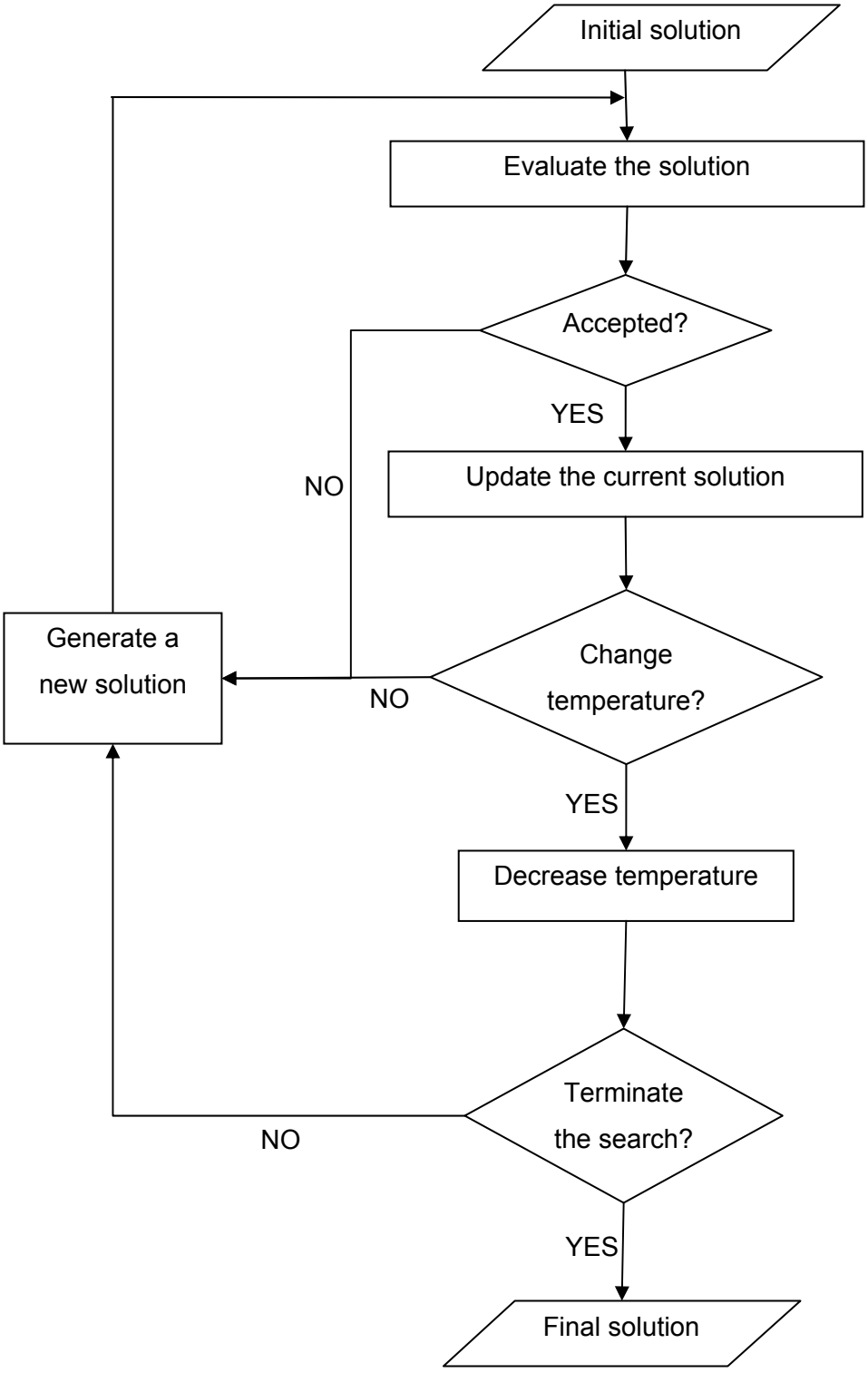

Figure 3-1 Flowchart of the HSSA algorithm

Performance index (PI) is the total cost of the optimization problems. It includes all design requirements such that structural/controller objective function(s), (J) and constraint(s), (f_c). A general type performance index is used in this study, which is based on weighting sum method. It can be defined as

$$PI = \sum_{i=1}^{noof} pw_i^o . J_i - \sum_{i=1}^{noc} pw_i^c . f_{c_i} \tag{3-8}$$

where pw^o and pw^c are denoted as penalty weight of objective function(s) and constraint(s), respectively. If the minimization of objective function is required pw^0 should have negative sign, since HSSA algorithm is a maximization type optimization method. If the constraint is an equality constraint, then the absolute value of f_c should be used. While, if the inequality constraint is requisited, $\max(0, f_c)$ should be used. The optimal solution of the objective function depends on the values of the penalty coefficients used. Users usually try different penalty coefficients to find the reasonable value, which requires some experimentation. In fact a coefficient that brings the constraints to the same order of magnitude with the objective function usually gives satisfactory results. If small penalty coefficients are used the distortion of the objective function is also small, while the optimum of it may not be near the true constraint optimum. On the other hand, when a large penalty coefficient is used, while the calculated optimum is closer to the true constrained optimum, the distortion may be so severe that objective function value may at its true global optimum.

A test problem is solved to compare HSSA algorithm with the other optimization algorithms used by Vanderplaats [48]. A parametric study will be carried out in this problem to see response of the program to its inputs.

3.3.2.1.1 Nonlinear optimization of a spring weight system by HSSA

Figure 3-2 shows a simple spring system supporting weights at the connections between the springs. This system was analyzed in the book of Vanderplaats [48] to

determine the equilibrium position by minimizing potential energy (PE). It is comprised of equally spaced five weights and six springs, shown in the undeformed position in Figure 3-2 (a) and the deformed position in Figure 3-2 (b).Problem definition is completely taken from Vanderplaats [48].

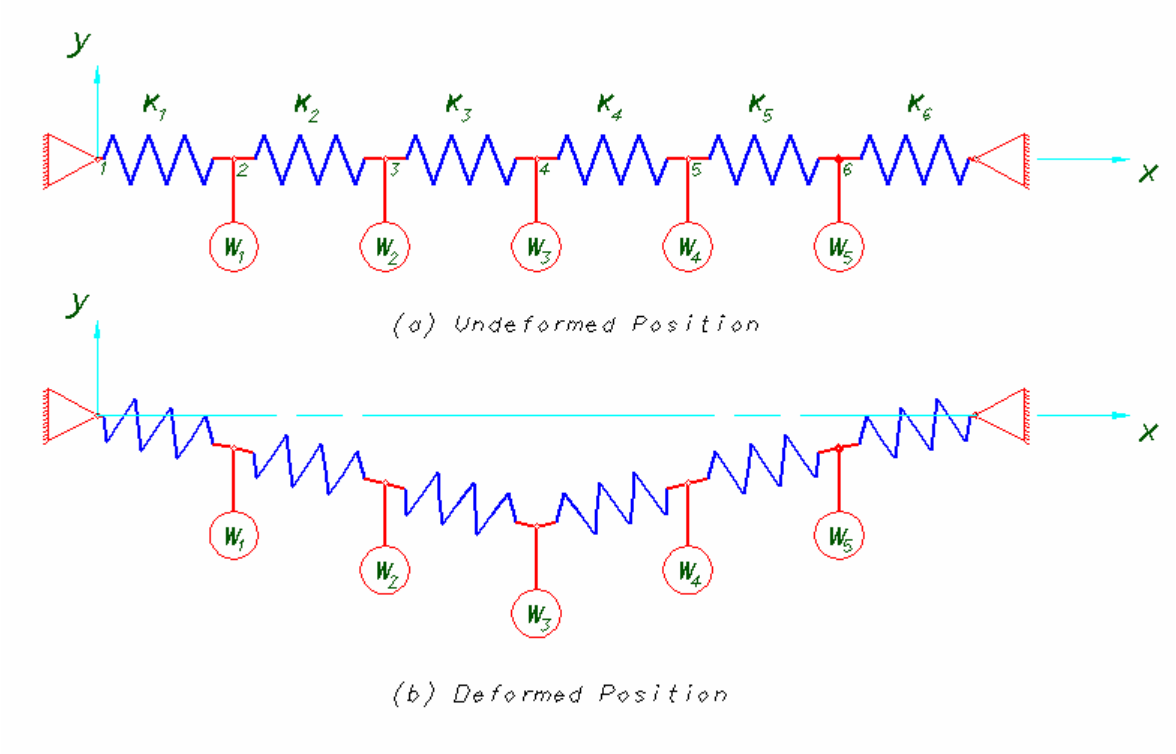

Figure 3-2 Spring and weight system

The deformation of spring i is

$$\Delta L_i = \sqrt{(X_{i+1} - X_i)^2 + (Y_{i+1} - Y_i)^2} - L_i^0 \tag{3-9}$$

where the length L^0 is taken to be 10 m for each spring, and there are a total of $N+1$ springs, with N being the number of weights (in Figure 3-2, $N = 5$).

The stiffness of spring i is taken to be

$$K_i = 500 + 200(\frac{N}{3} - i)^2 \qquad N/m \tag{3-10}$$

Weight W_j is defined to be

$$W_j = 50j \qquad N \tag{3-11}$$

where j corresponds to the joint where W_j is applied.

PE is

$$PE = \sum_{i=1}^{N+1} \frac{1}{2} K_i \Delta L_i^2 + \sum_{j=1}^{N} W_j Y_j \tag{3-12 }$$

where PE has units of Nm and the coordinates are positive as shown in the Figure 3-2.

Hide and seek annealing algorithm needs following inputs to run

- Initial guess for design parameters
- Upper/lower bound of design parameters
- Maximum iteration number to terminate program
- Maximum relative accuracy to terminate program

Since the program carries out a random walk in the design space an initial guess for design parameters does not affect the solution. It is only used to initiate program in a feasible region. Upper and lower bounds affect computation time directly with respect to the convergence of the program. When the problem is more definite for the designer finding global minimum will be also become easier. If designer does not know anything about the problem, he or she begins with a larger bound and run the

program a handful times. Then, according to results, some tighter bounds are set to get global optimum.

The maximum iteration number and relative accuracy are used for terminating the program. If program is terminated from the relative accuracy then the solution will be a global optimum. The convergence of the HSSA is verified theoretically by Belisie [32].

The program is run for 8 times with same inputs. Bounds are set to be reasonable physical values and initial design parameters are arithmetic average of bounds. Maximum iteration number and relative accuracy 50,000 and 10^{-8} are used for program convergence criteria, respectively. Other inputs of optimization algorithm are summarized in Table 3-1.

Table 3-1 Inputs of HSSA algorithm for 50,000 function evaluation

Design parameters (m)	X_2	X_3	X_4	X_5	X_6	Y_2	Y_3	Y_4	Y_5	Y_6
Initial solution	10	21	31	42	51	-3	-5	-7.5	-7.5	-5
Upper bound	11	22	32	43	52	0	0	0	0	0
Lower bound	9	20	30	41	50	-6	-10	-15	-15	-10

Program ends up with same optimal objective function for three different runs. Values of design parameters are close to each other. Differences between optimal design parameters are due to a large number of design parameters and significant digits of objective function. Results of the optimization are summarized in Table 3-2 and Table 3-3. Objective function values are converged to the same value in all iterations, which can be easily seen from Figure 3-3 and Figure 3-4. Figure 3-4 is rectangular zoomed region of Figure 3-3. In all iterations the objective function converged to 4,416 (Nm). In all runs program is terminated because the maximum number of iteration is exceeded the set limit.

Table 3-2 Optimum design parameters for 50,000 function evaluation

Optimum design variables (m)	*Run 1*	*Run 2*	*Run 3*	*Run 4*	*Run 5*	*Run 6*	*Run 7*	*Run 8*
X_1^*	10.25	10.39	10.31	10.32	10.35	10.27	10.34	10.27
X_2^*	20.91	21.10	21.02	21.01	21.08	20.97	21.05	20.94
X_3^*	31.53	31.70	31.62	31.62	31.67	31.58	31.65	31.55
X_4^*	41.94	42.10	42.02	42.02	42.08	41.99	42.05	41.95
X_5^*	51.63	51.79	51.71	51.70	51.76	51.68	51.73	51.65
Y_1^*	-4.33	-4.24	-4.29	-4.32	-4.28	-4.35	-4.25	-4.34
Y_2^*	-7.94	-7.87	-7.91	-7.97	-7.89	-7.96	-7.89	-7.95
Y_3^*	-9.78	-9.86	-9.86	-9.86	-9.86	-9.80	-9.84	-9.83
Y_4^*	-9.22	-9.41	-9.32	-9.31	-9.38	-9.26	-9.33	-9.23
Y_5^*	-5.83	-6.03	-5.94	-5.93	-5.99	-5.89	-5.96	-5.86

Table 3-3 Termination criteria for 50,000 function evaluation

	Run 1	Run 2	Run 3	Run 4	Run 5	Run 6	Run 7	Run 8
Optimum objective function	4410	4416	4415	4415	4416	4413	4416	4411
Relative accuracy	0.009	0.007	0.057	0.068	0.016	0.008	0.016	0.750
Number of accepted function evaluations	184	139	127	166	135	174	165	207

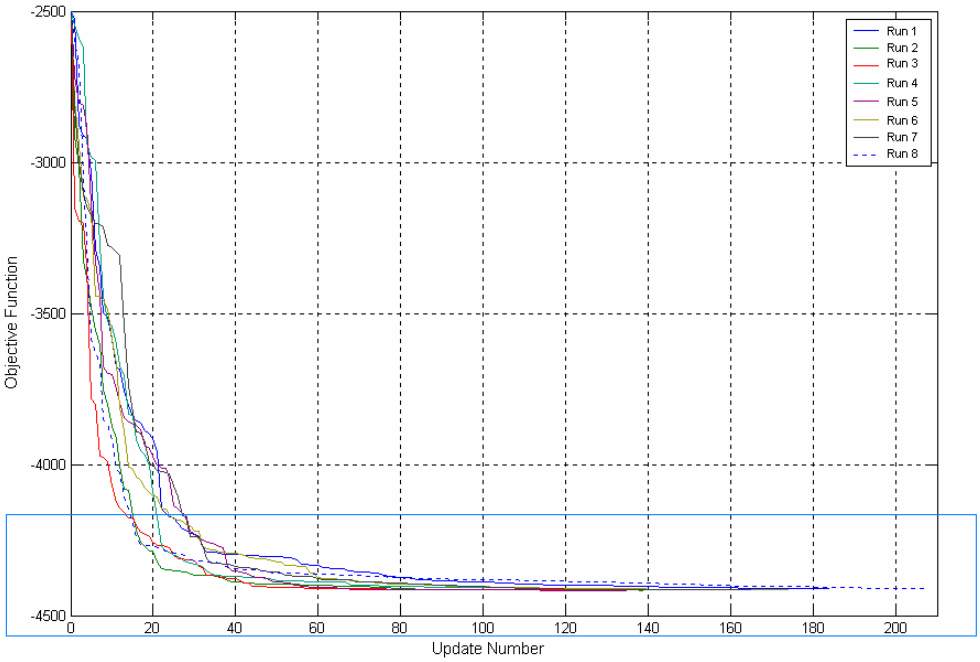

Figure 3-3 Objective function versus update number for 50,000 iterations

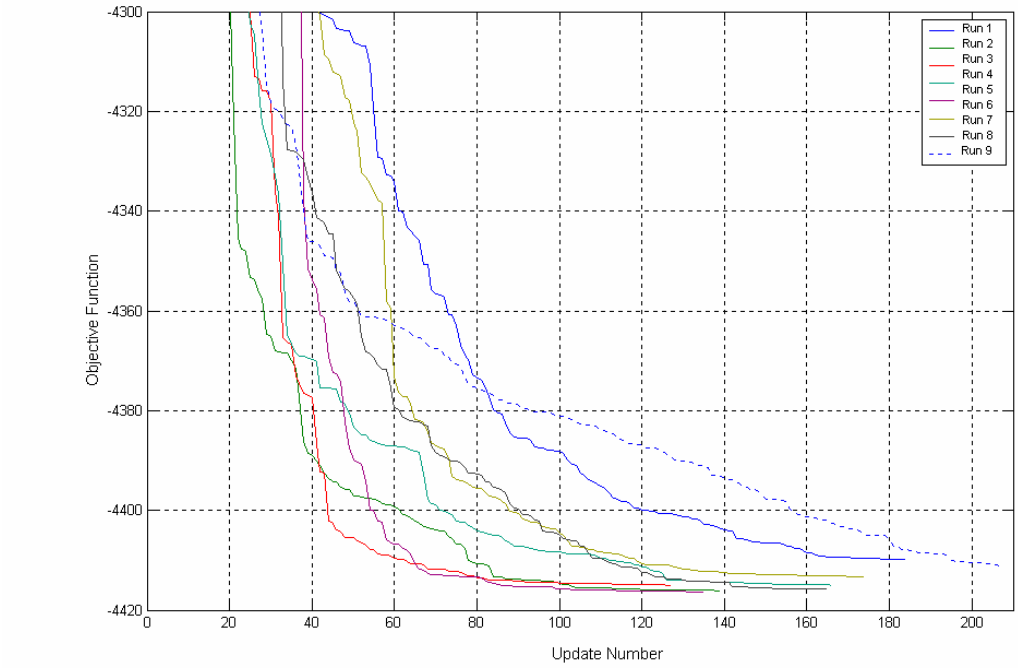

Figure 3-4 Zoomed objective function versus update number for 50,000 iterations

Design parameters can be also examined in a similar way. If history plots of ten design parameters are drawn, it is seen that all design parameters are converged to a constant value. Therefore, the final solution is the global optimum.

HSSA algorithm uses random walk to determine the next search point. Therefore, it may find the optimum solution in its first attempt. For example in these runs, the optimum solution is found at 39,887th function evaluation in the 1st iteration while it is found 49,979th function evaluation in the 7th iteration.

This example is a useful tool to see advantages and disadvantages of HSSA and also to verify it. Following six algorithms were used in [48] to solve defined problem:

1. Powell's method
2. Steepest descent
3. Fletcher-Reeves conjugate direction method
4. Davidon-Fletcher-Powell variable metric method
5. Broydon-Fletcher –Goldfarb-Shanno variable metric method
6. Newton's method

Type of first algorithm is the zero-order, 2nd -5th algorithms are the first-order, and 6th one is the second order optimization method. Table 3-4 gives the values of the design parameters and the optimum objective function for each of the seven methods. Bounds are taken similar to Table 3-1. Initial conditions are taken same as in reference [48], and are given in Table 3-4.

Table 3-5 gives the iteration history for each method. The number of function evaluations is listed only as a general purpose and is considered as an upper bound on the computational expense. In practice, the efficiency of the optimization algorithms is improved by careful programming, scaling of the variables, and less conservative termination criteria.

Table 3-4 Optimization results of several optimization algorithms [48] and HSSA

Design parameter (m)	Initial solution	Optimization method						
		1	2	3	4	5	6	HSSA
X_1	10	10.30	10.30	10.40	10.20	10.20	10.40	10.35
X_2	20	21.10	20.70	21.10	20.80	20.80	21.10	21.08
X_3	30	31.70	31.00	31.60	31.40	31.40	31.70	31.67
X_4	40	42.10	41.30	42.00	41.80	41.70	42.10	42.08
X_5	50	51.80	51.10	51.60	51.40	51.40	51.80	51.76
Y_1	0	-4.28	-2.65	-3.96	-4.64	-4.64	-4.28	-4.28
Y_2	0	-7.90	-5.25	-7.77	-8.19	-8.19	-7.90	-7.89
Y_3	0	-9.86	-7.35	-10.20	-10.00	-10.00	-9.86	-9.86
Y_4	0	-9.40	-7.63	-9.52	-9.18	-9.19	-9.40	-9.38
Y_5	0	-6.01	-4.97	-5.79	-5.42	-5.43	-6.01	-5.99

It is important to understand that this is only one simple problem to indicate the characteristics of the methods. It would not be meaningful to draw too many conclusions from this. However, it is probably safe, based on this and numerous other problems, to conclude that the more sophisticated methods usually converge more rapidly, and provide results that are more accurate. This is particularly true if the gradient information can be provided analytically rather than by finite difference.

HSSA algorithm converges to the final solution after a large number of function evaluations. But the number of accepted function evaluations becomes small. In a few accepted generation, the objective function decreased noticeably. A high number of function evaluation is required when bounds are vast. By making bounds tight then the final solution can be achieved in a smaller number of iterations. Bounds are made tighter by using information found in 50,000 iterations to validate this outcome. Program convergence criteria, maximum iteration number and relative accuracy are taken as 1,000 and 10^{-8}, respectively. Altered inputs of optimization algorithm are given in Table 3-6.

Table 3-5 Iteration history of objective functions of different optimization algorithms [48] and HSSA

Iteration no.	Optimization method						
	1	*2*	*3*	*4*	*5*	*6*	*HSSA*
0	0	0	0	0	0	0	-2,492
1	0	-60	-60	-60	-60	-1,256	-2,712
2	0	-126	-292	-292	-292	-1,618	-2,805
3	0	-151	-661	-666	-666	-1,987	-2,811
4	0	-194	-1,148	-941	-941	-2,175	-2,879
5	0	-223	-1,559	-1,430	-1,432	-2,330	-3,136
6	-78	-318	-1,895	-1,812	-1,812	-2,912	-3,330
7	-306	-398	-2,439	-2,123	-2,119	-3,076	-3,437
8	-683	-1,618	-2,828	-2,469	-2,471	-3,297	-3,675
9	-1,139	-1,900	-3,179	-2,519	-2,519	-3,402	-3,698
10	-1,722	-1,958	-3,540	-2,573	-2,572	-3,539	-3,703
11	-1,728	-2,010	-3,792	-3,202	-3,203	-4,219	-3,751
12	-1,732	-2,043	-4,014	-3,703	-3,700	-4,306	-3,796
13	-1,732	-2,101	-4,158	-3,823	-3,820	-4,355	-3,846
14	-1,734	-2,141	-4,198	-3,904	-3,902	-4,377	-3,860
15	-1,734	-2,355	-4,216	-4,149	-4,415	-4,391	-3,868
16	-1,739	-2,490	-4,307	-4,299	-4,298	-4,414	-3,871
17	-1,835	-2,540	-4,361	-4,336	-4,336	-4,416	-3,886
18	-1,987	-2,557	-4,390	-4,340	-4,340	-4,416	-3,941
19	-2,306	-2,588	-4,393	-4,340	-4,340	-4,416	-3,946
20	-2,623	-2,611	-4,393	-4,340	-4,340	-	-3,972
Final	-4,416	-3,964	-4,393	-4,378	-4,378	-4,416	-4,416
Number of accepted function evaluations	178	40	22	26	26	19	135
Number of function evaluations	465	587	331	383	383	378	50,000

Table 3-6 Inputs of HSSA algorithm for 1,000 function evaluation

Design parameter (m)	X_1	X_2	X_3	X_4	X_5	Y_1	Y_2	Y_3	Y_4	Y_5
Initial solution	10.35	21.15	31.65	42.05	51.75	-4.25	-7.85	-9.85	-9.40	-6.00
Upper bound	10.40	21.20	31.70	42.10	51.80	-4.20	-7.80	-9.80	-9.30	-5.90
Lower bound	10.30	21.10	31.60	42.00	51.70	-4.30	-7.90	-9.90	-9.40	-6.00

As expected, the optimum solution is found faster when bounds are set tighter. Program is run for three times with the same inputs. Results of these computer runs are summarized in Table 3-7, Table 3-8, and Figure 3-5. Each run gives same results and final design parameters are close to each other. Algorithm converged to global optimum rapidly after tighting bounds

Table 3-7 Optimum design parameters for 1,000 function evaluation

Optimum design parameter (m)	Computer run		
	1	2	3
X_1^*	10.361	10.357	10.358
X_2^*	21.103	21.101	21.100
X_3^*	31.690	31.694	31.695
X_4^*	42.093	42.094	42.096
X_5^*	51.769	51.775	51.773
Y_1^*	-4.263	-4.284	-4.287
Y_2^*	-7.846	-7.875	-7.894
Y_3^*	-9.860	-9.847	-9.850
Y_4^*	-9.405	-9.393	-9.403
Y_5^*	-6.010	-6.014	-6.013

Table 3-8 Termination criteria for 1,000 function evaluation

	Run 1	Run 2	Run 3
Optimum objective function	4,416	4,416	4,416
Relative Accuracy	0.004	0.0006	0.002
Number of accepted function evaluations	30	62	67

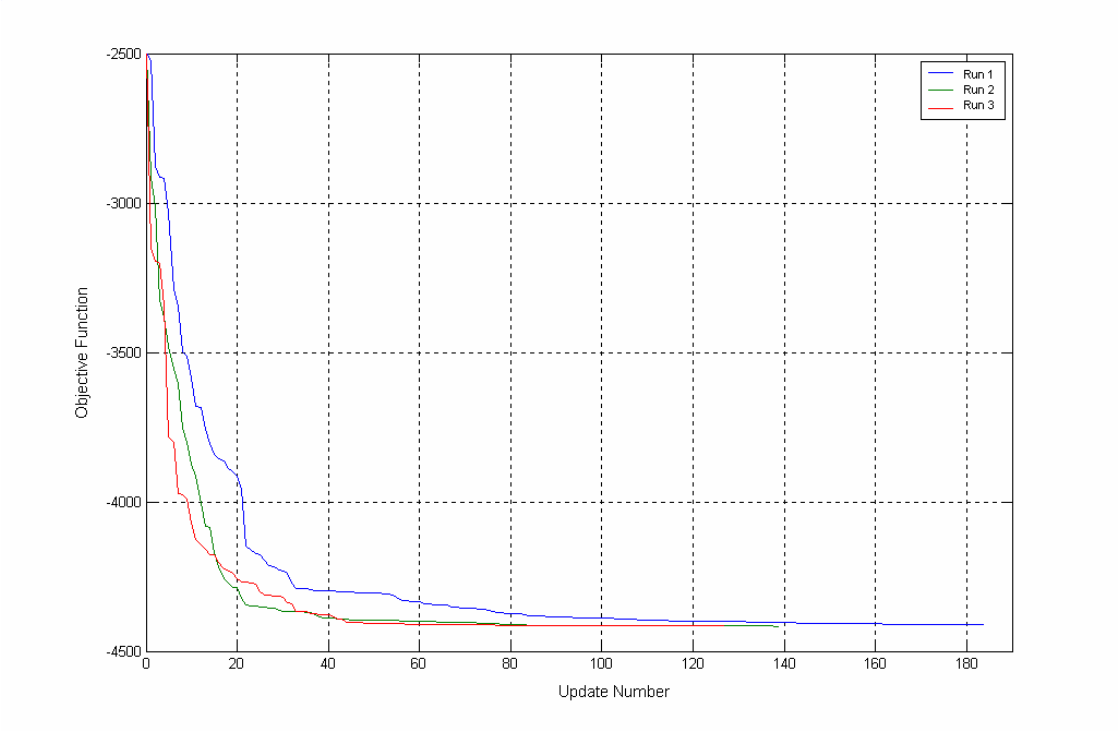

Figure 3-5 Objective function versus update number for 1,000 iterations

3.3.3 Quadratic Performance Index

In designing control systems a given performance index is used minimized or maximized via control vector. Quadratic performance index is used for minimization of

total energy of the system by minimizing sum of squares of both states and controller forces.

$$J_1 = \int_0^{\infty} \left(\{x\}^T [Q] \{x\} + \{u\}^T [P] \{u\} \right) dt \tag{3-13}$$

An advantage of using the quadratic optimal control scheme is that the system designed will be stable, except in the case where the system is not controllable. In designing control systems based on the minimization of quadratic performance index, it is required to solve the reduced matrix Riccati equation given in Eq. (3-14)

$$-[Q] = [A]^T [R] + [R][A] - [R][B][P]^{-1} [B]^T [R] \tag{3-14}$$

In this thesis work lqr function of MATLAB® is used in the solution of Riccati equation. Inputs of lqr function are A, B, Q, and P matrices while outputs are the Riccati matrix, controller gain matrix and closed loop eigen values. Function reference of lqr is given in Appendix D.

From Eq.(3-13), optimum quadratic performance index of the stable system for an arbitrary initial conditions, as $T_f \to \infty$, gives

$$J_1^* = \{x_0\}^T [R] \{x_0\} \tag{3-15}$$

where $[R]$ satisfies the Riccati equation.

Eq. (3-15) shows that optimal performance index depends on the initial states. This result is not very useful since the initial state is not available for practical problems. A simple way to compare performance indeces is taking trace of Riccati matrix [30]. By this way for any initial condition order of Ricatti matrix is minimized. Since Ricatti matrix is used in the calculation of feedback force, by minimizing trace of Riccati

matrix, dissipated actuator energy is also minimized. Hence, an upper bound on the dissipation energy can be expressed as

$$J_2 = \frac{1}{2} trace\left(\left[R\right]\right) \tag{3-16}$$

Consequently, two step optimization is carried out to minimize energy dissipation. Firstly, by solving reduced matrix Riccati equation closed loop gain matrix is optimized for any initial conditions. Then, in the upper level by using Eq. (3-16) other design parameters are optimized.

3.3.4 Robustness Measure of Patel and Toda

There are many works are done to guarantee various properties of a control system under finite ignorance. In this thesis work Patel and Toda's [49] robustness measure is used in controller design.

Consider the system described by

$$\left\{\dot{x}(t)\right\} = \left(\left[A_c\right] + \left[E(t)\right]\right)\left\{x(t)\right\} \tag{3-17}$$

where $\left[A_c\right]$ represents closed loop state matrix as defined by Eq. (2-29) and the uncertainty of the system assumed representable by $\left[E(t)\right]$. It can be shown that the system in Eq. (3-17) remains stable if $\left[E(t)\right]$ satisfies

$$\left\|\left[E(t)\right]\right\|_2 \le \mu \tag{3-18}$$

where

$$\mu = \frac{1}{\max \lambda\left(\left[L_y\right]\right)} \tag{3-19}$$

and $\left[L_y\right]$ is the solution of the Lyapunov equation given in Eq, (3-20), $\{\lambda\}$ denotes the eigenvalues of $\left[L_y\right]$

$$\left[A_c\right]^T \left[L_y\right] + \left[L_y\right]\left[A_c\right] = -2\left[I\right] \tag{3-20}$$

where $\left[I\right]$ is the identity matrix.

It is also shown by Toda and Patel [49] that

$$\mu \le \min\left[-\mathrm{Re}\,\lambda(A_c)\right] \tag{3-21}$$

Eq. (3-21) gives a bound on achievable robustness with this kind of measure. It is apparent that the ideas of robustness and stability margin are closely related. For pole placement designs by active feedback where eigenvalues are specified, the robustness measure μ in principle can be maximized up to $\min\left[-\mathrm{Re}\,\lambda\left(\left[A_c\right]\right)\right]$ by seeking a normal matrix with the desired eigenvalues, provided no additional constraints are imposed.

In this thesis, the same stability robustness measure is used with Liu and Begg [7]. They chosen first representation of the uncertainty margin. By maximizing Eq. (3-22) margin for the variation of the sytem uncertainity also maximized.

$$M_r = \frac{1}{\max \lambda\left(\left[L_y\right]\right)} \tag{3-22}$$

where M_r is the measure of stability robustness.

3.3.5 Controllability Measure of Liu

A system is said to be controllable at time t_0 if it is possible by means of an unconstrained control vector to transfer the system from any initial state $\{x(t_0)\}$ to any other state in a finite interval of time.

It is proved that in [46] system is completely state controllable if and only if the matrices $[B],[A][B],...,[A]^{n-1}[B]$ are linearly independent, or the nxn matrix

$$\left[[B] \ \vdots \ [A][B] \ \vdots \ \cdots \ \vdots \ [A]^{n-1}[B]\right] \tag{3-23}$$

is of rank n. This matrix is commonly called as the controllability matrix.

Hamdan and Nayfeh [50] propose a new measure of modal controbality which has connections with degree of controllability given in Eq. (3-23). Their controllability measure gives useful information on controllability of each mode with respect to each input.

It is known that the entries of the matrix $[S_A]^T[B]$ give information about the controllability of the modes from the inputs, where $[S_A]$ is the eigenvectors of system matrix. If the i[th] entry of the matrix $[S_A]^T[B]$ is zero $\left(\{s_{A_i}\}^T\{b_j\}=0\right.$, where $\left.\{b_j\}\right)$ is the j[th] column of $[B]$), then the i[th] mode is not controllable from the j[th] input. If the i[th] row of the $[S_A]^T[B]$ is a zero row, then this means that the i[th] mode is not controllable from all inputs.

One of the proposed method of controllability at [50], which is based on above information, uses magnitude of $\{s_{A_i}\}^T\{b_j\}$.

$$\left|\left\{s_{A_i}\right\}^T \left\{b_j\right\}\right| = \left\|\left\{s_{A_i}\right\}\right\| \left\|\left\{b_j\right\}\right\| \cos\theta_{ij} \tag{3-24}$$

where θ is taken to be acute; it gives indication of the distance between two one-dimensional subspaces. If the two subspaces are orthogonal, then $\left\{s_{A_i}\right\}$ lies in the left null-space of $\left\{b_j\right\}$ and the ith mode is uncontrollable from the jth input. If the angle is not 90 deg but near to it, then again this indicates that ith mode is not easily controllable from the jth input. The effect of $\left\|\left\{b_j\right\}\right\|$ on modal controllability can be appreciated if u_j is considered to be a unit current, then the two-norm of the vector $\left\{b_j\right\}$ represents the power injected by the jth input into the different channels of the state variables. Thus, if it is required to be compare the controllability of a mode from different inputs, the angles calculated from Eq. (3-24) give an indication of the suitability of the subspaces spanned by each $\left\{b_j\right\}$. Another factor is the norm of $\left\{b_j\right\}$. Higher norm indicates more power injected by the input, and thus more controllability.

Liu and Begg [42] used the singular value decomposition of the input matrix $[B]$ in defining controllability. This method can be used for both distinct and repeated modes. By using propesed technique modal controllability can be quantatitavely measured by associated singular values. Taking singular value decomposition of $[B]$ yields

$$[B] = [U][Svd_c][V]^T \tag{3-25}$$

where $[U]^T[U] = [I]$, $[V]^T[V] = [I]$, and

$$[Svd_c] = \begin{bmatrix} [\Sigma] & 0 \\ 0 & 0 \end{bmatrix} = \begin{bmatrix} diag(\sigma_i) & 0 \\ 0 & 0 \end{bmatrix} \tag{3-26}$$

where σ_i is the singular values of $[B]$.

By making same transformation and assumptions Liu found out that controller force is proportional to $[Svd_c]$. Therefore, the larger the value of the Euclidean nom $M_c = \|[\Sigma]\|_E$ the less energy is required to produce control forces and systems controllability increases as stated before.by Hamdan and Nayef, [50].

3.3.6 Frequency Constraint

Structural natural frequencies are calculated by solving Eq. (3-27) in structural analysis.

$$([M]^{-1}[K] - \omega^2[I])\{q\} = 0 \tag{3-27}$$

Frequency constraint can be applied as both equality constraint and inequality constraint depending on the design criteria. Equality and inequality constraint are inserted to performance index as

$$\omega - \omega_o = 0 \qquad or \qquad \omega - \omega_o \le 0 \tag{3-28}$$

where ω is structural natural frequency and ω_0 is desired structural natural frequency. Frequency constraint is nonlinear with respect to design parameters.

3.3.7 Mass constraint

Structural mass is used as equality constraint in both case studies. The formulation is given in Eq.(3-29)

$$M_t = \sum_{i=1}^{n_b} \rho_i a_i L_i \tag{3-29}$$

where ρ, a and L are density, cross sectional area, and length of the i^{th} bar element, respectively and n_b is the number of bar elements in the truss structure.

3.4 COMPUTATIONAL PROCEDURE

Visual Fortran® and MATLAB® are used to write modeling and optimization algorithms. There are three main programs are written by using these programs. These are

- Finite element modeler in MATLAB®
- Hide and Seek Algorithm in Visual Fortran®
- Performance index calculator in MATLAB®

HSSA algorithm is written in Visual Fortran® to accelerate the iteration part of the whole program. Other parts are written in MATLAB® by using its built-in functions.

The following analysis procedure is used in the optimization of structure/controller problem:

1. Initialize the optimization program by sending the following inputs to HSSA program
    - Upper/lower bound of design parameters
    - Initial guess of design parameters
    - Maximum number of iteration/relative accuracy
    - Number of design parameters

2. Calculate all initial values of the following optimization parameters
    - Objective function
    - Violation of frequency constraint
    - Violation of mass constraint
    - Performance index

3. Normalize all constraints by giving small perturbations to design parameters and recalculating optimization parameters

4. Send the performance index to HSSA program to set initial optimum value of the objective function

5. Check the relative accuracy and the maximum number of iteration, if satisfied go to step 9

6. Guess a new design family

7. Calculate optimization parameters

8. Compare the last maximum performance index with the current one.
    - If the current one is larger, set this design family and performance index as optimum. Calculate relative accuracy. Go back to step 5
    - If the current one is smaller go back to step 5

9. Quit from optimization program

CHAPTER 4

TWO BAR TRUSS CASE STUDY

In this chapter asimultaneous structure/controller optimization of a well-known two bar truss example is solved.

The geometry and material properties of this truss structure and all optimization parameters are taken the same as in Liu and Begg's work [17]. This basic problem is useful to understand both the theory and physics of the problem.

4.1 PROBLEM DEFINITION

The two bar truss structure shown in Figure 4-1 is 2-dof planar truss. A point mass is attached to intersection point of bar elements and the vibration level of this point is controlled by an axial force actuator. Actuator and external masses are taken as 0.5, 50 kg, respectively. Elastic modulus and density of material are taken as $73\ MPa$ and $2700\ kg/m^3$, respectively. Damping effects are completely neglected.

Design parameters are chosen as cross sectional areas of bar elements, number, and positions of actuators and closed loop gain matrix of controller.

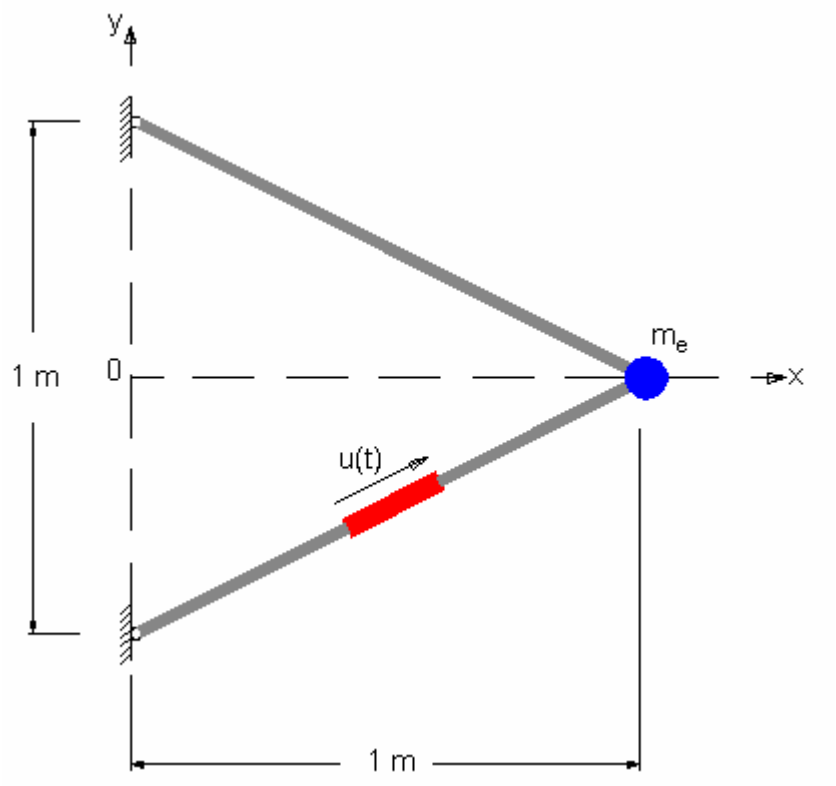

Figure 4-1 Two bar truss

Optimization problem can be defined as:

$$\min\left[\frac{tr(R)}{2}\right] \tag{4-1}$$

such that

$$M_t - 0.3019 = 0 \qquad (kg) \tag{4-2}$$

$$\omega_l - 161.08 = 0 \qquad (rad/s) \tag{4-3}$$

where R is the Riccati matrix, M_t is mass of truss structure, and ω_l is the lowest structural natural frequency.

Quadratic cost function given in Eq. (3-13) is set for minimizing states and control forces. Cost of QPI is chosen such that every state is penalized in same order while actuator energy is penalized 10^{-4} times smaller; i.e.,

$$[Q] = \begin{bmatrix} 1 & 0 & 0 & 0 \\ 0 & 1 & 0 & 0 \\ 0 & 0 & 1 & 0 \\ 0 & 0 & 0 & 1 \end{bmatrix} \tag{4-4}$$

$$[P] = 10^{-4}.I_{rxr} \tag{4-5}$$

where r is the number of actuators, $[Q]$ and $[P]$ are the state and control weighting matrices of QPI, respectively.

A linear state feedback control law is assumed to be applied such that

$$\{U(t)\} = -[G]\{x(t)\} \tag{4-6}$$

States are chosen as modal displacements and velocities of nodes. Therefore QPI includes both structural and controller objective function which are minimum displacements and velocities at nodes and minimum controller energy.

Structural type constraints are used in the design. Two structural design parameters are tried to be selected for three alternative placements of actuators. Since system is symmetrical, theoretically two different actuator positions are available as shown in Figure 4-2. For each configuration of actuators, the problem reduces to a two equation (one linear, one nonlinear) - two unknown set of equations in terms of structural constraints. Then the optimum closed loop gain matrix can be found by solving LQR problem by using solution of these equations for the each actuator

configuration. Therefore, the problem is reduced to a dynamic programming problem. Liu and Begg [17] did not include actuator positioning into their work and they solved problem for the configuration shown in Figure 4-1. Consequently, they run their programs to find exact solution, which can be found analytically.

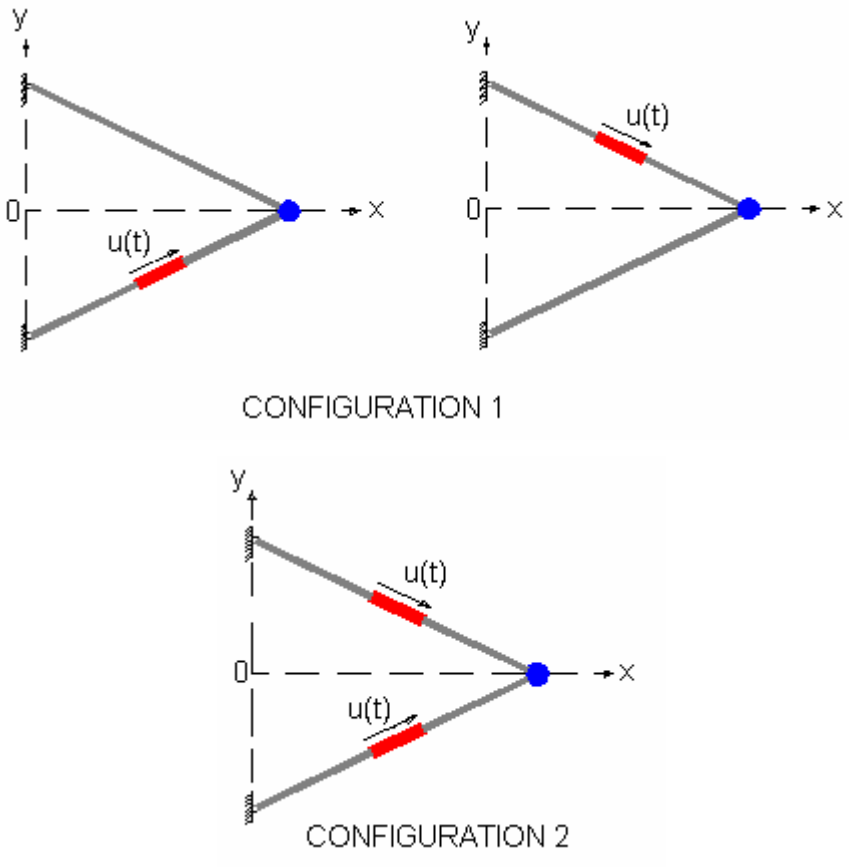

Figure 4-2 Positions of actuators

4.2 MATHEMATICAL MODELING

The mathematical modeling is carried out analytically to verify finite element, modal transformation, and optimization code.

4.2.1 Finite Element Modeling

Before modeling, elements and nodes are numerarized as custom case for all finite element models as shown in Figure 4-3.

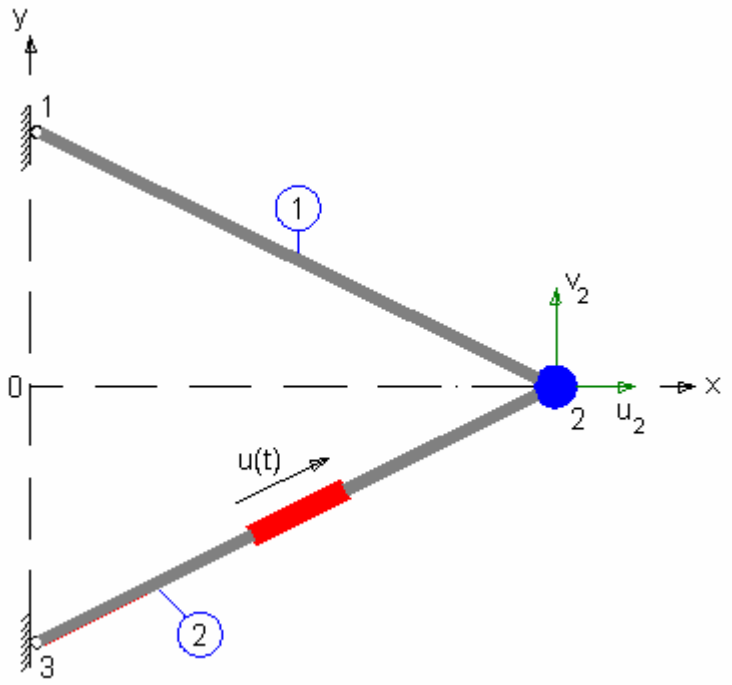

Figure 4-3 Finite element model

Derivation of elemental matrices and assembling of global structure matrices are given in Appendix D. Results of finite element code and these analytical solutions are crosschecked for verification.

Structural mass, stiffness, and direction of actuator force matrices for one actuator case are derived as given through Eq. (4-7)- (4-9).

$$[K] = \begin{bmatrix} 52.235(a_1 + a_2) & 26.117(a_2 - a_1) \\ 26.117(a_2 - a_1) & 13.059(a_1 + a_2) \end{bmatrix} \quad (N/mm) \tag{4-7}$$

$$[M] = \begin{bmatrix} 0.0010062(a_1 + a_2) + 50.25 & 0 \\ 0 & 0.0010062(a_1 + a_2) + 50.25 \end{bmatrix} (kg) \tag{4-8}$$

$$\{F_a\} = \begin{bmatrix} 0.89 \\ 0.45 \end{bmatrix} \tag{4-9}$$

where a_i are the elemental cross sectional areas.

Then by using equations above a modal state transformation can be carried out. To avoid the calculation of eigenvalues symbolically a modal transformation is not applied in the analytical solution. Therefore, a state space transformation in spatial coordinates can be derived by choosing states as nodal displacements and velocities. System and input matrices are given in Eq. (4-10)-(4-11) and the derivation of matrices is given in Appendix D.

$$[A]=\begin{bmatrix} 0 & 0 & \vdots & 1 & 0 \\ 0 & 0 & \vdots & 0 & 1 \\ \cdots & \cdots & \vdots & \cdots & \cdots \\ \dfrac{52235(a_1+a_2)}{0.0010062(a_1+a_2)+50.25} & \dfrac{26117(a_2-a_1)}{0.0010062(a_1+a_2)+50.25} & \vdots & 0 & 0 \\ \dfrac{26117(a_2-a_1)}{0.0010062(a_1+a_2)+50.25} & \dfrac{13059(a_1+a_2)}{0.10062(a_1+a_2)+50.25} & \vdots & 0 & 0 \end{bmatrix} \tag{4-10}$$

$$\{B\}=\begin{bmatrix} 0 \\ 0 \\ \cdots \\ \dfrac{0.89}{0.0010062(a_1+a_2)+50.25} \\ \dfrac{0.45}{0.0010062(a_1+a_2)+50.25} \end{bmatrix} \tag{4-11}$$

These matrices can be used in design of the optimal controller. Constraints can be also derived analytically. Again, the derivations are given in Appendix D.

$$W_t=(m_t)_1+(m_t)_2=0.0030187(a_1+a_2)\,(kg) \tag{4-12}$$

$$\omega_l=\sqrt{\frac{65300(a_1+a_2)-\sqrt{(39200(a_1+a_2))^2+(52200\,(a_2-a_1))^2}}{2(0.0010062\,(a_1+a_2)+50.25)}} \tag{4-13}$$

Then, this two equation two unknown system can be solved by using MATLAB®. Cross sectional areas of bar elements are found approximately 50 mm^2. Similar derivations can be done for two-actuator case, which are given in Appendix D. Frequency and mass constraints cannot be satisfied for two actuators case at the same time. Constraint plots both configurations are given Figure 4-4. For two actuator case, as it can be seen from the figure, constraint curves does not intersect. However, when penalty weight of the constraints are small, program may choose this configuration also as a solution..

Contour plots of objective functions can be drawn also by using MATLAB® contour function for each positions of actuators. Graphical solution of the optimization problem is given in Figure 4-5 and Figure 4-6 for both configurations. For a two-actuator case, as mentioned before, by accepting some error in both constraints an optimal solution can be found. Value of the optimum objective function for one-actuator and two-actuator cases are approximately 3840 and 210, respectively. This means that, if penalty weight of constraints is decreased, then program will choose two-actuator case. Because, improvement of the objective function is greater than the penalization of constraints.

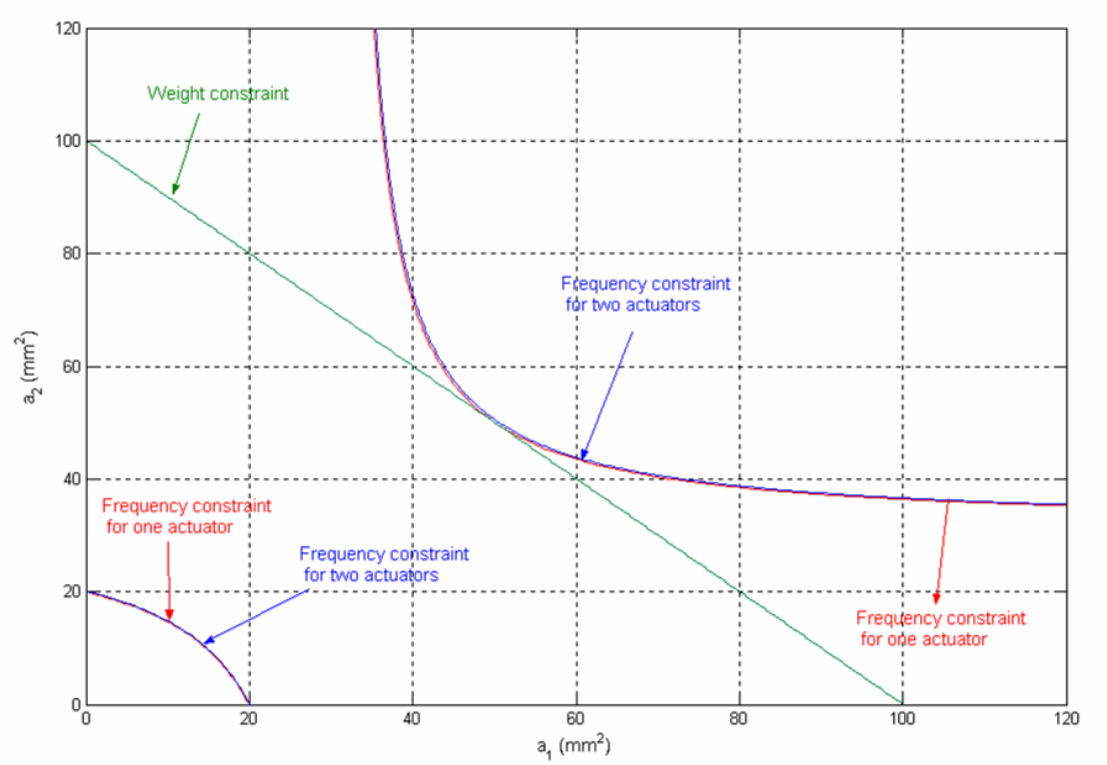

Figure 4-4 Two bar problem structural constraints plot

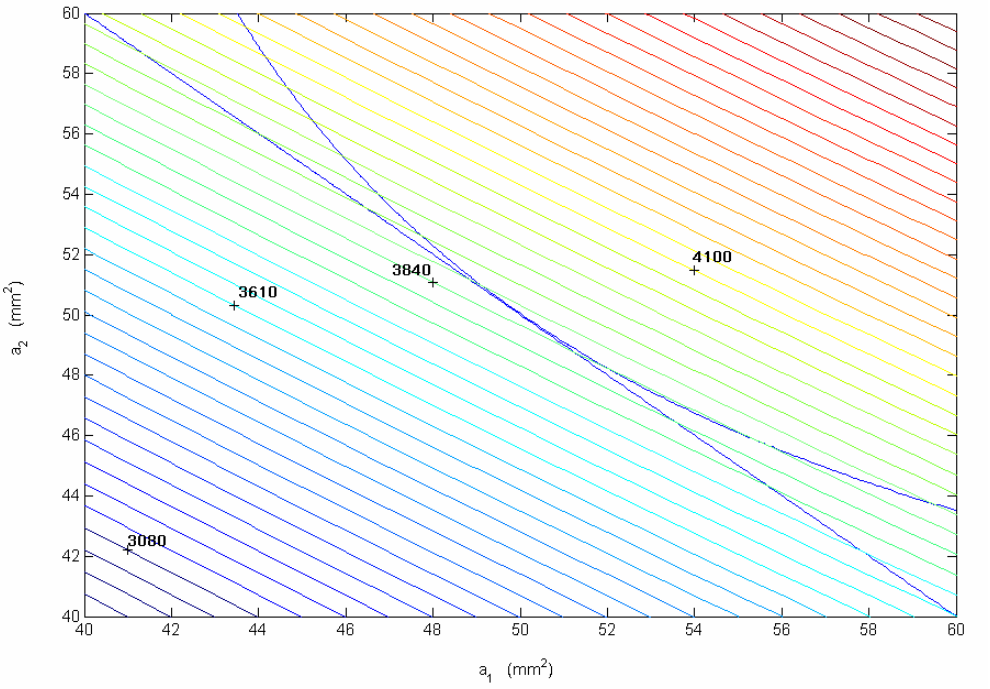

Figure 4-5 Graphical solution for one actuator case

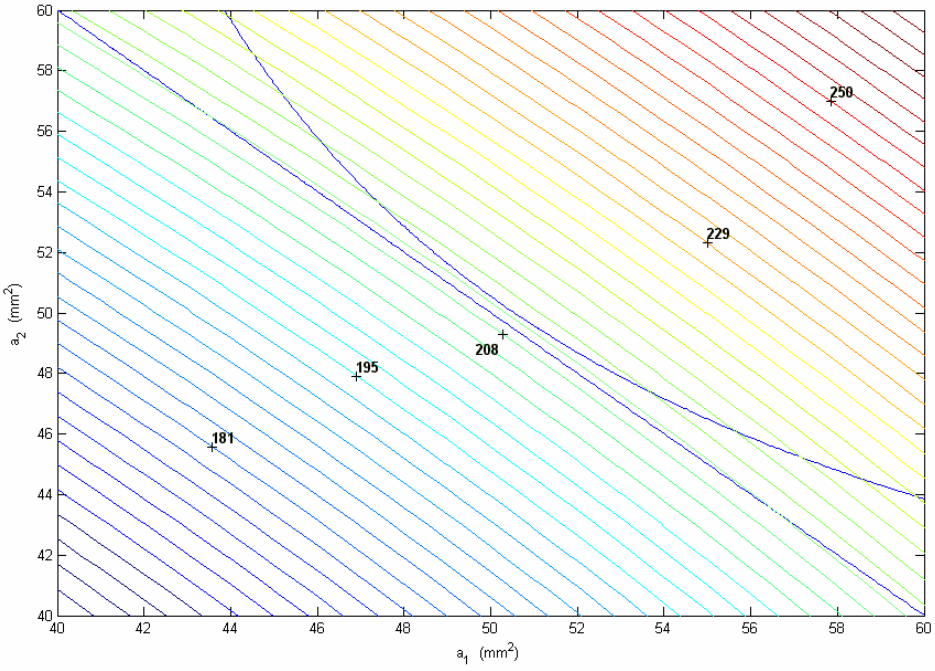

Figure 4-6 Graphical solution for two actuator case

4.3 RESULTS OF OPTIMIZATION ALGORITHM

HSSA requires some inputs as mentioned in Chapter 3. A parametric study of the algorithm is carried out for this simple example. These parameters and optimization results are summarized in Table 4-1 through Table 4-4. Lower and upper bounds of cross sectional areas are taken as 40 mm^2 and 60 mm^2 ,respectively in case 12. Whereas, in other case studies they are taken as 0.000001 mm^2 and 200 mm^2 , respectively.

Table 4-1 Inputs of optimization algorithm for different case studies

Case no.	Frequency constraint		Mass constraint		Maximum number of iteration	Initial values of cross sectional areas (mm^2) *	
	Penalty weight	Normalization constant	Penalty weight	Normalization constant			
	pw_c	nc	pw_c	nc		$(a_1)_0$	$(a_2)_0$
1	100	113	100	21,240	1,000	100	**100**
2	1	113	1	21,241	1,000	100	**100**
3	0.01	113	0.01	21,241	1,000	100	**100**
4	0.01	220	0.01	29,021	1,000	200	**200**
5	0.01	17	0.01	10,291	1,000	10	**10**
6	0.01	1	0.01	566	1,000	**10**	**10**
7	1	1	1	566	1,000	**10**	**10**
8	1	17	1	10,291	1,000	**10**	10
9	1	17	1	10,291	5,000	**10**	10
10	1	17	1	10,291	10,000	**10**	10
11	100	17	100	10,291	10,000	**10**	10
12	100	70	100	10,291	10,000	**60**	60

* actuator placed bar elements are shown in bold characters.

Table 4-2 Results of optimization for different case studies

Case no.	Optimum cross sectional areas (mm^2) *		Optimal objective function	Violation of mass constraint (kg)	Violation of frequency constraint (rad/s)	Relative accuracy	Update no
	$(a_1)_0$	$(a_2)_0$	J^*	$W_t - (W_t)_o$	$\omega_l - \omega_o$		
1	**52.59**	47.27	3893	0.05	-0.0004	270049	6
2	**55.20**	45.39	3963	0.58	0.0018	89	8
3	**70.56**	**30.36**	220	16.51	0.0276	982	6
4	**83.15**	**25.64**	250	24.54	0.0265	1827	8
5	**80.25**	**8.59**	208	78.63	0.0337	151	2
6	**10.00**	**10.00**	31	89.12	-0.0242	1	0
7	**46.52**	**57.35**	220	-1.45	0.1164	89	3
8	**36.01**	61.53	3520	9.23	-0.0007	61	5
9	**39.97**	62.90	3623	7.33	-0.0004	0.9	13
10	**36.65**	63.25	3618	7.67	0.0003	0.7	12
11	**48.05**	52.05	3829	0.13	0.0003	879148	7
12**	**51.05**	48.97	3875	0.06	0.0000	2799	8

* actuator placed bar elements are shown in bold characters.

**selected optimum solution of the problem is highlighted.

Following conclusions are derived from these case studies:

- Case 1 through 3 show that if the penalty weights of constraints decrease, solution of the optimization problem switches from one actuator to two-actuator case. This conclusion is also made in the analytical solution.

- Changing the initial guess; (i.e., case 3-7), affects normalization constants and this changes penalty weight of the constraints. Therefore, results of the optimization problem may switch according to the penalty weights. If violation of the constraints larger than the desired, the penalty weight should be increased.

- The maximum number of iteration is increased from case 8 to case 10. This input affects convergence of the problem. This can be seen from the change in

the final relative accuracy of the optimization problem. As the maximum number of iteration increases, the relative accuracy of the optimization algorithm decreases.

- Violation of the constraints strictly depends on the penalty weight of constraints. Therefore, as it can be seen from case 10 and 11, increasing penalty weights forces the optimization algorithm to satisfy the constraints.

- Side bounds of the design parameters and maximum number of iteration strictly depend on each other. If bounds of the design parameters become tighter; i.e., case 12, for the same number of function of evaluation, a more accurate result is found. Therefore, if the design parameters are not bounded, then the number of function evaluation should increased. Then, according to the results, bounds can be made tighter to find the optimal solution.

Consequently, the optimum solution of the problem is given in case 12. Iteration histories are shown in Figure 4-7 through Figure 4-13. All parameters converge to the constant value. Figure 4-13 shows that HSSA algorithm finds global optimum.

Optimum gain values for the controller can be transformed from modal coordinates to spatial coordinates or can be used as they are. Optimum design parameters are summarized in Table 4-3 and Table 4-4. In Table 4-4, highlighted elements of closed loop gain vector correspond to nodal velocities in x and y direction, respectively. Other two elements correspond to displacement of node 2 in x and y direction, respectively.

Optimal structural and controller characteristics are given in Table 4-5. The closed loop poles are placed on left side of the complex plane, indicating a stable system. If the controlled system matrix is examined, it can be seen that insertion of an actuator adds damping and stiffness besides mass to the system.

Table 4-3 Optimum structural design parameters

Notation	Optimum cross sectional areas of bar elements $\left(mm^2\right)$
a_1^*	51.05
a_2^*	48.97

*actuator placed bar element is highlighted.

Table 4-4 Optimum controller design parameters

Coordinate System	Notation	Optimum Closed Loop Gain Vector			
Modal coordinates	G_{mc}^*	-17,7640	-91,919	-560	-579
Spatial coordinates	G_{sc}^*	785,900	420,570	2,461	2,617

Table 4-5 Structural parameters of optimum system

Mass of truss structure (kg)	0.3019
Total mass of structure (kg)	0.8019
Structural natural frequencies (rad/s)	161.01
	322.15

Table 4-6 Closed loop poles of the optimum system

Closed loop poles of the optimum system	p_1= -601
	p_2= -219 + 57i
	p_3= -219 – 57i
	p_4= -88

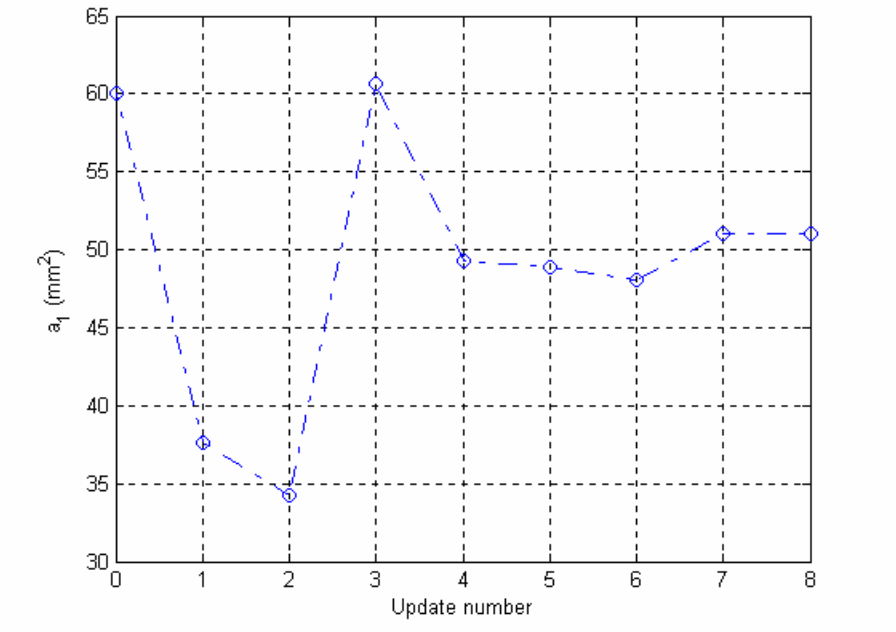

Figure 4-7 Iteration history of cross sectional area of element number 1

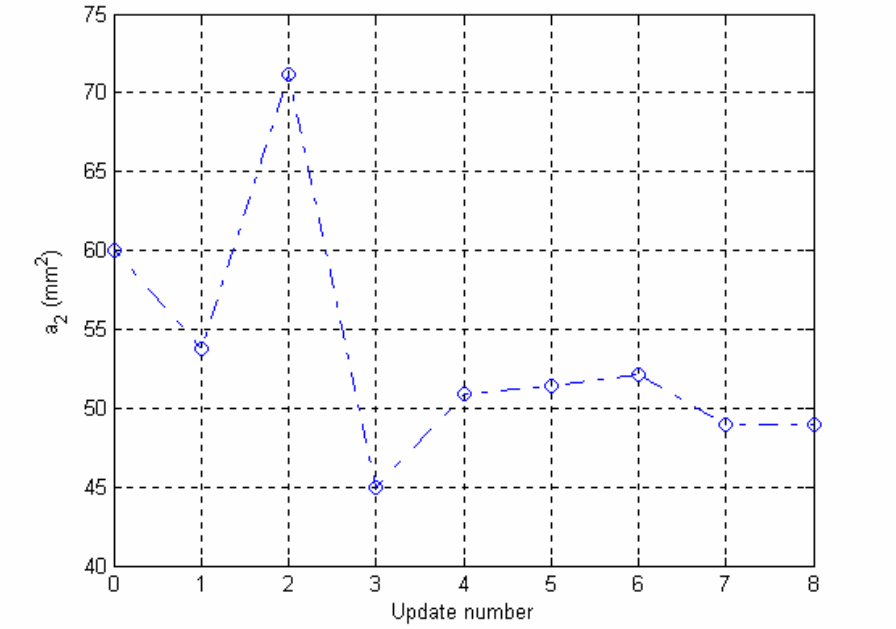

Figure 4-8 Iteration history of cross sectional area of element number 2

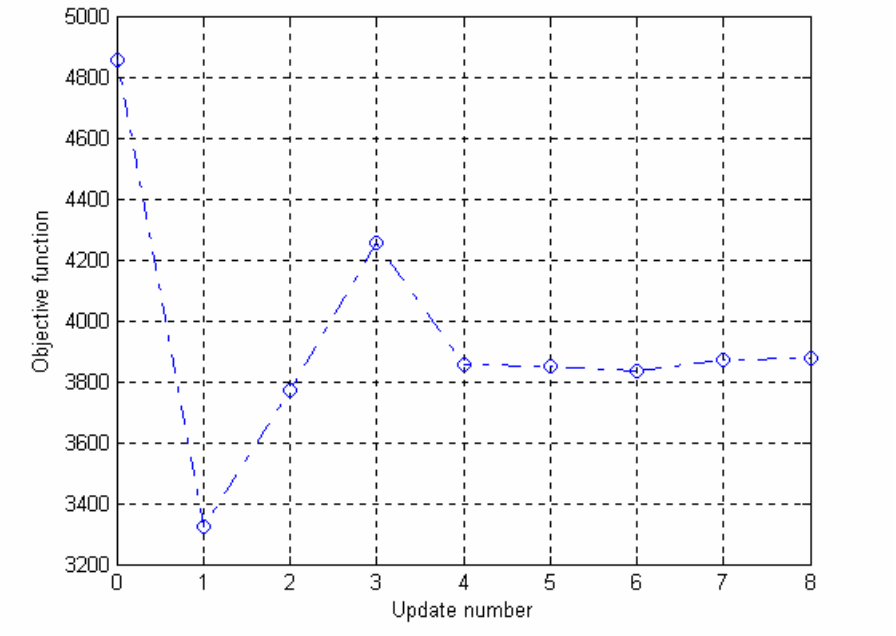

Figure 4-9 Iteration history of objective function

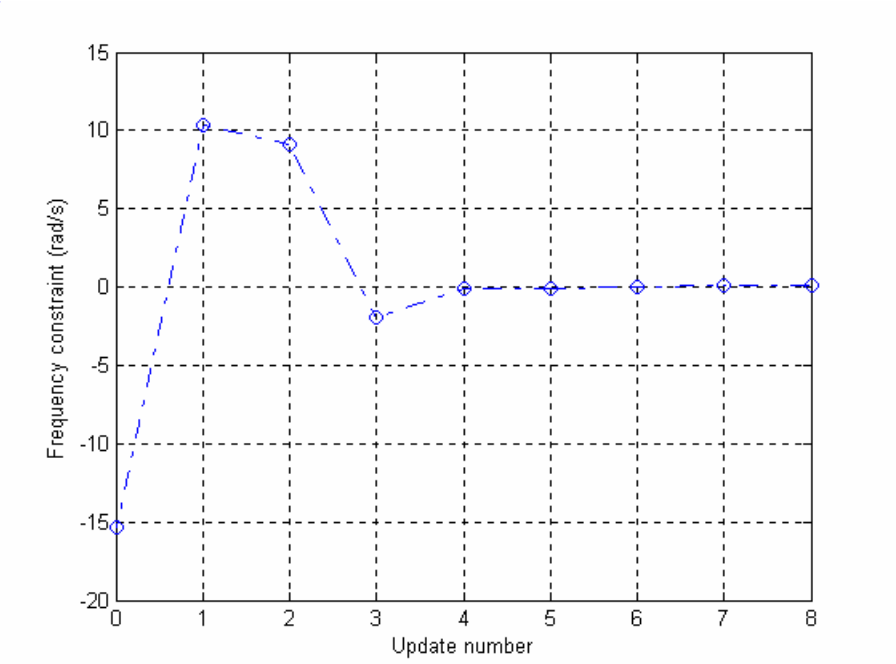

Figure 4-10 Iteration history of frequency constraint

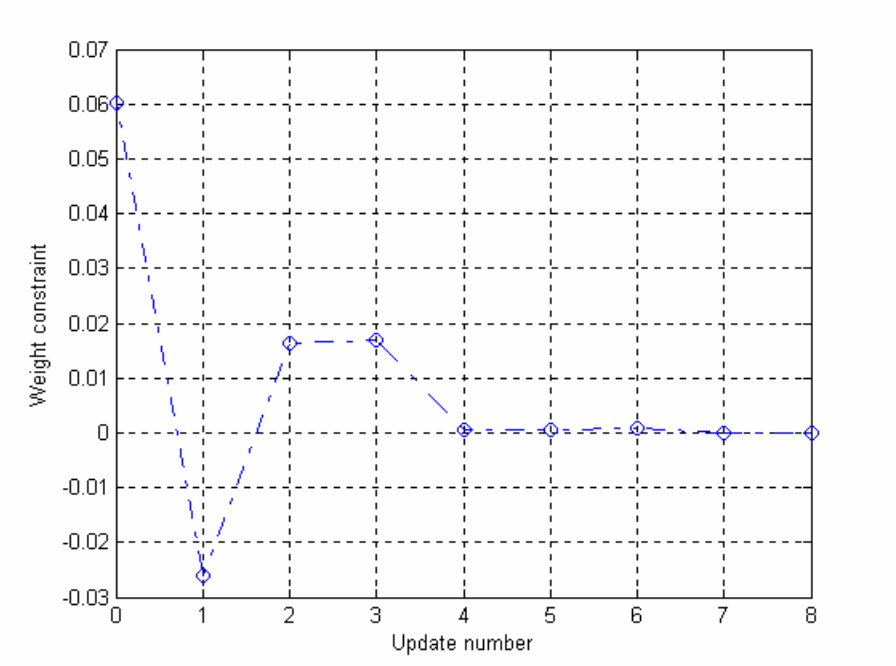

Figure 4-11 Iteration history of mass constraint

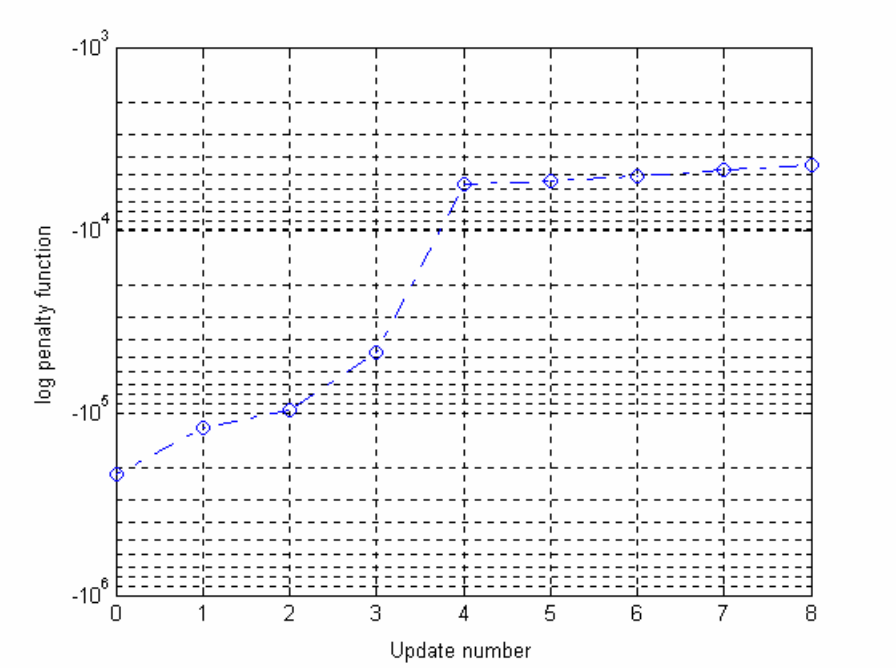

Figure 4-12 Iteration history of penalty function

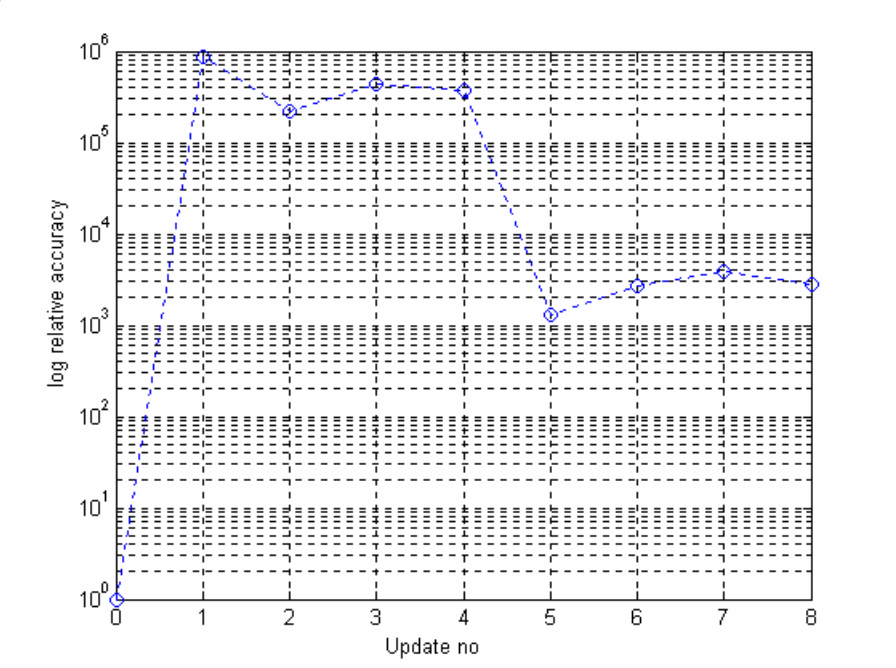

Figure 4-13 Iteration history of relative accuracy

4.4 DISCUSSION

Optimization of a two-bar truss problem is verified analytically. It is shown that the optimal system satisfies performance requirements with one actuator case.

Liu and Begg [17] solved this problem for one actuator case. They found the same optimal cross sectional areas, but did not give the resulting optimal closed loop gain values. The results of two solutions for cross sectional areas of bar elements are equal, which shows that in both cases same mathematical model is used in the controller design. The minimum value of the quadratic performance index found by Liu and Begg is 5,874, however in this study the same quantity is found as 3875. The reason for difference may be explained by the usage of elements of closed loop gain vector as design parameters and reduced matrix Riccati equation as constraint, so Liu and Begg's result cannot be defined as global optimum closed loop gain values. In fact, there is a unique solution for reduced matrix Ricatti equation, which minimizes

QPI optimally. In other words, they could optimize all design parameters by using single level optimization procedure.

HSSA algorithm works efficiently except its termination criterion. Convergence of the algorithm to the global optimum is rigorously proved. But it is terminated by the maximum number of iterations in all runs. Relative accuracy cannot be satisfied thoroughly although program finds global optimum. For complicated optimization problems relative accuracy cannot be satisfied in reasonable number of iteration. Therefore, results of different runs should be compared to accept the solution as optimum.

CHAPTER 5

PARABOLIC SHAPE MULTI-TRUSS CASE STUDY

In this chapter, a simultaneous structural/controller optimization problem of a parabolic shape truss structure controlled by four identical axial force actuators is considered.

The geometry and material properties of this truss structure and optimization parameters are again taken similar to Liu and Begg's work [17]. This problem is used to show the efficiency of the optimization method for large-scale problems; i.e., vibration suppression of a large truss structure.

5.1 PROBLEM DEFINITION

The parabolic shape truss structure considered is shown in Figure 5-1. It is a 20-dof planar truss. Elastic modulus and density of the material are taken as $73\,MPa$ and $2{,}700\,kg/m^3$, respectively. Nodal coordinates are given in Appendix F.

Design parameters are chosen as the cross sectional areas of bar elements (a_i), shape parameters (h_t and h_b), positions of actuators and closed loop gain matrix of the controller. Actuator number may be also used as a design parameter, but it would increase computational time. Therefore, the number of actuators is assumed equal to the number of modes which is required for the system to be controllable.

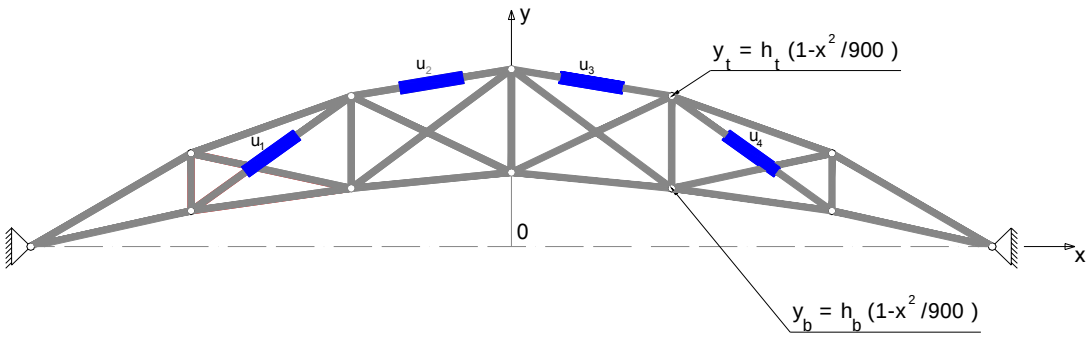

Figure 5-1 Parabolic shape truss structure

The optimization problem is very similar to the two-bar truss problem handled in Chapter 4, but only the frequency constraint is switched to an inequality constraint. A multiobjective optimization problem is solved in the second case study, which is also solved, by Liu and Begg [17]. The objective function and constraints of the first case study are defined by Eq. (5-1), Eq.(5-3), and Eq. (5-4), respectively. Corresponding optimization parameters for the second and third case studies are given by Eq.(5-2), Eq.(5-3), and Eq. (5-4). In the first and second case studies, actuator placed truss elements are not removed from the truss structure by the optimization algorithm. While in the third case study, actuator placed bar elements are removed from the structure.

$$\min\left[\frac{tr(R)}{2}\right] \tag{5-1}$$

$$\min\left[\frac{tr(R)}{2}\right] - 10{,}000(M_r + M_c) \tag{5-2}$$

such that

$$M_t - 3{,}000 = 0 \ (kg) \tag{5-3}$$

$$-\omega_l + 10 \le 0 \ \ (rad/s) \tag{5-4}$$

Performance indeces of these optimization problems are given in Eq. (5-5) and Eq. (5-6).

$$PI = \left[\frac{tr(R)}{2} \right] + pw_w^c abs\left(M_t - 3{,}000\right) + pw_f^c \max\left(0{,}10 - \omega_l\right) \tag{5-5}$$

$$PI = \left[\frac{tr(R)}{2} \right] - 10{,}000(M_r + M_c) + pw_w^c abs\left(M_t - 3{,}000\right) + pw_f^c \max\left(0{,}10 - \omega_l\right) \tag{5-6}$$

Since the number of design parameters is large, it is necessary to apply side constraints to size and shape parameters in order to bound the design space. Also structural design parameter linking is used between the cross sectional areas of the bar elements. Cross sectional areas of the symmetric bar elements about y axis are linked. Actuator positions are linked similar way. Hence, possible position of actuators decrease from 25 to 12 and two actuator are placed. Design parameter linking scheme is given in Appendix E.

States are chosen as the modal displacements and velocities of the nodes again and linear state feedback is applied. Therefore, QPI minimizes the energy of the structure and the controller.

Effects of high order natural frequencies are neglected and the controller design is carried out for lowest four natural frequencies. In the Liu and Begg's design, structural damping ratio is assumed as 0.1% for all modes. This is a conservative estimate of damping, which is mostly used in aerospace industry.

Structural type constraints are used in the design. Total mass of the structure is required to be 3,000 kg. Lowest natural frequency of the damped structure is required to be greater than 10 rad/s (1.6 Hz).

Optimization parameters are summarized in Table 5-1.

5.2 MATHEMATICAL MODELING

Mathematical modeling of the system is carried out in two steps, which are FEM and modal transformation. FEM is carried out by using the full dof's of the system. Element and node numbers can be seen in Figure 4-3. Modal reduction is used in modal state transformation. Controller is designed for the reduced model which is formed by using the lowest four lowest natural frequencies.

Table 5-1 Inputs of optimization algorithm

		Bounds	Initial Guess
Design parameters	Cross sectional areas $(a_i,\ i = 1 \cdots 13)$ $\left(cm^2\right)$	$0.0001 \le a_i \le 100$	50
	Shape variables (m)	$4 \le h_t \le 6$ $0 \le h_b \le 2$	$h_t = 5$ $h_b = 1.5$
	Actuator positions	On elements $1-12$	Shown in Figure 5-1
	Closed loop gain matrix (8x4)	No bounds	Not applicable
Constraints	Mass constraint (kg)	$W_t - 3{,}000 = 0$	
	Frequency constraint (rad/s)	$\omega_i^2 \ge 100$	
	Penalty weight of mass constraint	100	
	Penalty weight of frequency constraint	1	
Objective function	State weighting matrix	$[Q] = [I]_{4x4}$	
	Control weighting matrix	$[P] = 10^{-4}.[I]_{4x4}$	
HSSA method	Maximum number of iterations	20,000	
	Relative accuracy	10^{-4}	

* penalty weights of constraints are taken different from [17].

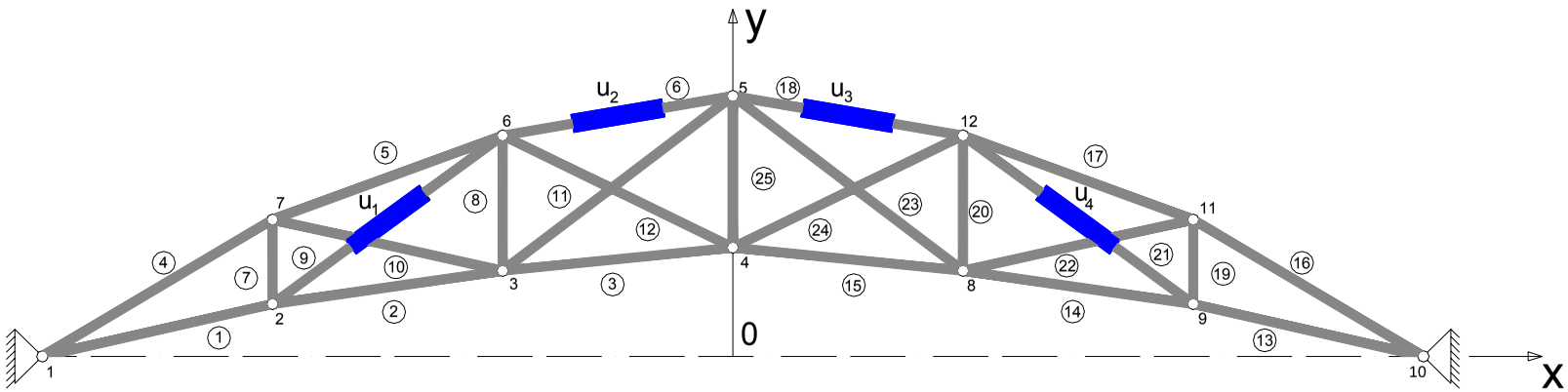

Figure 5-2 Finite element model of parabolic shape multi-bar truss case

5.3 OPTIMIZATION RESULTS OF PARABOLIC SHAPE MULTI-BAR TRUSS CASE STUDY

The results of both the optimization problems given in the following section are the final results of the optimization after certain number of runs.

5.3.1 Single Objective Optimization Using QPI

An optimization of parabolic shape truss is achieved very successfully after 20,000 iteration. The HSSA algorithm updates the design 32 times and converges to an optimum solution. The objective function of the optimization problem improved by 99%. Penalty weights of frequency and mass constraints are 1 and the normalization constants are 10^7 and $6{,}500$, respectively. Both constraints are satisfied. The convergence histories of the objective function and constraints are shown in Figure 5-2 through Figure 5-4.

The iteration histories of the cross sectional areas of the bar elements are given in Appendix F. Optimal actuator positions are parallel to the 4^{th} and the 6^{th} bar elements. The cross sectional areas of these truss members becomes very small; i.e, 2 cm^2 and 6 cm^2, respectively. This means the diameters of these truss members are approximately 2.5 cm and 4.8 cm, respectively. In fact, for such long truss members these diameters are not practical.

Optimal shape parameters, h_t and h_b are found as 5.6 and 0.9 m, respectively. Convergence histories of shape parameters are given in Figure 5-5 and Figure 5-6.

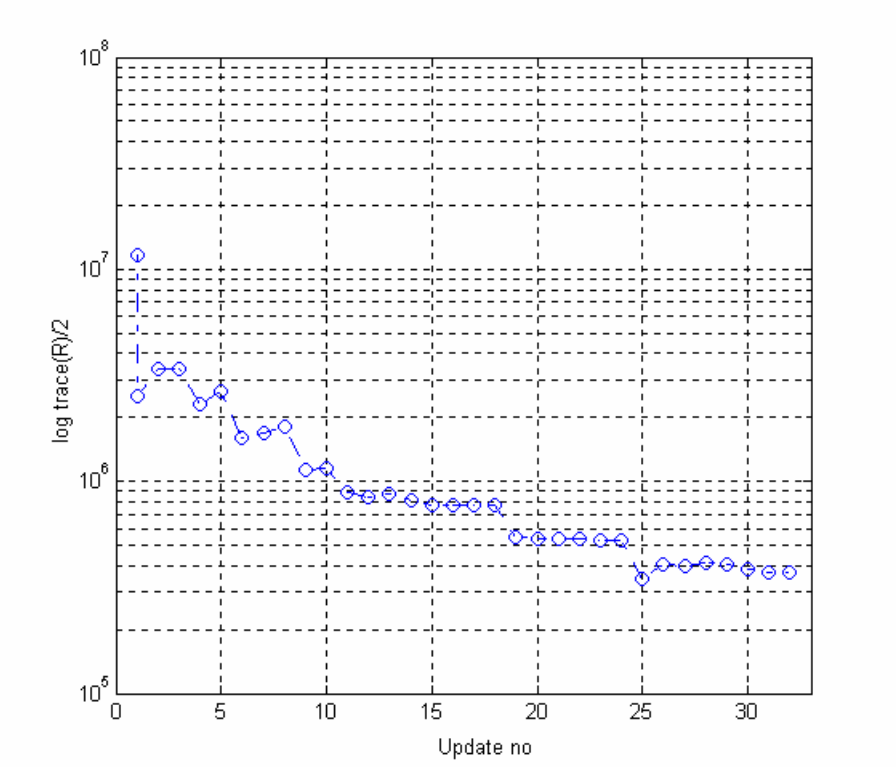

Figure 5-2 Iteration history of objective function for single objective optimization, Case I

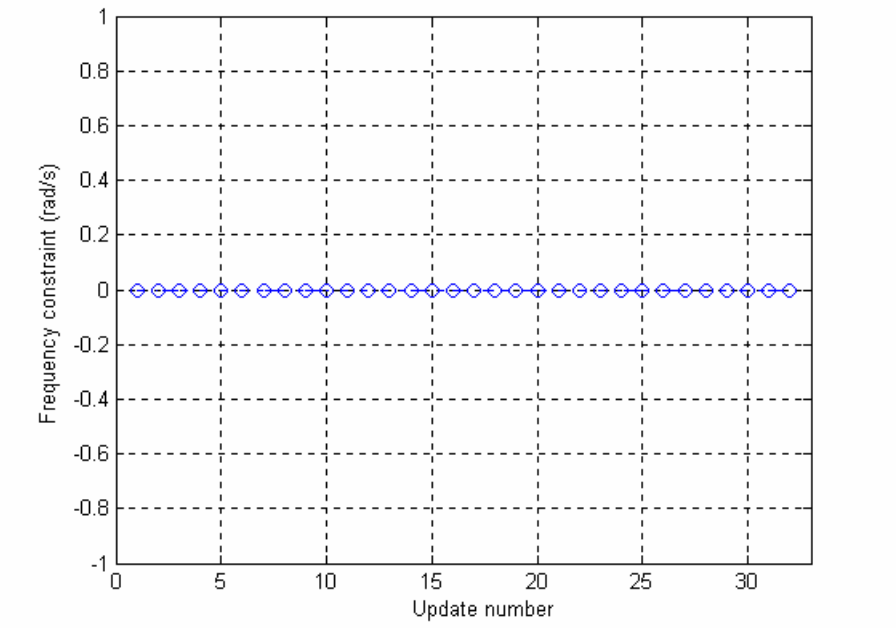

Figure 5-3 Iteration history of frequency constraint for single objective optimization, Case I

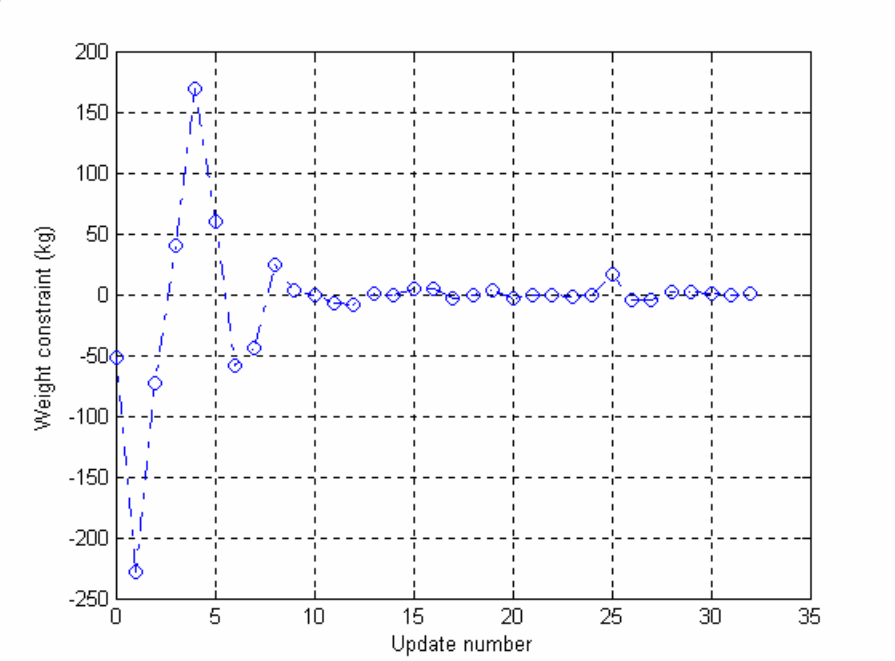

Figure 5-4 Iteration history of mass constraint for single objective optimization, Case I

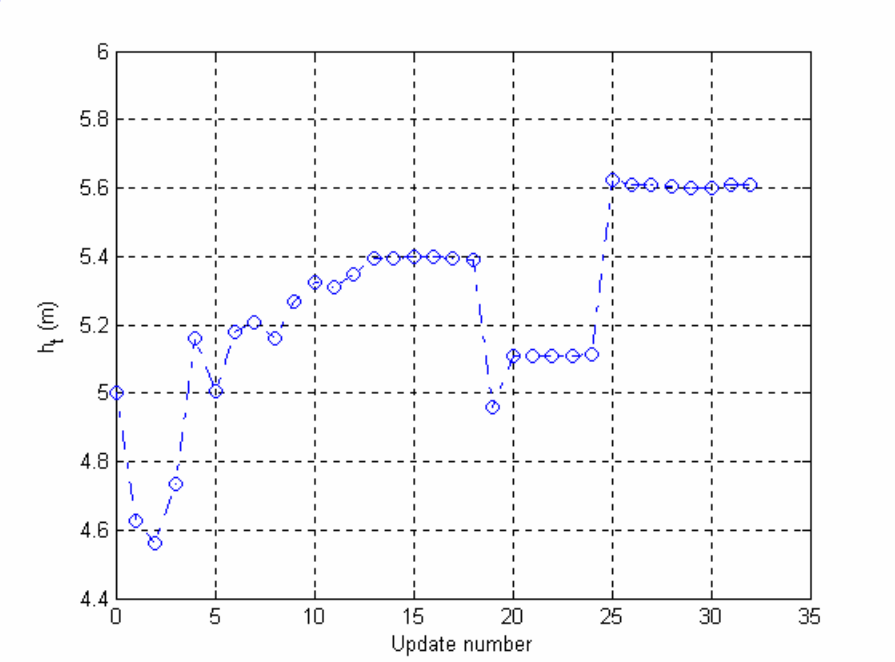

Figure 5-5 Iteration history of top shape parameter for single objective optimization, Case I

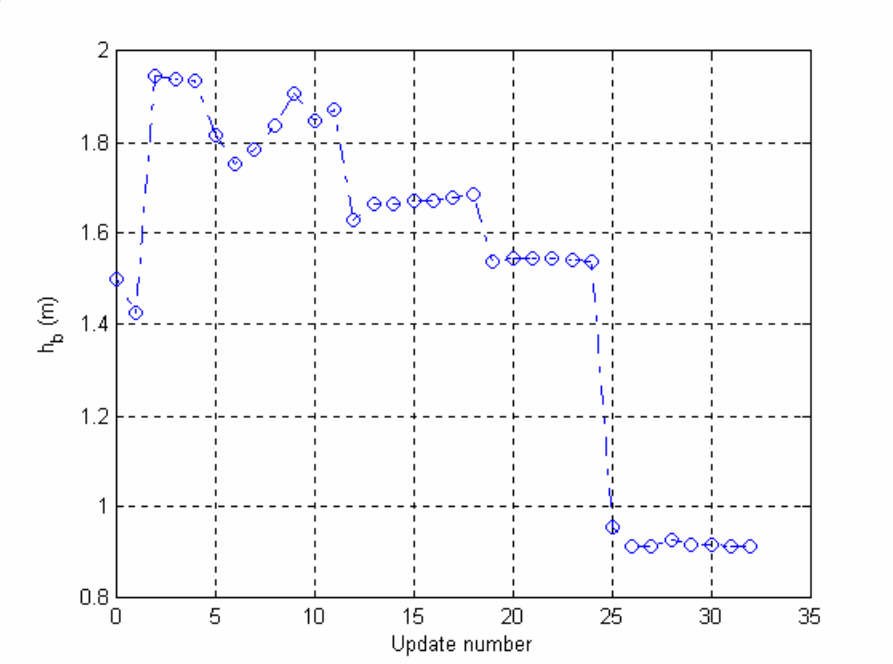

Figure 5-6 Iteration history of bottom shape parameter for single objective optimization, Case I

The Iteration history of performance index is given in Figure 5-7. It converges to the final solution smoothly. The relative accuracy of the optimization algorithm is 1,562. The plot of relative accuracy versus update number is given in Figure 5-8. Although, the relative accuracy is not converged, its fluctuation decreases.

Finally, optimal solutions of cross sectional areas and actuator positions are summarized in Table 5-2.

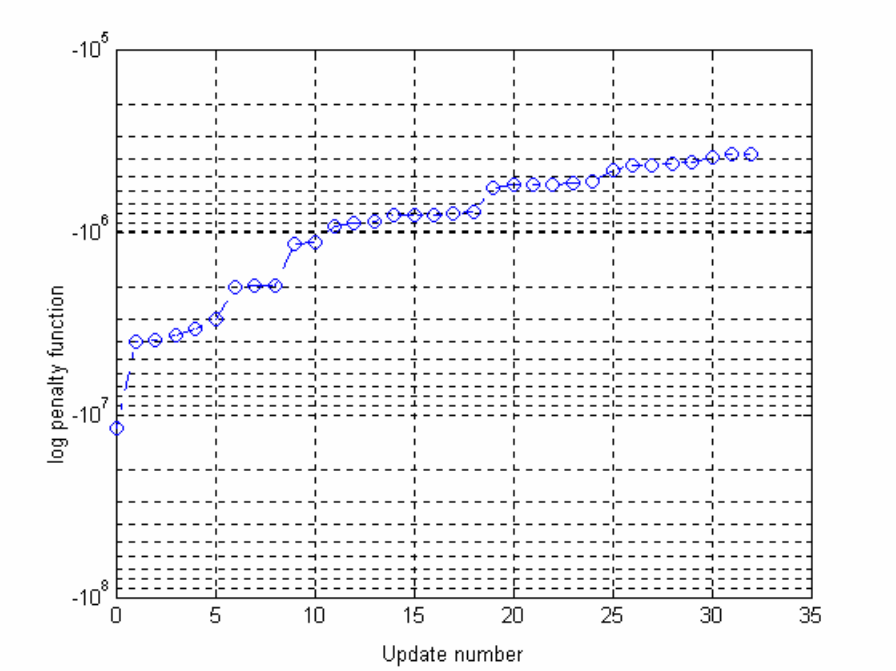

Figure 5-7 Iteration history of performance index for single objective optimization, Case I

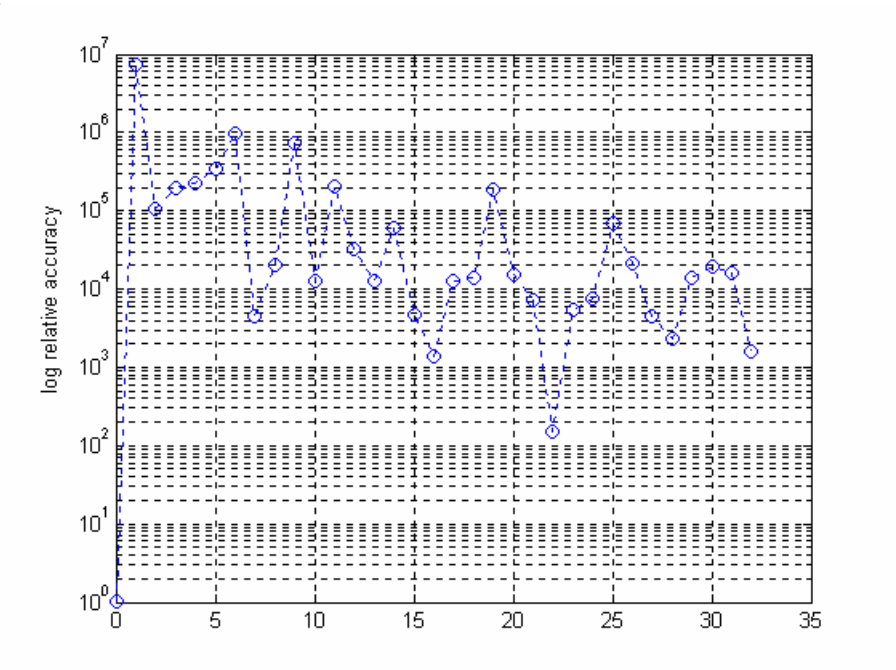

Figure 5-8 Iteration history of relative accuracy for single objective optimization, Case I

Table 5-2 Optimal structural design parameters for single objective optimization, Case I

Optimal cross sectional areas of the bar elements (cm^2)												
a_1	a_2	a_3	a_4	a_5	a_6	a_7	a_8	a_9	a_{10}	a_{11}	a_{12}	a_{25}
a_{13}	a_{14}	a_{15}	a_{16}	a_{17}	a_{18}	a_{19}	a_{20}	a_{21}	a_{22}	a_{23}	a_{24}	
36	83	33	2	57	6	51	95	85	54	72	47	23

*actuator placed bar elements are highlighted.

Optimal closed loop gains and optimal closed loop poles are calculated by using same precision with the optimization algorithm. While suboptimal closed loop gains and optimal closed loop poles are calculated firstly by using values given in Table 5-2 and than by removing 4^{th}, 6^{th}, 16^{th} and 18^{th} bar elements. Optimal closed loop poles of optimal and suboptimal (truncated) systems are given in Table 5-3. Closed loop poles of optimal system lie in the left-side of the complex plane which means stable system. For suboptimal systems optimal closed loop gain matrix is calculated again. Therefore, closed loop poles of suboptimal system also lie in the left-side of the complex plane and system is stable. Optimal closed loop gain matrix is given in Eq.(5-7) and suboptimal closed loop gain matrices for bar elements removed and unremoved cases are given in Eq. (5-9) and Eq.(5-8), respectively.

Table 5-3 Optimal and Suboptimal closed loop poles for second case of multi-objective optimization

Closed loop poles	Optimal system	Suboptimal system	Suboptimal system (Bar elements are removed)
p_1	-68.87	-68.57	-108.46
p_2	-66.69	-66.39	-105.16
p_3	-115.75	-115.86	-57.66
p_4	-112.79	-112.89	-55.33
p_5	-9.72	-9.50	-1.12+0.44i
p_6	-10.42	-10.21	-1.12-0.44i
p_7	-17.24	-16.82	-4.63
p_8	-15.95	-15.52	-3.84

$$G^* = \begin{bmatrix} 2,787 & -27,203 & 211,620 & -728,720 & 278 & -1,642 & -3,126 & -6,384 \\ 22,779 & 27,049 & -265,170 & 327,010 & 2,267 & 1,633 & 3,917 & 2,865 \\ 2,788 & 27,203 & 211,620 & 728,720 & 278 & 1,642 & -3,126 & 6,384 \\ 22,779 & -27,049 & -265,170 & -327,010 & 2,267 & -1,633 & 3,917 & -2,865 \end{bmatrix} \quad (5\text{-}7)$$

$$G_s^* = \begin{bmatrix} 2,489 & -25,373 & 210,270 & -722,270 & 253 & -1,572 & 3,120 & -6,322 \\ 21,757 & 25,578 & -262,150 & 327,040 & 2,213 & 1,585 & -3,889 & 2,862 \\ 2,489 & 25,373 & 210,270 & 722,270 & 253 & 1,572 & 3,120 & 6,322 \\ 21,757 & -25,578 & -262,150 & -327,040 & 2,213 & -1,585 & -3,889 & -2,862 \end{bmatrix} \quad (5\text{-}8)$$

$$G_{sr}^* = \begin{bmatrix} 36 & 111 & 140,300 & 430,560 & 56 & 26 & 2,487 & 4,036 \\ -62 & -3,338 & -156,760 & 247,480 & -95 & -796 & -2,779 & -2,320 \\ -36 & 111 & 140,300 & -430,560 & -56 & 26 & 2,487 & -4,036 \\ 62 & -3,338 & -156,760 & 247,480 & 95 & -796 & -2,779 & 2,320 \end{bmatrix} \quad (5\text{-}9)$$

Lowest four structural natural frequencies of optimal and suboptimal systems are given in Table 5-4. Lowest structural natural frequency of the system is greater than zero for optimal and first suboptimal system, which means that system has not any rigid body modes. While suboptimal system nearly losts its structural integrity when bar elements are removed from the system. Furthermore, this system violates frequency constraint. Therefore, these elements can not removed from the structure.

Table 5-4 Optimal and Suboptimal structural natural frequencies of structure for single objective optimization, Case I

Structural natural frequencies (rad/s)	Optimal system	Suboptimal system	Suboptimal system (Bar elements are removed)
ω_1	10.07	9.87	0.13
ω_2	16.59	16.16	4.21
ω_3	67.77	67.42	56.48
ω_4	114.26	114.37	106.8

5.3.2 Multiobjective Optimization Using QPI, Robustness and Controllability Measures

This case is solved in two different manners. In the first case, problem is solved similar to Liu and Begg's [17] work in which truss members parallel to actuators are not removed. While in the second case, cross sectional areas of the bar elements are set to very small values which means that they are removed from the structure without transforming the system to a mechanism.

5.3.2.1 Optimization Results without Removing Actuator Placed Bar Elements

HSSA algorithm updates the design 23 times for 20,000 function evaluations and then converges to an optimum solution. Quadratic performance index is minimized 99% of the initial system's performance index. Robustness of the system is improved 50% and controllability of the system is improved 200%. Both controllability and QPI iteration history is converged, but robustness is not converged. History plots of objective functions are given in Figure 5-9 through Figure 5-11.

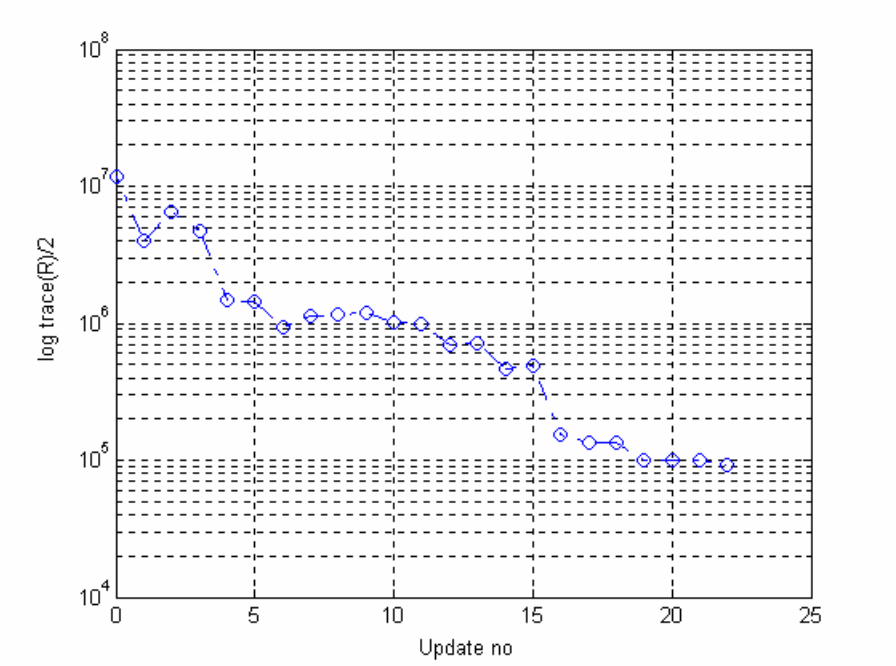

Figure 5-9 Iteration history of QPI for multiobjective optimization, Case II

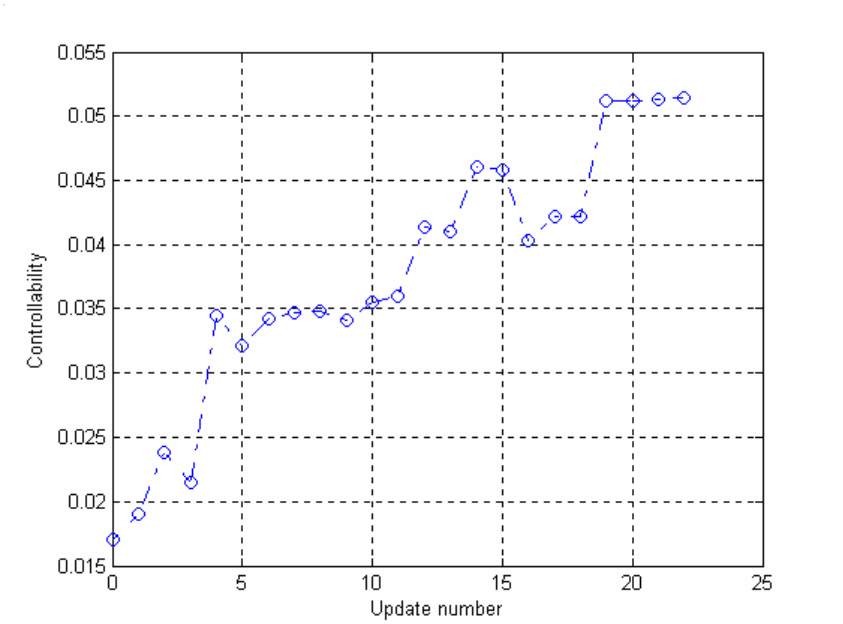

Figure 5-10 Iteration history of controllability of system for multiobjective optimization, Case II

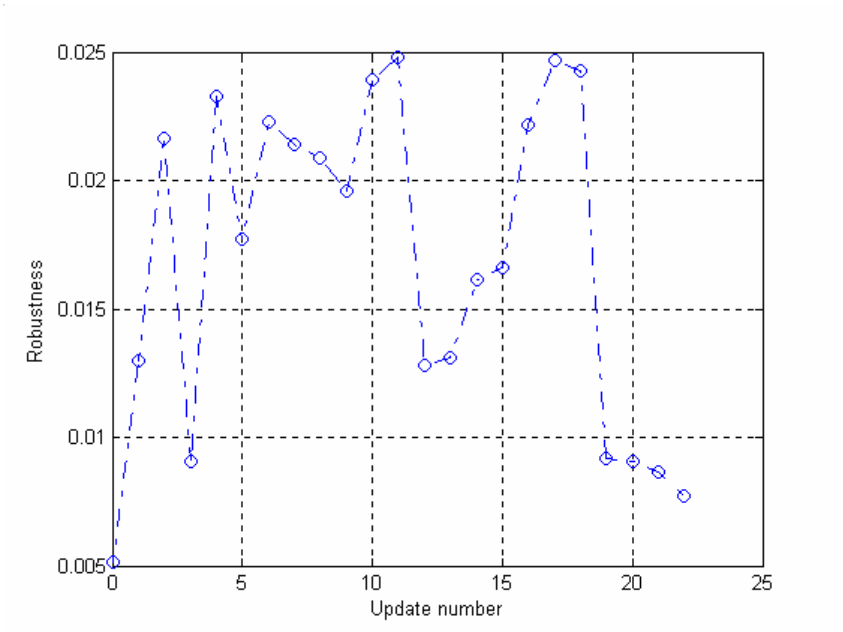

Figure 5-11 Iteration history of stability robustness of system for multiobjective optimization, Case II

Penalty weights of frequency and mass constraints are 1 and 10,000 respectively. Normalization constants are similar to the single objective case, since initial guesses are not changed. Both constraints are satisfied. Constraint convergence histories are shown in Figure 5-14 and Figure 5-15.

Iteration histories of performance index and relative accuracy are given in Figure 5-12 and Figure 5-13, respectively. Logarithmic scale is used for both performance index and relative accuracy. Although, the relative accuracy is not converged, its fluctuation decreases and performance index converges.

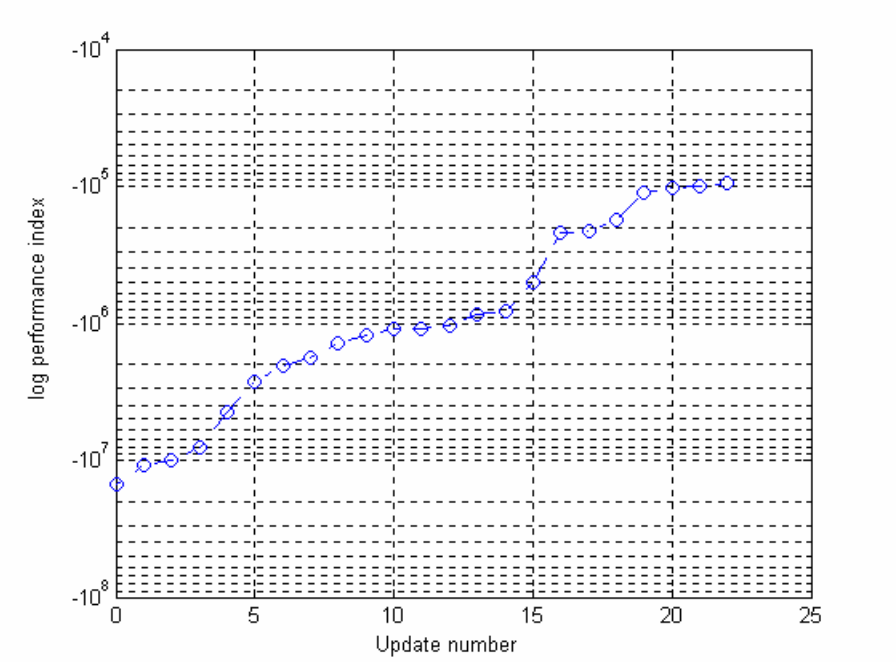

Figure 5-12 Iteration history of performance index for multiobjective optimization, Case II

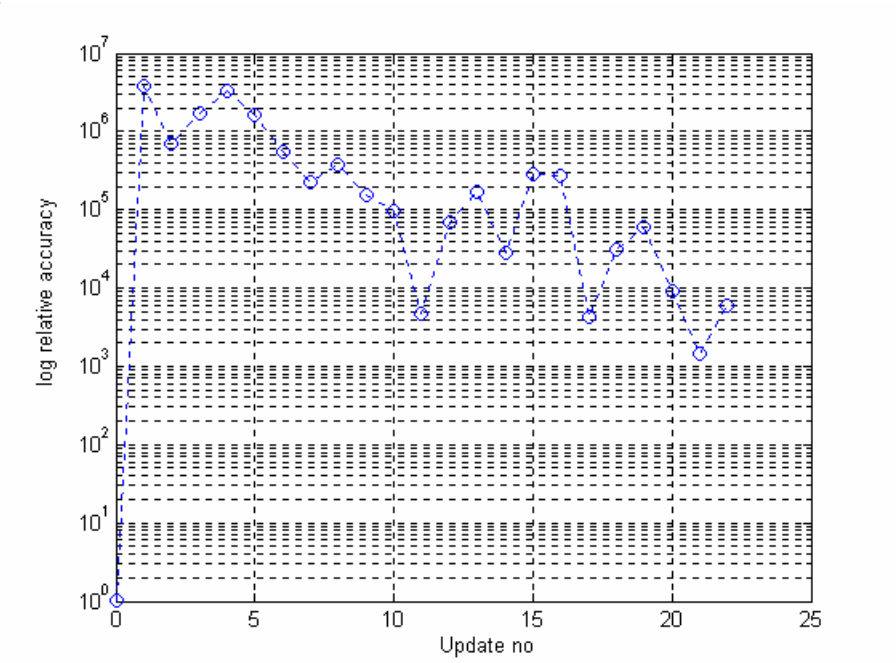

Figure 5-13 Iteration history of relative accuracy for multiobjective optimization, Case II

Design parameters are also converged for this case. The cross sectional areas of the 3rd and 11th bar elements attain again small values. Optimal actuator positions are parallel to the 3rd and the 4th bar elements. Again, in the solution, one of the actuator placed bar element is removed from the optimal system.

Optimal shape parameters h_t and h_b are found as 5.87 m and 0.58 m, respectively.

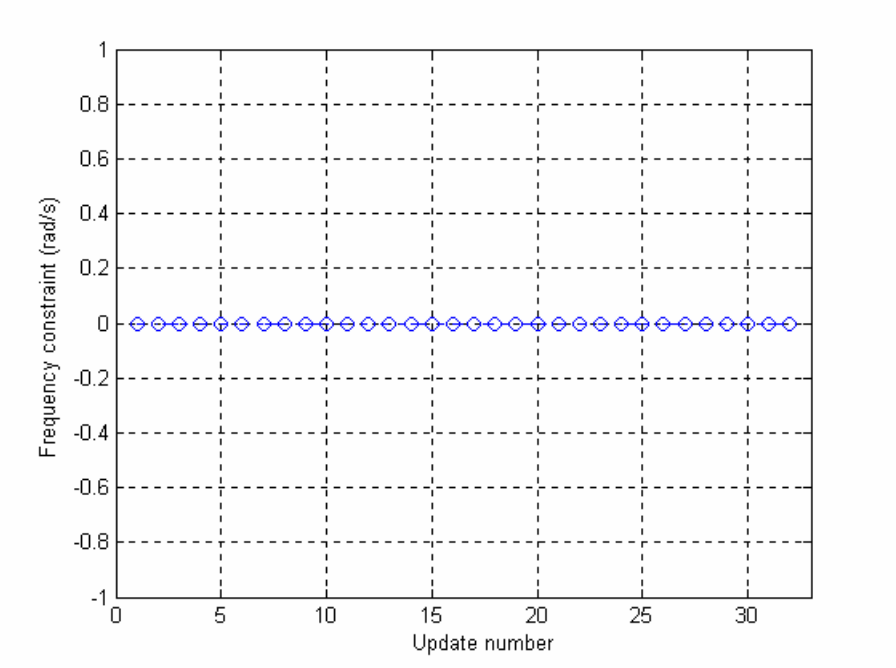

Figure 5-14 Iteration history of frequency constraint for multiobjective optimization, Case II

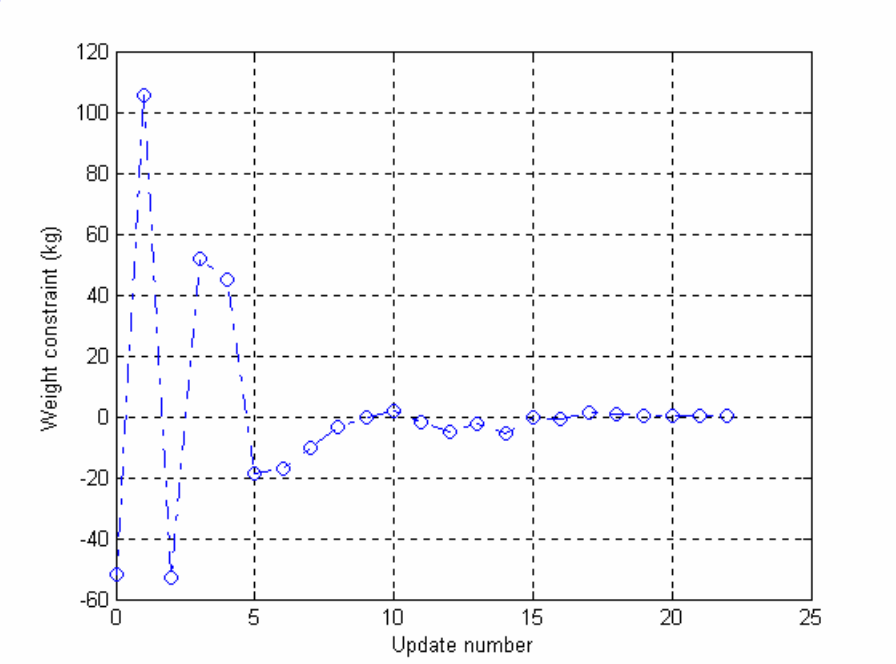

Figure 5-15 Iteration history of mass constraint for multiobjective optimization, Case II

Finally, optimal solutions of cross sectional areas and actuator positions are summarized in Table 5-5.

Table 5-5 Optimal structural design parameters for multi-objective optimization, Case II

Optimal cross sectional areas of the bar elements (cm^2)												
a_1	a_2	a_3	a_4	a_5	a_6	a_7	a_8	a_9	a_{10}	a_{11}	a_{12}	a_{25}
a_{13}	a_{14}	a_{15}	a_{16}	a_{17}	a_{18}	a_{19}	a_{20}	a_{21}	a_{22}	a_{23}	a_{24}	
7	61	0.3	16	37	62	99	79	76	89	0.05	97	75

*actuator placed bar elements are highlighted.

Optimal closed loop gains and optimal closed loop poles are calculated by using same precision with the optimization algorithm. While suboptimal closed loop gains and optimal closed loop poles are calculated firstly by using values given in Table 5-5 and than by removing 3rd, 4th, 15th and 16th bar elements. Optimal closed loop poles of

optimal and suboptimal (truncated) systems are given in Table 5-6. Optimal closed loop gain matrix is given in Eq.(5-7) and suboptimal closed loop gain matrices for bar elements removed and unremoved cases are given in Eq. (5-9) and Eq.(5-8), respectively.

Table 5-6 Optimal and Suboptimal closed loop poles for multi-objective optimization, Case II

Closed loop poles	Optimal system	Suboptimal system	Suboptimal system (Bar elements are removed)
p_1	-10.24	-10.24	-1.12
p_2	-12.25	-12.25	-2.08
p_3	-59.34	-59.33	-56.04
p_4	-55.27	-55.27	-52.12
p_5	-53.75	-53.75	-55.37
p_6	-56.13	-56.13	-52.97
p_7	-21.27	-21.27	-21.27
p_8	-20.76	-20.76	-20.76

$$G^* = \begin{bmatrix} -10{,}932 & -26{,}875 & -182{,}430 & -157{,}980 & -979 & -1{,}280 & -3{,}325 & -2{,}762 \\ -6{,}3567 & 121{,}810 & -1{,}235 & -49{,}107 & -570 & 5{,}803 & -23 & -858 \\ 10{,}932 & -26{,}875 & -182{,}430 & 157{,}980 & 979 & -1{,}280 & -3{,}325 & 2{,}762 \\ 6{,}357 & 121{,}810 & -1{,}235 & 49{,}107 & 570 & 5{,}803 & -23 & 858 \end{bmatrix} \quad (5\text{-}10)$$

$$G_s^* = \begin{bmatrix} -10{,}932 & -26{,}875 & -182{,}430 & -157{,}980 & -979 & -1{,}280 & -3{,}325 & -2{,}762 \\ -6{,}357 & 121{,}810 & -1{,}235 & -49{,}107 & -570 & 5{,}803 & -23 & -858 \\ 10{,}932 & -26{,}875 & -182{,}430 & 157{,}980 & 979 & -1{,}280 & -3{,}325 & 2762 \\ 6{,}357 & 121{,}810 & -1{,}235 & 49{,}107 & 570 & 5{,}803 & -23 & 858 \end{bmatrix} \quad (5\text{-}11)$$

$$G_{sr}^* = \begin{bmatrix} 66 & 26{,}516 & -176{,}700 & -108{,}730 & 90 & 1{,}263 & -3{,}267 & -2{,}015 \\ 31 & -121{,}680 & 705 & -24{,}420 & 42 & -5{,}796 & 13 & -453 \\ -66 & 26{,}516 & -176{,}700 & 108{,}730 & -90 & 1{,}263 & -3{,}267 & 2{,}015 \\ -31 & -121{,}680 & 705 & 24{,}420 & -42 & -5{,}796 & 13 & 453 \end{bmatrix} \quad (5\text{-}12)$$

Lowest four structural natural frequencies of optimal and suboptimal systems are given in Table 5-7. Lowest structural natural frequency of the system is greater than zero for optimal and first suboptimal system, which means that system has not any rigid body modes. While suboptimal system nearly losts its structural integrity when bar elements are removed from the system. Furthermore, this system violates frequency constraint. Therefore, these elements can not removed from the structure.

Table 5-7 Optimal and Suboptimal structural natural frequencies of structure for multi-objective optimization, Case II

Structural natural frequencies (rad/s)	Optimal system	Suboptimal system	Suboptimal system (Bar elements are removed)
ω_1	11.20	10.82	0.26
ω_2	21.01	21.01	21.02
ω_3	54.93	57.37	54.05
ω_4	57.26	55.37	54.15

5.3.2.2 Optimization Results by Removing Actuator Placed Bar Elements

HSSA algorithm updates the design 15 times for 10,000 number of iterations and converges to optimum solution. QPI is minimized 98.6% of the initial system's performance index. While the robustness of the system is improved 96.97%, the controllability of the system is improved 227%. Graphs of these objective functions are given in Figure 5-16 through Figure 5-18. although the objective functions controllability, and trace of Riccati matrix do not converge, performance index and relative accuracy are converged as shown Figure 5-19 and Figure 5-20, which are the convergence criteria of the optimization algorithm.

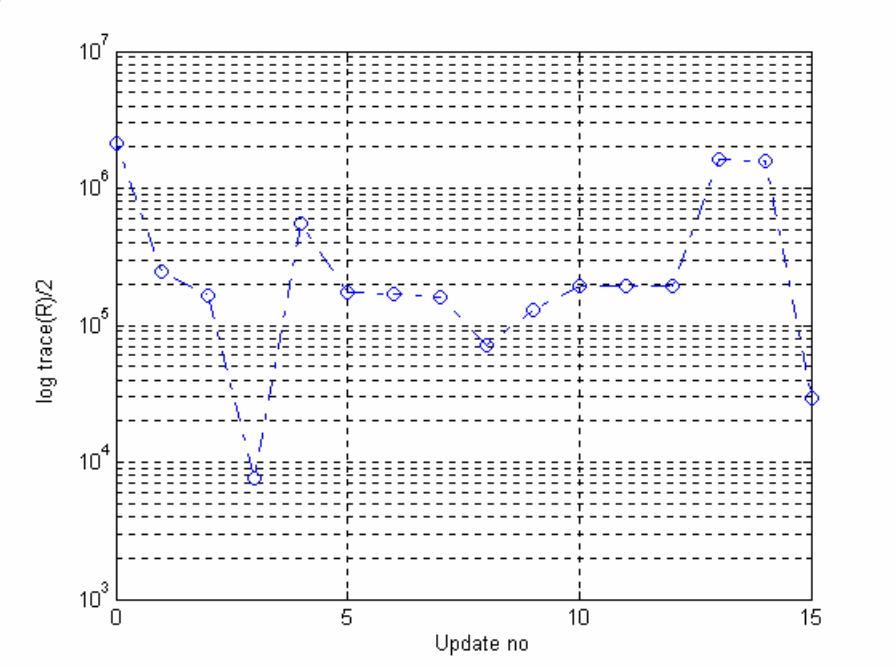

Figure 5-16 Iteration history of QPI for of multiobjective optimization, Case III

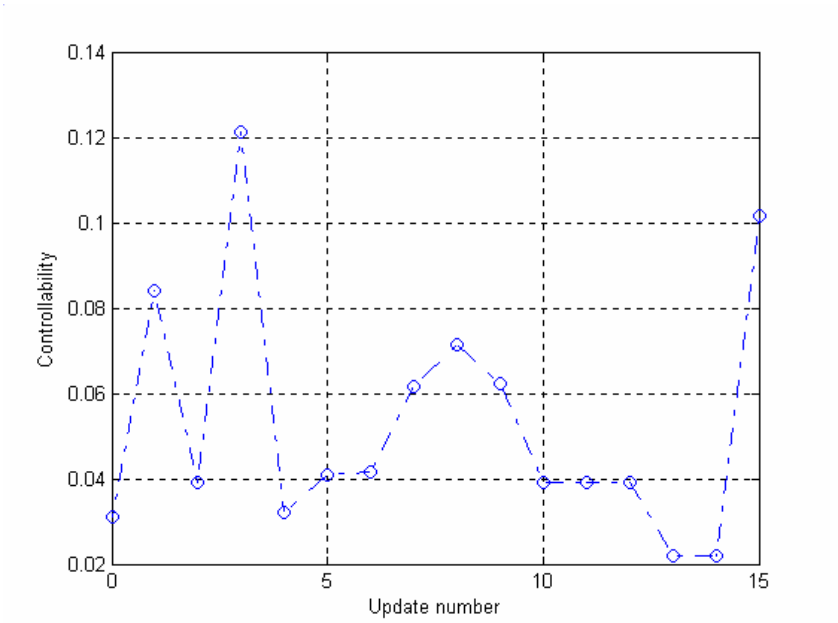

Figure 5-17 Iteration history of controllability for multiobjective optimization, Case III

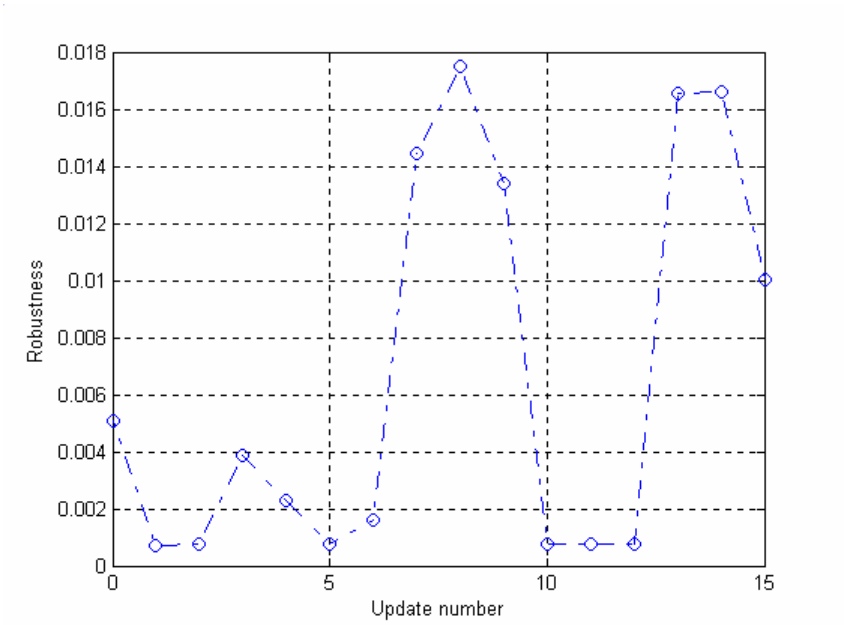

Figure 5-18 Iteration history of robustness for multiobjective optimization, Case II

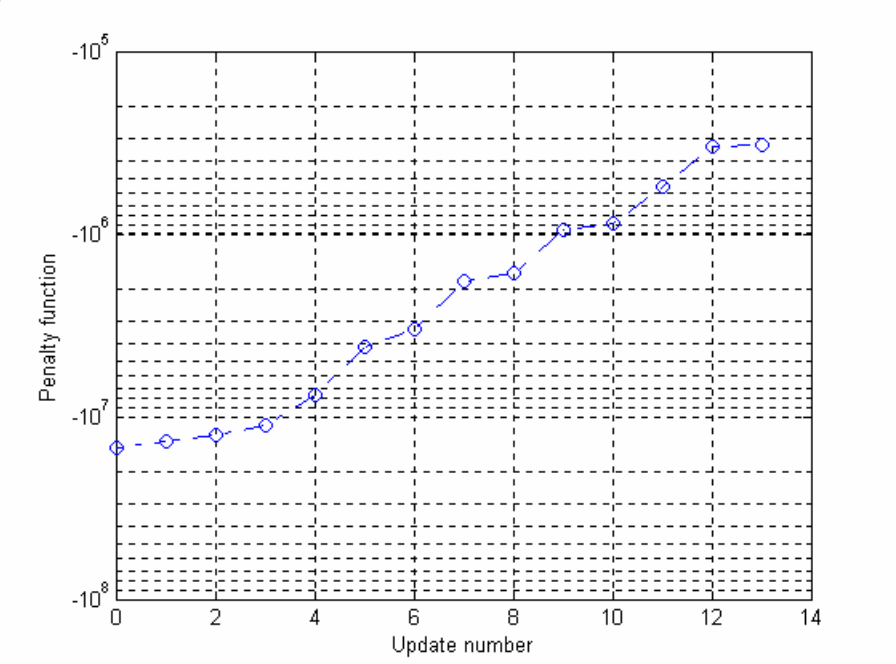

Figure 5-19 Iteration history of performance index for multiobjective optimization, Case III

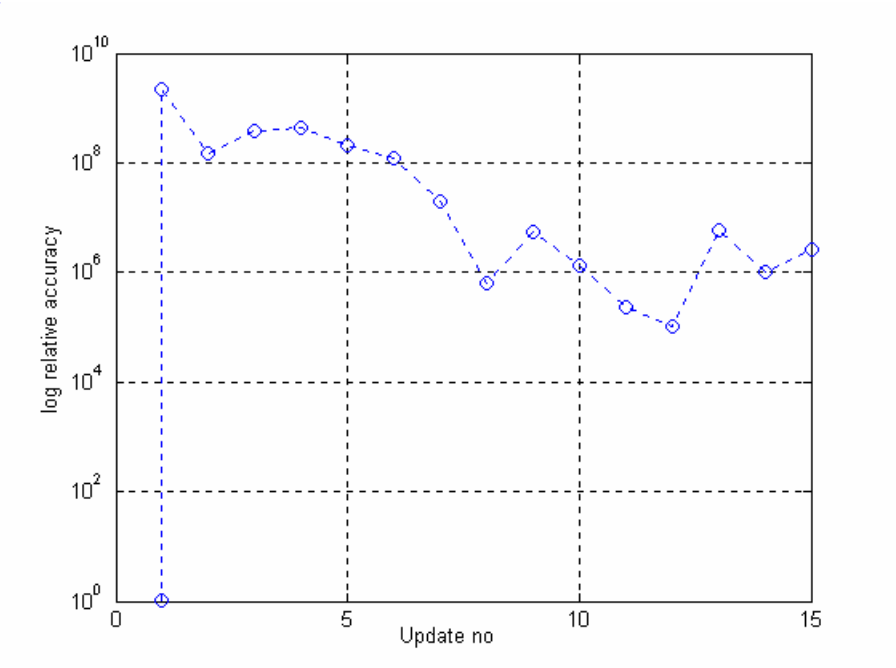

Figure 5-20 Iteration history of relative accuracy for multiobjective optimization, Case III

Penalty weights of frequency and mass constraints are 1 and 10,000, respectively. Normalization constants are similar to the others since initial guesses are not changed. Both mass and frequency constraints are satisfied and their iteration histories are shown in Figure 5-21 and Figure 5-22, respectively.

Design parameters are also converged to optimal solutions for this case. There is no actuator removed from the system except to automatically removed actuator placed bar elements. Optimal actuator positions are parallel to the 7^{th} and the 11^{th} bar elements.

Optimal shape parameters h_t and h_b are found as 4.68 m and 1.74 m, respectively.

Finally, optimal solutions of the cross sectional areas of the bar elements and actuator positions are summarized in Table 5-8.

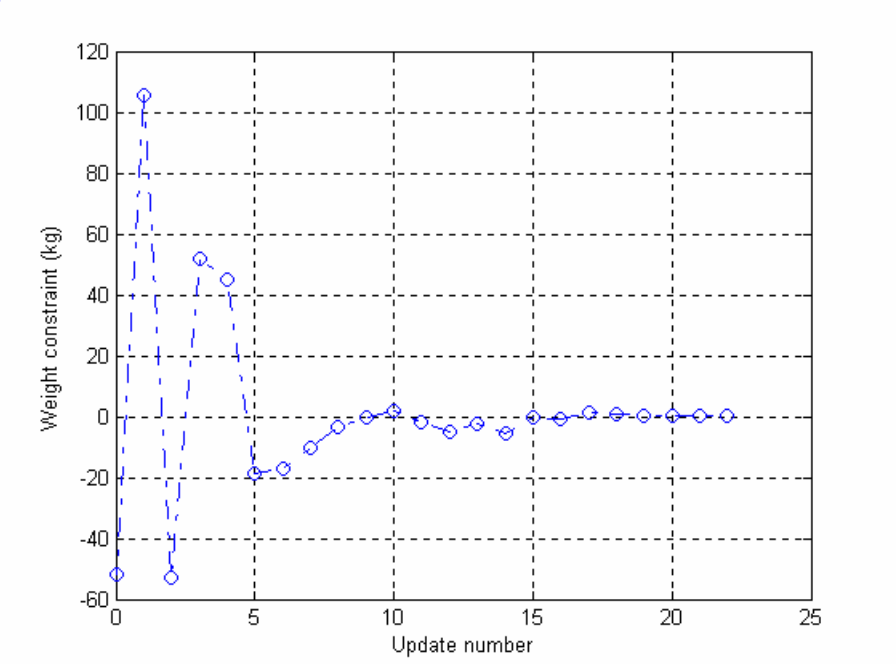

Figure 5-21 Iteration history of mass constraint for multiobjective optimization, Case III

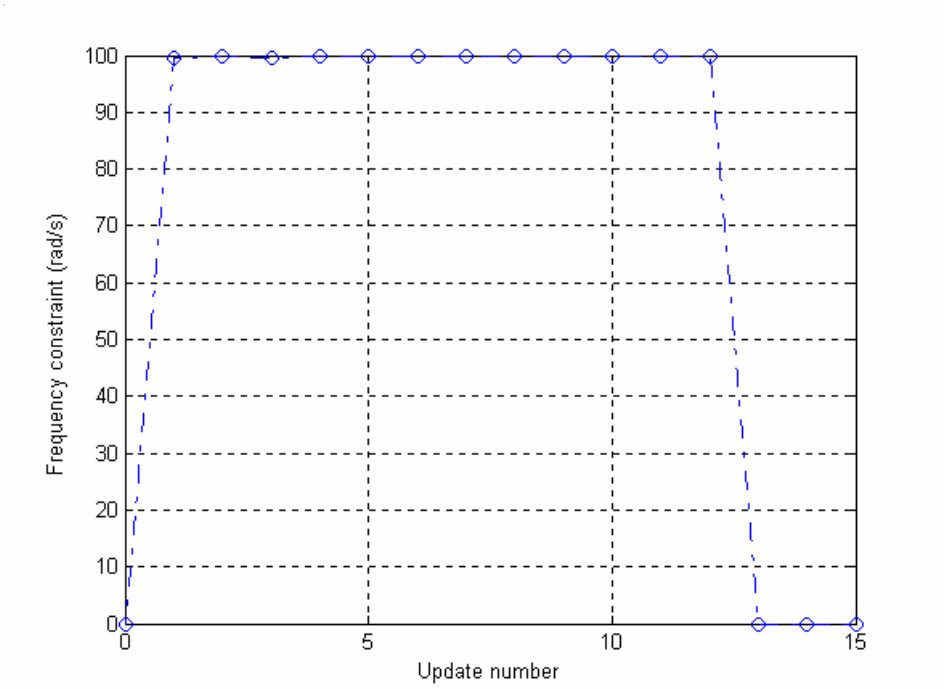

Figure 5-22 Iteration history of frequency constraint for multiobjective optimization, Case III

Table 5-8 Optimal structural design parameters for multi-objective optimization, Case III

Optimal cross sectional areas of the bar elements (cm^2)												
a_1	a_2	a_3	a_4	a_5	a_6	a_7	a_8	a_9	a_{10}	a_{11}	a_{12}	a_{25}
a_{13}	a_{14}	a_{15}	a_{16}	a_{17}	a_{18}	a_{19}	a_{20}	a_{21}	a_{22}	a_{23}	a_{24}	
48	63	75	36	6	16	0	47	96	89	0	93	76

* actuator placed bar elements are highlighted.

Optimal closed loop gains and optimal closed loop poles are calculated for exactly same optimal design parameters and truncated design parameters. Optimal closed loop poles of optimal and suboptimal (truncated) system are given in Table 5-9. Results are close to each other and system does not become unstable due to truncation. Optimal closed loop gain matrix is given in Eq.(5-14) and suboptimal closed loop gain matrix is given in Eq.(5-13).

Table 5-9 Optimal and Suboptimal closed loop poles for multi-objective optimization, Case III

Closed loop poles	Optimal system	Suboptimal system
p_1	-46.52	-47.46
p_2	-42.37	-43.28
p_3	-79.51	-80.27
p_4	-70.69	-71.51
p_5	-12.65	-12.50
p_6	-14.31	-14.14
p_7	-16.30	-16.65
p_8	-13.87	-14.20

$$G^* = \begin{bmatrix} -16,289 & -19,406 & 96,136 & 134,880 & -1,212 & -1,293 & 2,169 & 1,802 \\ -19,159 & 2,956 & 52,703 & -11,261 & -1,427 & 197 & 1,188 & -150 \\ -16,289 & 19,406 & 96,136 & -134,880 & -1,212 & 1294 & 2,169 & -1802 \\ -19,159 & -2,956 & 52,703 & 11,261 & -1,426 & -197 & 1,188 & 150 \end{bmatrix} \quad (5\text{-}13)$$

$$G_s^* = \begin{bmatrix} 15{,}891 & -20{,}259 & -98{,}250 & 139{,}320 & 1{,}197 & -1{,}321 & -2{,}171 & 1{,}842 \\ 18{,}598 & 3{,}155 & -53{,}156 & -1{,}1923 & 1{,}402 & 206 & -1{,}174 & -158 \\ 15{,}891 & 20{,}259 & -98{,}250 & -139{,}320 & 1{,}197 & 1{,}321 & -2{,}171 & -1{,}842 \\ 18{,}598 & -3{,}156 & -53{,}156 & 11{,}923 & 1{,}402 & -206 & -1{,}174 & 158 \end{bmatrix} \quad (5\text{-}14)$$

Lowest four structural natural frequencies of optimal and suboptimal system are given in Table 5-10. Lowest structural natural frequency of the system is greater than zero which means that system has not any rigid body modes. Therefore, structural integrity is preserved while removing bar elements.

Table 5-10 Optimal and Suboptimal structural natural frequencies of structure for multi-objective optimization, Case III

Structural natural frequencies (rad/s)	Optimal system	Suboptimal system
ω_1	13.46	13.29
ω_2	15.04	15.38
ω_3	44.40	45.32
ω_4	74.98	75.76

5.4 DISCUSSION

In this case study, a parabolic shape truss structure is optimized by three different methods. In the first case, single objective, QPI, is used and the global optimum is found. The result requires removal of the all actuator placed truss elements from the system. In the second case, a multi-objective optimization is applied. Performance index is converged, and elements of the performance index are also converged, except robustness. Both mass and frequency constraints are satisfied exactly. In this case, the result requires removal of one of the actuator placed elements from the structure. Therefore, as a third case, this problem is solved by initially removing actuator placed bar elements from the system. Improvement percentages of objective functions are calculated by using initial performance criterion and optimal one. If initial

performance indexes are taken equal, in the third case improvement of the objective functions becomes better.

The second case is the one solved by Liu and Begg. They used five different optimization algorithms and compared the results. One of them is SA, which improves QPI 95.3%, robustness 1141% and controllability 26.8%. However, it violates mass constraint -2.4% which is equal to 72 kg. All other algorithms are violating mass constraint while two of them also violate frequency constraint. Maximum improvement on performance index is 97.3%, robustness is 2521.9% and controllability is 68.4%.

It seems that the objective function is optimized similarly in our case, the robustness is improved better, but controllability becomes worse. However, this conclusion cannot be done with the available results given in this paper [17]. The initial performance index of case II and Liu and Begg's are not equal. The reason for the difference may be explained by the usage of elements of closed loop gain matrix as design parameters and reduced Riccati equation as constraint. Therefore, their result cannot be declared as the global optimum closed loop gain matrix. In fact, there is a unique solution for Ricatti equation, which minimizes QPI optimally. In other words, they could optimize all design parameters by using single level optimization procedure. As a result, the difference between the optimized solution and the initial performance index becomes large, which seems like better improvement is achieved by them.

In the solutions of three case studies, if optimal cross sectional area of a bar element is attained physically meaningless value, this element may be removed from the structure. But, if an actuator is not placed parallel to this element, system may become unstable or lost its structural integrity. In such a case, system should have rigid body modes or closed loop poles lie in the left-half of the complex plane. When OPI is minimized for positive-definete $[Q]$ matrix, closed loop system always becomes stable. For three case studies, system becomes stable after optimal and suboptimal systems as expected. But, structural natural frequencies become near to zero when bar elements are removed from the system for case I and II. This means

that structure is very sensitive to these design parameters. While these cross sectional areas seems negligible in engineering sense, it affects structural performance drastically. Therefore, for this type optimization problems sensitivity analysis should carried out before removing smaller elements from the structure.

CHAPTER 6

CONCLUSION

6.1 SUMMARY AND DISCUSSION

In this thesis, a simultaneous structure and controller optimization is carried out. Two case studies are considered to see interaction between the structural and the controller design parameters. First case study is a simple two bar truss problem, which can be also solved analytically. Second case study is a larger one, in which different performance indices and solution methodologies are used.

In the structural analysis, finite element modeling of the truss structures is carried out by using bar elements. Actuators and external masses are also added to the finite element model. In the model, actuators are defined only by their masses, and it is assumed that they only exert axial force. External masses are lumped into the corresponding nodes.

A mathematical modeling is carried out by using displacement based finite element modeling procedure. Firstly, elemental stiffness, mass, and force matrices are calculated and then structural ones are assembled from these matrices.

From the equation of motion, a modal state transformation is performed to decouple differential equations. By using modal model, large-scale problems can easily be reduced to smaller models, based on system dominant eigenvalues. For the first case study, which is a 2 dof model, modal model reduction does not performed. For the second case study, system model is reduced from twenty dof to four dof. This simplifies calculation of the performance index. However, this procedure can lead to

errors due to the reduction of high order natural frequencies, whose value is acceptable.

In the first case study, the number of actuators is selected as a design parameter. The two-bar truss structure is a two dof system. Hence, it may be uncontrollable by using single actuator. If the structural natural frequencies become identical, single actuator cannot control the structure. However, when the system is examined in this manner, it can be seen that the geometry does not allow identical natural frequencies for any cross sectional area combination. In fact, in such a case controller forces will become very large, which means that the performance index becomes very large. Consequently, optimization algorithm eliminates these type of solutions.

The equality of the system dof with the number of actuators guarantees system controllability for any value of design parameters, which is applied for the second case study. Since modal reduction is also applied for this case, the number of actuators is taken as four which is defined as twenty at the beginning. Design parameter linking is also considered for this problem. Cross sectional areas and actuator elements are linked about the symmetry axis. Modal reduction is applied by using lowest four eigenvalues of the system. As a result, the controllable system is optimized in a shorter time with a reasonable accuracy.

In both case studies, a sensor model is not used and it is assumed that all states can be measured exactly. In fact, this is not a realistic case, but the problem renders complexity including regulator design.

The definition of the optimization includes controller objective functions and two structural constraints. The controller objective function is based on LQR theory, which aims minimization of the system energy and controller forces. For the second case study, measure of controllability and stability robustness are also added to the performance index as an objective function. Maximization of these performance indices guarantees system performance against to the uncertainities of the system model. The lowest structural natural frequency and the mass of the truss structure are used as structural constraints. Mass constraint is used frequently in structural

analysis. In fact, it is usually selected as an objective function of the structural optimization problems. Because, it is directly related to the cost or the functionality of the structure; as in the case of satellites. A frequency constraint affects dynamic characteristics of the system. Cross sectional areas of bar elements, the number and the positions of the actuators, and closed loop gain matrix are used as the design parameters.

A penalty weight is used to emphasize order of the required fullfilment of the optimization parameters with respect to conflicting design requirements. However, in optimization, physics of the problem is lost when performance index is calculated. Therefore, next to penalizing weight, optimization parameters should be multiplied by a normalization factor to get them to the same order of magnitude. This factor is calculated before the iteration loop of the optimization by giving small perturbation to the initial design family and calculating elements of performance index for both cases, namely initial and perturbated ones. Then, the ratio of the initial and perturbated design optimization parameters is used as the normalization factor.

Two-optimization programs are used in the solution of problems. HSSA algorithm is used for guessing new design families randomly by using Metropolis criteria. This program can solve both linear and nonlinear optimization problems in discrete or continuous design space. However, it has drawbacks in satisfying inequality constraints, since it generates design families randomly. This increases iteration number and computation time. HSSA algorithm ends up with global optimum, if the relative accuracy of the system is converged to a value, which is verified theoretically. Second optimization algorithm includes the solution of reduced matrix Riccati equation by MATLAB® lqr function. According to the LQR theory, by solving reduced matrix Riccati equation QPI is globally optimized for an arbitrary initial condition. System is optimized in higher level again by averaging out all initial conditions by optimizing trace of the Riccati matrix. In summary, HSSA algorithm guesses the cross sectional areas of the bar elements, the positions, and the number of actuators. Then, lqr function finds global optimum closed loop gain matrix for this candidate design family. If HSSA algorithm converges, then all design parameters are certainly said to be global optimum.

Firstly, a two bar truss problem is solved analytically to verify the solution method and the mathematical modeling and optimization codes. Same results are attained from the graphical solution and the numerical solution. The optimization problem includes a nonlinear frequency constraint, a nonlinear objective function and a linear mass constraint. Both constraints are applied as equality constraints. Therefore, the violation of constraints can take positive or negative values. Since both cases should be penalized, absolute value of the vialotion is used in the performance index. If the constraint and design parameters for each actuator position are examined, a set of equations for two unknowns are obtained. For a single actuator case one solution can be found for this set of equations, while there is no unique solution for the two actuator case.

Parametric study is carried out to see the sensitivity of the optimization code to its inputs. Optimization inputs are bounds and initial guesses of design parameters, maximum number of iterations, relative accuracy, and penalty weights of constraints. Bounds and maximum number of iterations are proportional to each other. The iteration number is increased by increasing bounds of the design parameters. The initial guess does not affect the system performance. This parameter is used only for the search inside the bounds. The first case study is very proper to show the effect of penalty weights to the results of the optimization.

The two-bar truss problem was solved by Liu and Begg [17] to compare five different optimization algorithms. They did not optimize neither number nor positions of actuators in their work. One actuator is placed on one of the bar elements. They found the same cross sectional areas by using different algoritms, but they did not give resulting optimum values of the closed loop gain matrix in their paper. They found optimum objective function as 5,874. However, corresponding value found in this study is 3875. Since they used random search methods for the solution of Lyapunov equation, they could not find global optimum gain values and objective function.

In the second case study, a twenty-bar and four-actuator element system is optimized. This problem is solved for three different cases. In the first case, the objective function is QPI and constraints are the frequency and the mass constraint.

The frequency constraint is applied as an inequality constraint while mass constraint is applied as an equality constraint. In the second and third case studies, this problem is solved for three objective functions, which are QPI, measure of stability robustness and controllability. The mass and frequency constraints remained same as the first case study. Since from the results of the first two cases, it is seen that algorithm forces to removal of the bar elements, which are parallel to the actuators, in the third case study, optimization problem is solved by removing actuator parallel bar elements automatically. As seen from the results, removing bar elements parallel to the actuators give smaller performance index.

In case I and II same bar elements are attained small values. In engineering sense, these elements should removed from the structure. But, when these elements removed from the stsructure and controller is optimized for this system. As expexted system becomes stable. However, structural natural frequencies become very small and frequency constraint is violated for this case. This sitution is due to sensitivity of the structure to these design parameters. In the case II stability robustness is maximized. Therefore, this system become more robust to variation in the design parameters. Only first natural frequency is affected from the removal of the actuators.

6.2 CONCLUSION

This basic structural/controller model is studied properly in the optimization of coupled systems. Although, the performance index is quite complicated, the optimization algorithm finds the optimal solution in a small number of iteration for heurastic type optimization. Selection of penalty weights drastically affects result of optimization problems. Constraints should multiplied by a normalization constant to decide penalty weights according to design requirements only. Program always terminated from maximum number iterations. Relative accuracy criterion should improved.

Two-bar truss problem and parabolic shape multi-bar truss problem are considered. For the first case both constraints are satisfied when single actuator is used. While for the two actuator case it is satisfied with 0.6% error, which is meaningless according to engineering intuition. If penalty weights of constraints are decreased, improvement of

the objective function becomes more important. Since objective function is smaller for two actuator case than single actuator case, program finds two actuator case as a solution of the optimization problem. Liu and Begg [17] solved this problem for one actuator case. The quadratic performance index of Liu and Begg is 5,874, however in this study it is found as 3875.

Parabolic shape multi-bar truss problem is optimized for three different cases. In the first case, QPI is optimized globally. Actuator placed bar elements are removed from the structure. In the second case study, multiobjective optimization is carried out. This case is also solved by Liu and Begg [17]. If the results are compared, it is seen that they could not satisfy mass constraint for all algorithms. Only robustness is maximized and a better result are obtained than the one obtained in this work. It seems objective function is optimized same order in our case, robustness is improved better, but controllability becomes worse. They used elements of closed loop gain matrix as design parameters and reduced Riccati equation as constraint. So Liu and Begg's closed loop gain values cannot be global optimum and they may optimize all design parameters by using single level optimization procedure. As a result, the difference between the optimized solution and the initial performance index becomes large, which seems like better improvement is achieved. In the third case, actuator placed bar elements are removed from the structure automaticaly, in which optimization ends up with smaller performance index.

Sensitivity analysis should carried out in the structure/controller simultaneous design to decide removal of the small sized bar elements. Also, closed loop gain matrix should calculated again after fixing size of structural design parameters.

6.3 FUTURE WORK

Simultaneous structure and controller optimization is a very wide subject, which becomes highly popular in the last century. This thesis subject can be improved from many different directions from this basic model.

FEM can be improved by adding other element types; i.e., beam, shell, solid, etc. Actuator and sensor dynamics can be considered. From the controller point of view, regulator design may be included.

Optimization algorithms used in this work are proper for the solution of these type problems. However, different optimization parameters may be used in the design. Different objective functions and constraints can be added. Finally, laboratory tests should be carried out to verify results of the optimization.

REFERENCES

[1] Utku, S., Incorporating Intelligence into Engineering Products: Adaptive Structures, 1st Ed., 1998 Fulbright Lectures.

[2] Dunn, H. J., “Experimental Results of Active Control on a Large Structure to Suppress Vibration”, Journal of Guidance, Control, and Dynamics, Vol. 15, No. 6, 1992, pp. 1334-1341.

[3] Crawley, E. F., ”Intelligent Structures for Aerospace: A technology Overview and Assessment”, AIAA Journal, Vol. 32, No.8, 1994, pp.1689-1699.

[4] Burdisso, R. A. and Haftka, R. T., “Optimal Location of Actuators for Correcting Distortions in Large Truss Structures”, AIAA Journal, Vol. 27, No. 10, 1989, pp.1406-1411.

[5] Onada, J., Sano, T., and Kamiyana, K., “Active, Passive, and Semiactive Vibration Suppression by Stiffness Variation”, AIAA Journal, Vol. 30, No. 12, 1992, pp. 2922-2929.

[6] Haftka, R., Martinovic, Z., and Hallauer, W., “Enhanced Vibration Controllability by Minor Structural Modifications,” AIAA Journal, Vol. 23, No. 8, pp. 1260-1266.

[7] Liu, X. and Begg, D. W., “On Simultaneous Optimization of Smart Structures-Part I: Theory”, Computer Methods in Applied Mechanics and Engineering, 184, 2000, pp. 15-24.

[8] Gilbert, M. G. and Schmidt, D. K., “Integrated Structure/Control Law design by Multilevel Optimization”, Journal of Guidance, Control, and Dynamics, Vol. 14, No. 5, 1991, pp. 1001-1007.

[9] Schulz, G. and Heimbold, G., “Dislocated Actuator/Sensor Positioning and Feedback Design for Flexible Structures”, Journal of Guidance, Control and Dynamics, Vol. 6, No.5, 1983, pp. 361-367.

[10] Onada, J. and Watanabe, N., “Vibration Suppression by Variable-Stiffness Members,” AIAA Journal, Vol. 29, No. 6, pp. 977-983.

[11] Darby, A. P. and Pellegrino, S., “Modeling and Control of a Flexible Structure Incorporating Inertial Slip-Stick Actuators”, Journal of Guidance, Control and Dynamics, Vol. 22, No. 1, 1999, pp. 36-42.

[12] Sun, C. T. and Wang, R. T., “Enhancement of Frequency and Damping in Large Space Structures with Extendible Members”, AIAA Journal, Vol. 29, No 12, 1991, pp. 2269-2271.

[13] Hyde, T. T and Anderson, E. H., “Actuator with Built-In Viscous Damping for Isolation and Structural Control”, AIAA Journal, Vol. 34, No. 1, 1996, pp.129-135.

[14] Matunaga, S., Yu, Y., and Ohkami, Y., “Vibration Suppression Using Acceleration Feedback Control with Multiple Proof- Mass Actuators”, AIAA Journal, Vol. 35, No. 5, 1997, pp. 856-862.

[15] Sepulveda, A. E., Jin, I. M., and Schmit, L. A., “Optimal Placement of Active Elements in Control Augmented Structural Synthesis”, AIAA Journal, Vol. 31, No. 10, 1993, pp. 1906-1915.

[16] Li, Y., Onada, J, and Minesugi, K., “Simultaneous Optimization of Piezoelectric Actuator Placement and Feedback for Vibration Suppression”, Acta Astronautica, Vol. 50, No. 6, pp. 335-341.

[17] Liu, X. and Begg, D. W., “On Simultaneous Optimization of Smart Structures-Part II: Algorithms and Examples”, Computer Methods in Applied Mechanics and Engineering, 184, 2000, pp. 25-37.

[18] Jin, I. M. and Schmit, L. A., “Control Design parameter Linking for Optimization of Structural/Control Systems, AIAA Journal, Vol. 30, No. 7, 1992, pp. 1892-1900.

[19] Jin, I. M. and Schmit, L. A., “Improved Control Design parameter Linking for Optimization of Structural/Control Systems”, AIAA Journal, Vol. 31, No. 11, 1993, pp. 2111-2120.

[20] Vanderplaats, G. N., Numerical Optimization Techniques for Engineering Design: With Applications, 1st Ed., 1984, McGraw Hill, Inc.

[21] Sedaghati, R., Suleman, A., and Tabarrok, B., “Structural Optimization with Frequency Constraints Using the Finite Element Force Method”, AIAA Journal, Vol. 40, No. 2, 2002, pp. 382-388.

[22] Canfield, R. A., “High-Quality Approximation of Eigenvalues in Structural Optimization,” AIAA Journal, Vol. 28, No. 6, 1990, pp. 1116-1122.

[23] Wang, B. P., “Closed Form Solution for Minimum Weight Design with a Frequency Constraint,” AIAA Journal, Vol. 29, No. 1, pp. 152-154.

[24] Czyz, J. A. and Lukasiewicz, S. A., “Multimodal Optimization of Structures with Frequency Constraints”, AIAA Journal, Vol. 33, No. 8, 1995, pp. 1496-1502.

[25] Kajiwara, I., Tsujiko, K., and Nagamatsu, A., “Approach for Simultaneous Optimization of a Structure and Control Systems”, AIAA Journal, Vol. 32, No.4, 1994, pp. 866-873.

[26] Canfield, R. A. and Meirovitch, L., “Integrated Structural Design and Vibration Suppression Using Independent Modal Space Control”, AIAA Journal, Vol. 32, No. 10, 1994, pp. 2053-2060.

[27] Sunar, M. and Rao, S. S.,”Optimal Selection of Weighting Matrices in Integrated Design of Structures/Controls”, AIAA Journal, Vol. 31, No. 4, 1993, pp. 714-720.

[28] Cheng, F. Y. and Li, D., “Multiobjective Optimization of Structures with and without Control”, Journal of Guidance, Control, and Dynamics, Vol. 19, No. 3, 1996, pp. 392-397.

[29] Slater, G. L. and McLaren, M. D., “Disturbance Model for Control/Structure Optimization with Full State Feedback”, Journal of Guidance, Control and Dynamics, Vol. 16, No. 3, 1993, pp. 523-533.

[30] Rao, S. S., Pan, T., and Venkayya, V. B., “Optimal Placement of Actuators in Actively Controlled Structures Using Genetic Algorithms”, AIAA Journal, Vol. 29, No.6, 1991, pp. 942-943.

[31] Fleming P. J., Purshouse R. C., “Evolutionary algorithms in control systems engineering: a survey”, Control Engineering Practice, Vol. 10, 2002, pp. 1223-1241.

[32] Bélisle C. J. P., Romeijn H. E., and Smith R.L., Hide-and-Seek: A Simulated Annealing Algorithm for Global Optimization, Department of Industrial and Operations Engineering, Technical Report 90-25, University of Michigan, Ann Arbor, 1990.

[33] Karslı, G., Simulated Annealing for the Generation of Pareto Fronts with Aerospace Applications, M.S. Thesis, Aeronautical Engineering Department, METU, Ankara, January 2004.

[34] Onada, J. and Hanawa, Y., “Actuator Placement Optimization by Genetic and Improved Simulated Annealing Algorithms”, AIAA Journal, Vol. 31, No.6, pp. 1167-1169.

[35] Fonseca, I. M. and Bainum, P. M., “Large Space Structure Integrated Structural and Control Optimization, Using Analytical Sensitivity Analysis,” Journal of Guidance, Control and Dynamics, Vol. 24, No. 5, 2001, pp. 978-982.

[36] Sobieszczanski-Sobieski, J., Bloebaum, C. L., and Hajela, P., “Sensitivity of Control-Augmented Structure Obtained by a System Decomposition Method”, AIAA Journal, Vol. 29, No. 2, 1991, pp. 264-270.

[37] Missoum, S. and Gürdal, Z., “Displacement- Based Optimization for Truss Structures Subjected to Static and Dynamic Constraints”, AIAA Journal, Vol. 40, No. 1, 2002, pp. 154-161.

[38] Onada, J. and Watanabe, N., “Integrated Direct Optimization of Structure/Regulator/Observer for Large Flexible Spacecraft”, AIAA Journal, Vol. 28, No. 9, 1990, pp. 1677-1685.

[39] Khot, N. S. and Heise, S. A., “Consideration of Plant Uncertainties in the Optimum Structural-Control Design”, AIAA Journal, Vol. 32, No. 3, 1994, pp. 610-615.

[40] Lim, K. B. and Junkins, J. L., ”Robustness Optimization of Structural and Controller Parameters”, Journal of Guidance, Control and Dynamics, Vol.12, No.1, 1989, pp. 89-96.

[41] Rao, S. S., Pan, T., and Venkayya, V. B., “Robustness Improvement of Actively Controlled Structures through Structural Modifications”, AIAA Journal, Vol. 28, No. 2, 1990, pp. 353-361.

[42] Liu, Z., Wang, D, Hu, H., and Yu, M., ”Measures of Modal Controllability and Observability in Vibration Control of Flexible Structures”, Journal of Guidance, Control and Dynamics, Vol. 17, No. 6, 1994, pp. 1377-1380.

[43] Onada, J. and Haftka, R. T., “ An Approach to Structure/Control Simultaneous Optimization for Large Flexible Spacecraft”, AIAA Journal, Vol. 25, No. 8, 1987, pp. 1133-1138.

[44] Liu, W. and Hou, Z., “Model Reduction in Structural Vibration Control and Its Application”, 16th ASCE Engineering Conference, 2003.

[45] Locatelli, G., Langer, H., Müller, M., and Baier, H., “Simultaneous Optimization of Actuator Placement and Structural Parameters by Mathematical and Genetic Optimization Algorithms”, Institute of Lightweight Structures, Aerospace Department, Munich University.

[46] Ogata, K., Modern Control Theory, 3rd Ed., 1997, Prentice Hall, Inc.

[47] Cook, R. D., Malkus, D. S., and Plesha, M. E., Concepts and Applications of Finite Element Analysis, 1989, 3rd Ed., John Wiley and Sons.

[48] Vanderplaats, G. N., Numerical Optimization Techniques for Engineering Design: with Applications, 1st Edition, 1984, McGraw-Hill, Inc.

[49] Patel, R. V. and Toda, M., “Quantitative Measures of Robustness for Multivariable Systems”, TP8-A, Proceedings of JACC, San Francisco, CA, 1980.

[50] Hamdan, A: M. A. and Nayfeh, A. H., “Measures of Modal Controllability and Observability for First- and Second-Order Linear Systems”, Journal of Guidance, Control and Dynamics, Vol. 12, No. 3, May-June 1989.

[51] Carmichael, D. G., Structural Modeling and Optimization: A General methodology for Engineering and Control, 1st Ed., 1981, Ellis Horward Limited.

[52] Nicholas M. B., Finite Element Analysis on Microcomputers, 1988, McGraw-Hill Book Company.

[53] Pantling, C.M. and Shin, Y.S., “Active Vibration Control Method and Verification for Space Truss Using APDL”.

[54] Irons, B. and Shrive N., Finite Element Primer, 1983, John Wiley & Sons, Inc.

[55] Lu, P. and Khan, A., “Nonsmooth Trajectory Optimization: An Approach Using Continuous Simulated Annealing”, Journal of Guidance, Control and Dynamics, Vol. 17, No. 4, July-August 1994.

[56] Utalay S., Trajectory and Multidisciplinary Design Optimization of Missiles Using Simulated Annealing, M.S. Thesis, Aeronautical Engineering Department, METU, Ankara, January 2000.

[57] Midkiff, J., www.eng.vt.edu/eng/materials/classes/MSE2094_NoteBook/ 97ClassProj/num/midkiff/theory.html, Last updated:2000, Last accessed:2001.

[58] Adams, V. and Askenazi, A., Building Better Products with Finite Element Analysis, 1st Ed., 1999, OnWord Press.

[59] Kelly, S. G., Fundamentals of Mechanical Vibrations, International editions 1993, McGraw-Hill.

[60] MATLAB® Manual, Version 6.5.0 Release 13, 2002.

APPENDIX A

DEFINITIONS OF FINITE ELEMENT METHOD

These definitions are completely taken from references [57] and [47]

degree-of-freedom (dof) - name given to the freedom of movement for an object in any given direction. Any unconstrained object has six degrees-of-freedom (translation in three directions and rotation in three directions).

design parameters - variables that can be created to aid in testing multiple design variations. Can be on geometry (dimensions), material properties, etc

element - one individual piece used in a finite-element analysis model.

geometric nonlinearity - type of nonlinearity in structural analysis caused by large deformation. If the geometry changes enough during the course of the analysis, the stiffness will also change (even if the material property does not). Imagine a thin piece of sheet metal. It may stay within the linear range of the material property, but still show a large deflection. This results in nonlinearity because the stiffness (which is a function of both material and geometry), changes during the simulation.

material nonlinearity - type of nonlinearity in structural analysis caused by nonlinear relationship between stress and strain for the material used. The material property (Young's Modulus) changes over the course of the analysis, and cannot be input as one number. This can be caused by a material (such as a metal) being loaded above it's yield stress value. It can also be caused by a material that has an inherently

nonlinear stress-strain curve. This nonlinearity requires an iterative solution (performed in many steps).

matrix algebra - a form of mathematics where sets of simultaneous equations are represented by rows and columns of numbers.

mesh - collection of finite-elements that together represent a geometric body for FEA.

node – connection points of finite elements.

nodal dof – displacements or rotations at a node.

optimization - design study where software automatically finds the best design.

two-dimensional element - element whose geometry is defined by a 2-d area. Represents a solid whose cross section is unchanging in the direction into the page. Can be used for linearly extruded cross section solids or axisymmetric solids of revolution. Only valid if geometry, loads, and boundary conditions are symmetric.

APPENDIX B

MODAL STATE SPACE TRANSFORMATION

This part is completely taken from reference [59]

B.1 NORMALIZED MODE SHAPES

A mode shape corresponding to a specific natural frequency of an n-dof system is unique only to a multiplicative constant. The arbitrariness can be alleviated by requiring the mode shape to satisfy the normalization constraint. It is convenient to normalize mode shapes by requiring that the kinetic energy scalar product of a mode shape with itself is equal to one. That is,

$$(\{V_i\},\{V_i\})_M = \{V_i\}^T [M]\{V_i\} = 1 \tag{B-1}$$

If the mode shape, $\{V_i\}$, is normalized according to above equation, then from Rayleigh's quotient,

$$\{V_i\}^T [K]\{V\}_i = (\{V_i\},\{V_i\})_K = \omega_i^2 \tag{B-2}$$

The orthogonality relations, the normalization constraint and the subsequent result of the choice of normalization, are summarized by

$$(\{V_i\},\{V_i\})_M = \delta_{IJ} \tag{B-3}$$

and

$$(\{V_i\},\{V_i\})_K = \omega_i \delta_{iJ} \tag{B-4}$$

where δ_{ij} is the Kronecker delta.

B.2 MODAL MATRIX

The modal matrix $[S]$ for an n-dof system is the nxn matrix whose columns are the normalized mode shapes. Let

$$[E] = [S]^T [M][S] \tag{B-5}$$

Let e_{ij} represent the element in the ith row and jth column of $[E]$. Then

$$\begin{aligned} e_{ij} &= \sum_{r=1}^{n} ([S]^T)_{ir} ([M][S])_{rj} \\ &= \sum_{r=1}^{n} V_{ri} \sum_{s=1}^{n} \{M_{rs}\}\{S_{sj}\} \\ &= \sum_{r=1}^{n} \sum_{s=1}^{n} V_{ri} \{M_{rs}\} V_{sj} \\ &= \{V\}_i^T [M]\{V_j\} \end{aligned} \tag{B-6}$$

Using the definition of the kinetic energy scalar product, the preceding equation becomes

$$e_{ij} = (\{V_i\},\{V_j\})_M \tag{B-7}$$

Since the modal matrix is defined using mode shapes, Eq. (B-7) implies

$$e_{ij} = \delta_{ij} \tag{B-8}$$

Thus $[E]$ is the *nxn* identity matrix and Eq. (B-1) becomes

$$[S]^T [M][S] = [I] \tag{B-9}$$

In a similar fashion it is shown that

$$[S]^T [K][S] = [\Omega] \tag{B-10}$$

where $[\Omega]$ is a *nxn* diagonal matrix with the squares of the natural frequencies along the diagonal. That is,

$$[\Omega] = \begin{Bmatrix} \omega_1^2 & 0 & 0 & \cdots & 0 \\ 0 & \omega_2^2 & 0 & \cdots & 0 \\ 0 & 0 & \omega_3^2 & \cdots & 0 \\ \vdots & \vdots & \vdots & \ddots & \vdots \\ 0 & 0 & 0 & \cdots & \omega_n^2 \end{Bmatrix} \tag{B-11}$$

B.3 PROPORTIONAL DAMPING

The diferential equations for a linear *n* dof system with proportional viscous damping are

$$[M]\{\ddot{q}\} + (\alpha[K] + \beta[M])\{\dot{q}\} + [K]\{q\} = \{F\} \tag{B-12}$$

The undamped system has *n* natural frequenciews and normalized mode shapes. The nonsingular modal matrix $[S]$ exists. Principal coordinates for the undamped syatem are defined by Eq. (2-16). Using the principal coordinates as dependent variables in Eq. (B-12) and premultiplying by $[S]^T$ leads to

$$[S]^T[M][S]\{\ddot{s}\} + (\alpha[S]^T[K][S] + \beta[S]^T[M][S])\dot{s} + [S]^T[K][S]\{s\} = [S]^T \quad \text{(B-13)}$$

Eq. (B-9) and (B-10) allow Eq. (B-13) to be rewritten as

$$\{\ddot{s}\} + (\alpha\omega_i^2[S] + \beta)\{\dot{s}\} + \omega_i^2\{s\} = \{H\} \quad \text{(B-14)}$$

The differential equations represente by Eq. (B-14) are uncoupled. The ith equation for the forced vibrations of a one dof system

$$\ddot{s}_i + 2\zeta_i\omega_i^2\dot{s} + \omega_i^2 s = h_i \quad \text{(B-15)}$$

where ζ_i is called the modal damping coefficient for mode i :

$$\zeta_i = \frac{1}{2}\left(\alpha\omega_i + \frac{\beta}{\omega_i}\right) \quad \text{(B-16)}$$

Then Eq. (B-14) can be written as

$$\{\ddot{s}\} + [\Lambda]\{\dot{s}\} + [\Omega]\{s\} = [S]^T\{F\} \quad \text{(B-17)}$$

where Λ is a *nxn* diagonal matrix with the twice of the modal damping coefficient multiply by the natural frequency along the diagonal. That is,

$$[\Lambda] = \begin{Bmatrix} 2\zeta_1\omega_1 & 0 & 0 & \cdots & 0 \\ 0 & 2\zeta_2\omega_2 & 0 & \cdots & 0 \\ 0 & 0 & 2\zeta_3\omega_3 & \cdots & 0 \\ \vdots & \vdots & \vdots & \ddots & \vdots \\ 0 & 0 & 0 & \cdots & 2\zeta_n\omega_n \end{Bmatrix} \quad \text{(B-18)}$$

APPENDIX C

HIDE AND SEEK SIMULATED ANNEALING OPTIMIZATION ALGORITHM

C.1 SIMULATED ANNEALING OPTIMIZATION ALGORITHM

This part is completely taken from reference [48].

Simulated annealing is a class of stochastic optimization algorithm for the following problem

$$\begin{aligned} &\min f(x) \\ &x \in S \end{aligned} \tag{C-1}$$

where the feasible region $S \subset R^n$ is a compact set, and f a continuous function defined on S. The problem is to find an $x^* \in S$ so that $f^* = f(x^*) \leq f(x)$ for all $x \in S$. The algorithm searches for a global optimum by simulating the physical phenomenon of annealing.

Simulated Annealing is an optimization algorithm, which is suitable for large-scale optimization problems, especially ones where a desired global extreme is hidden among many poorer, local extremes. It is applicable both to continuous and discrete optimization problems.

SA depends on the analogy with thermodynamics, specifically with the way that liquids freeze and crystallize, or metals cool and anneal. At high temperatures, the molecules of a liquid move freely with respect to one another. If the liquid is cooled

slowly, thermal mobility is lost. The atoms line themselves up and form a pure crystal, which is the state of minimum energy for this system. For slowly cooled systems, nature is able to find this minimum energy state. In fact, if a liquid metal is cooled quickly or quenched, it does not reach this state but rather ends up in a polycrystalline state having higher energy. So the essence of the process is slow cooling, allowing sample time for redistribution of the atoms as they lose mobility. SA simulates this physical annealing process ensuring that a low energy state will be achieved.

The minimization algorithm is based on Boltzmann probability distribution;

$$\Pr ob(E) \propto \exp(-\frac{E}{kT}) \tag{C-2}$$

which expresses the idea that a system in thermal equilibrium at temperature T has its energy probabilistically distributed among all different energy states E. Even at low temperature, there is a chance of a system being in a high energy state, so, for the system to get out of a local energy minimum in favor of finding a better, more global, one. The quantity k, Boltzmann's constant, is a constant of nature that relates temperature to energy. In other words, the system sometimes goes uphill as well as downhill; but the lower the temperature, the less likely is any significant uphill excursion.

Metropolis, in 1953, incorporated these principles into numerical calculations. A simulated thermodynamic system was assumed to change its configuration from energy E_1 to energy E_2 with probability,

$$p = \exp\left(-\frac{E_2 - E_1}{kT}\right) \tag{C-3}$$

Notice that if $E_2 < E_1$, this probability is greater than unity, in such cases the change is arbitrarily assigned a probability equal to unity. This general scheme of always taking a downhill step while sometimes taking an uphill step, has come to be known as the

Metropolis criterion. To make use of Metropolis criterion, one must provide the following elements:

- A description of possible system configurations
- A generator of random changes in the configuration
- An objective function E whose minimization is the goal of the procedure
- A control parameter T and an annealing schedule which tells how it is lowered from high to low values.

In simulated annealing, the state of a system corresponds to the design vector x, energy to the value of the augmented cost function, f, and the metropolis criterion to

$$\beta_T = \min\left(1.0, e^{\frac{f(x_2)-f(x_1)}{T}}\right) \tag{C-4}$$

where x_1 and x_2 are two different design points.

C.2 HIDE-AND-SEEK SIMULATED ANNEALING ALGORITHM

Past applications of simulated annealing have been mainly in discrete optimization problems such as famous traveling salesman problem. For application in trajectory optimization for a continuous dynamic system, a continuous SA algorithm is required. One of the major differences between a discrete and continuous SA algorithm is the choice of a cooling schedule for the temperature parameter, which parameterizes the decrease of acceptance probabilities for deteriorations.

More recently, a SA algorithm for continuous optimization (maximization), called Hide-and-Seek, was developed by Bélisle et. al [16]. This algorithm has two distinct features: an adaptive cooling schedule and a continuous random walk process for generating a sequence of feasible points. Convergence of the algorithm to the global optimum is rigorously proved. The user supplies the bounds on the design vector.

Within the bounded design space, the feasible region is specified by criteria set up by the user, and disjoint feasible regions are allowed.

Hide-and-Seek is a powerful yet simple and easily implemented continuous simulated annealing algorithm for finding the maximum of a continuous function over a compact body. The algorithm begins with any feasible interior point. In each iteration it generates a candidate successor point by generating a uniformly distributed point along a direction chosen at random from the current iteration point. The candidate point is then accepted as the next iteration point according to the Metropolis criterion parameterized by an adaptive cooling schedule. The sequence of iteration points converges in probability to a global optimum.

Hide-and-Seek proceeds roughly as follows. The stating point, x_0, is generated randomly and a large initial temperature, T_0, is selected. In the k^{th} step, a direction, Φ_k, on the surface of the unit sphere in the search space is chosen from the uniform distribution. Then choose λ_k from the uniform distribution $\Lambda_k = (\lambda \in R : x_k + \lambda\Phi_k \in S)$ Set $y_{k+1} = x_k + \lambda\Phi_k$. The next search point, x_{k+1}, is determined by

$$x_{k+1} = \begin{cases} y_{k+1} & \text{if} \quad V_k \in [0, \beta_T(x_k, y_{k+1})] \\ x_k & \text{if} \quad V_k \in [\beta_T(x_k, y_{k+1}), 1] \end{cases} \qquad \text{(C-5)}$$

where V_k is a random variable with uniform distribution on $[0,1]$; and T is the current temperature. It should be noted that from the above equation, even if $f(y_{k+1})$ represents a deterioration in the objective function; i.e., $f(y_{k+1}) < f(x_k)$, the probability of acceptance of y_{k+1} as the next iteration point is high if the temperature T is high. T is updated (decreased) by the cooling schedule

$$T = 2 \cdot \frac{\left(f^* - f(x_k)\right)}{\chi^2_{1-p}(n)} \tag{C-6}$$

only when $f(\chi_k)$ is greater than all previous objective function values, where $0 < p < 1$ and $\chi^2_{1-p}(n)$ is the $100.(1-p)$ percentile point of the chi-square distribution with n dof [49]. This cooling schedule generates the next point that would give an improvement in function value over current iteration point with probability at least p. Performance of the algorithm is insensitive to different choices of p. When f^* is not known, the authors of Hide-and-Seek have developed a heuristic estimator $\hat{f}$ for f^*

$$\hat{f} = f_1 + \frac{f_1 - f_2}{(1-p)^{-n/2} - 1} \tag{C-7}$$

where f_1 and f_2 are the current two largest function values and the parameter p corresponds to the probability that the real maximum is larger than this estimator.

C.3 AN EXAMPLE OF SINGLE-OBJECTIVE HSSA

C.3.1 Zermelo's Trajectory Optimization Algorithm

Zermelo's problem is well known problem in literature. In this trajectory optimization problem, a ship must travel through a region of strong currents. The magnitude and the direction of the currents, known as function of position, are as below;

$$u = u(x, y) \quad , \quad v = v(x, y) \tag{C-8}$$

In the Eq. (C-8), (x, y) are rectangular coordinates and (u, v) are the velocity components of the current in the x and y directions, respectively. The magnitude of the ship's velocity relative to water is V, a constant. The optimal control problem is to

steer the ship in such a way as to minimize the time necessary to go from an initial point (x_i, y_i) to final point (x_f, y_f). the equations of motion are as below;

$$\begin{aligned} \dot{x} &= V\cos\theta + u(x,y) \\ \dot{y} &= V\sin\theta + v(x,y) \end{aligned} \tag{C-9}$$

θ, in the above equation is the heading angle of the ship's axis relative to the fixed coordinate axes, and (x, y) represents the position of the ship shown in Figure C-1.

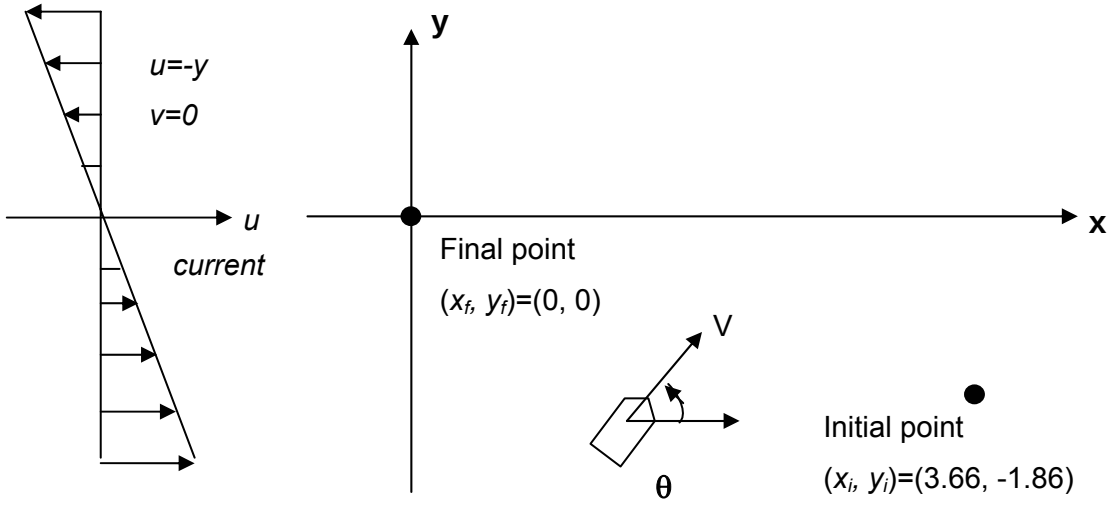

Figure C-1 Zermelo's trajectory optimization problem

Analytic solution that is obtained by Bryson [50] for this problem is given in Table C-1.

Table C-1 Results of the analytical solution

t_f	5.46
x_f	0.0
v_f	0.0
θ_i	105°
θ_f	240°

C.3.2 Solution of the Problem with Simulated Annealing

To solve the Zermelo's optimal control problem by Hide and Seek continuous simulated annealing, the problem is transformed into nonlinear programming problem.

Then the nonlinear problem is as below;

$$\begin{aligned} &\text{minimize } t_f \\ &\quad \text{s.t. } G(p) = 0 \\ &\quad p_l \le p \le p_u \end{aligned} \tag{C-10}$$

where p is the optimization parameters and includes the steering angles $\theta_i \ (1 \cdots N)$ and t_f, G is the equality constraint and equals to range error [51].

N is the number of evenly-spaced time nodal points on the trajectory. The optimization parameters are total time and the value of the steering angles at these nodes.

In the solution procedure of the Zermelo's trajectory problem 10 nodes are used and the state values between the nodes found by the cubic spline interpolation between the just right and left nodes. To handle the equality constraints a penalty function approach is used. According to this approach the nonlinear problem is converted as Eq. (C-11);

$$f = -t_f - k_1 \left| x(t_f) \right| - k_2 \left| y(t_f) \right| \tag{C-11}$$

where, k_1 and k_2 are penalty coefficients and have positive values. The choices of k_i affect the accuracy of the i^{th} constraints.

Initial parameters that are used in Hide and Seek Simulated Annealing are tabulated in Table C-2 and the results are in Table C-3.

Table C-2 Initial parameters used in Hide and Seek

Number of intervals	10
Initial $\theta_i \quad i = 1 \cdots 10$	3°
x_i	3.66
y_i	-1.86

Table C-3 Results of Hide and Seek

t_f (s)	5.458
x_f	0.004
v_f	0.01
θ_i	105.9°
θ_f	237.1°
number of function evaluations	43189
number of accepted function evaluation number	87

The resultant trajectory of the problem is given in Figure C-2. In Figure C-3 final steering angle vs. time graph is given.

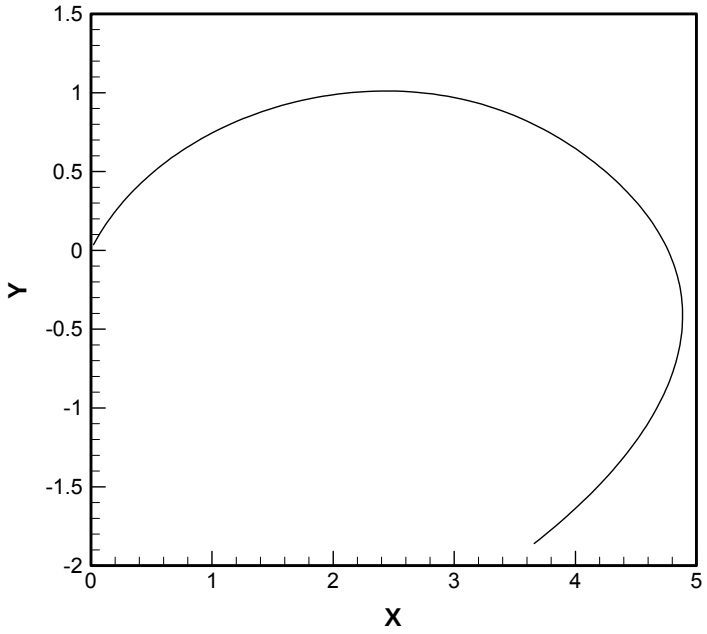

Figure C-2 Final trajectory of the Zermelo optimization problem

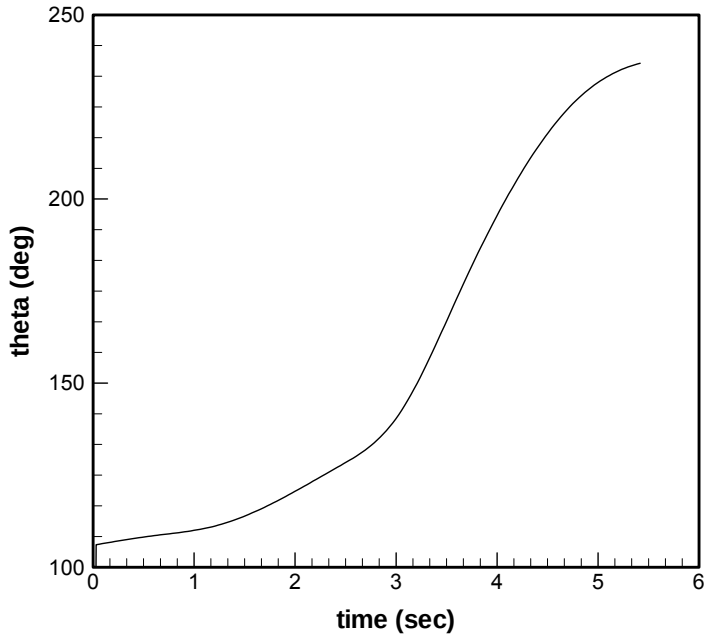

Figure C-3 Final steering angle-time graph of Zermelo optimization problem

APPENDIX D

LINEAR QUADRATIC REGULATOR FUNCTION

This part is completely taken from reference [60].

lqr

Design linear-quadratic (LQ) state-feedback regulator for continuous plant

Syntax

$$[G,R,e] = lqr(A,B,Q,P) \tag{D-1}$$

$$[G,R,e] = lqr(A,B,Q,P,N) \tag{D-2}$$

Description

Eq.(D-2) calculates the optimal closed loop gain matrix G such that the state-feedback law given at Eq.(2-15) minimizes the quadratic cost function

$$J(t) = \int_0^\infty \left(x^T Q x + U^T P U + 2x^T N U \right) dt \tag{D-3}$$

for the continuous-time state-space model given at Eq. (2-26)

The default value $N = 0$ is assumed when N is omitted.

In addition to the state-feedback gain G, lqr returns the solution R of the associated Riccati equation

$$[A]^T[R]+[R][A]-([R][B]+[N])[P]^{-1}([B]^T[R]+[N]^T)+[Q]=0 \quad \text{(D-4)}$$

and the closed loop eigenvalues

$$[e]=eig([A]-[B][G]) \quad \text{(D-5)}$$

Note that G is derived from R by

$$[G]=[P]^{-1}([B]^T[R]+[N]^T) \quad \text{(D-6)}$$

Limitations

The problem data must satisfy:

- The pair (A,B) is stabilizable.
- $P>0$ and $Q-N.P^{-1}.N^T \geq 0$
- $\left(Q-N.P^{-1}.N^T, A-B.P^{-1}.N^T\right)$ has no unobservable mode on the imaginary axis.

APPENDIX E

MATHEMATICAL MODELLING OF TWO BAR CASE STUDY

Mathematical modelling of the two bar case study is given below for each configuration of actuator.

E.1 FINITE ELEMENT MODELLING

FEM is drawn symbolically for cross sectional areas of bar elements. Structural matrices are derived for each configuration by hand is given below.

E.1.1 Configuration 1: Single Actuator

Positions of the actuator is given in Figure E-1.

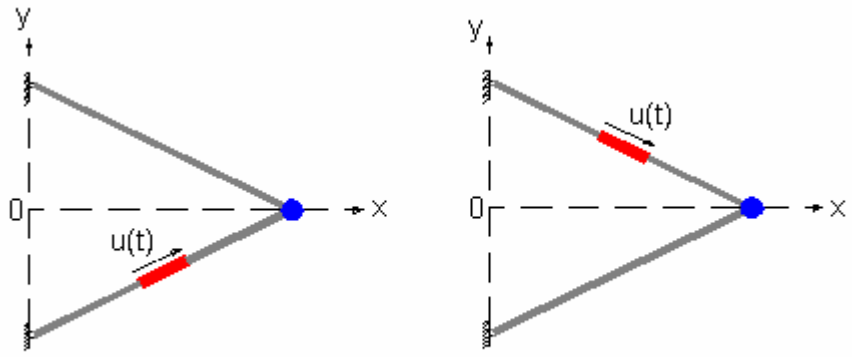

Figure E-1 Single actuator placed case

Elemental structural matrices for bar elements are calculated as follows:

ELEMENT-1

$$L_1 = \sqrt{(1000-0)^2 + (0-500)^2} = 1118.03\ (mm) \tag{E-1}$$

$$t_1 = \frac{X_2 - X_1}{L_1} = \frac{1000-0}{1118.03} = 0.89 \tag{E-2}$$

$$t_2 = \frac{Y_2 - Y_1}{L_1} = \frac{0-500}{1118.03} = -0.45 \tag{E-3}$$

$$[k_1] = \frac{E_1 a_1}{L_1}\begin{bmatrix} t_1^2 & t_1 t_2 \\ t_1 t_2 & -t_2^2 \end{bmatrix} = a_1 \begin{bmatrix} 52.235 & -26.117 \\ -26.117 & 13.059 \end{bmatrix} (N/mm) \tag{E-4}$$

$$(m_t)_1 = a_1 \rho_1 L_1 = a_1 (mm^2)\, 2700\ 10^{-9} \left(\frac{kg}{mm^3}\right) 1118.03 (mm^3)$$
$$(m_t)_1 = 0.0030187 a_1\ (kg) \tag{E-5}$$

$$[m_1] = \frac{a_1 \rho_1 L_1}{6}\begin{bmatrix} 2 & 0 \\ 0 & 2 \end{bmatrix} = a_1 \begin{bmatrix} 0.0010062 & 0 \\ 0 & 0.0010062 \end{bmatrix} (kg) \tag{E-6}$$

ELEMENT-2

$$L_2 = \sqrt{(1000-0)^2 + (0-(-500))^2} = 1118.03\ (mm) \tag{E-7}$$

$$t_2 = \frac{Y_2 - Y_3}{L_2} = \frac{0-(-500)}{1118.03} = 0.45 \tag{E-8}$$

$$[k_2] = \frac{E_2 a_2}{L_2}\begin{bmatrix} t_1^2 & t_1 t_2 \\ t_1 t_2 & -t_2^2 \end{bmatrix} = a_2 \begin{bmatrix} 52.235 & 26.117 \\ 26.117 & 13.059 \end{bmatrix} (N/mm) \tag{E-9}$$

$$(m_t)_2 = a_2 \rho_2 L_2 = a_2 \left[mm^2\right] 2700\ 10^{-9} \left[\frac{kg}{mm^3}\right] 1118.03 \left[mm^3\right] \tag{E-10}$$

$$(m_t)_2 = 0.0030187 a_2\ (kg)$$

$$\left[m_2\right] = \frac{a_2 \rho_2 L_2}{6} \begin{bmatrix} 2 & 0 \\ 0 & 2 \end{bmatrix} = a_2 \begin{bmatrix} 0.0010062 & 0 \\ 0 & 0.0010062 \end{bmatrix} (kg) \tag{E-11}$$

$$\left[m_a\right] = \frac{m_{act}}{2} \begin{bmatrix} 1 & 0 \\ 0 & 1 \end{bmatrix} = \begin{bmatrix} 0.25 & 0 \\ 0 & 0.25 \end{bmatrix} (kg) \tag{E-12}$$

$$\left\{f_a\right\} = \begin{bmatrix} 0 & 0 \\ t_1 & t_2 \end{bmatrix}^T \begin{bmatrix} -1 \\ 1 \end{bmatrix} = \begin{Bmatrix} 0.89 \\ 0.45 \end{Bmatrix} \tag{E-13}$$

Next step is assembling elemental structural mass and stiffness matrices, controller force matrices and external mass matrices.

EXTERNAL MASS:

$$\left[M_e\right] = m_e \begin{bmatrix} 1 & 0 \\ 0 & 1 \end{bmatrix} = \begin{bmatrix} 50 & 0 \\ 0 & 50 \end{bmatrix} (kg) \tag{E-14}$$

SYSTEM MATRICES:

$$\left[M\right] = \left[m_1\right] + \left[m_2\right] + \left[(m_a)_1\right] + \left[M_e\right]$$

$$\left[M\right] = \begin{bmatrix} 0.0010062(a_1 + a_2) + 50.25 & 0 \\ 0 & 0.0010062(a_1 + a_2) + 50.25 \end{bmatrix} \left(kg\right) \tag{E-15}$$

$$\left\{F_a\right\} = \begin{Bmatrix} 0.89 \\ 0.45 \end{Bmatrix} \tag{E-16}$$

E.1.2 Configuration 2: Two Actuator

Two actuators are placed on both bar elements as shown Figure E-2.

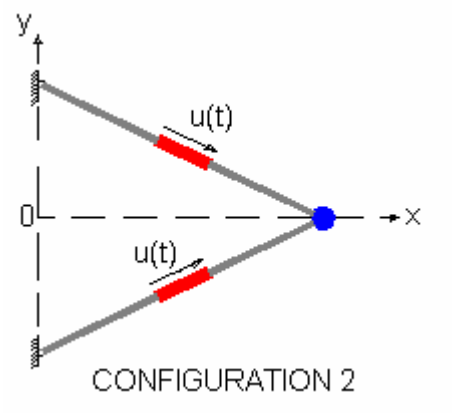

Figure E-2 Two actuator placed case

Element stiffness and mass matrices are calculated in similar way as mentioned above. Since actuator element does not have stiffness and damping contribution to finite element model, stiffness matrix is same as one-actuator case. Only mass matrix is changed such that half of the actuator mass will be added to both nodal dof. Consequently, mass matrix of the two-actuator configuration is as follows:

$$[M] = [m_1] + [m_2] + [(m_a)_1] + [(m_a)_2] + [M_e]$$

$$[M] = \begin{bmatrix} 0.0010062(a_1 + a_2) + 50.5 & 0 \\ 0 & 0.0010062(a_1 + a_2) + 50.5 \end{bmatrix} \ (kg) \qquad \text{(E-17)}$$

Actuator force matrix should also revise. Since two actuators are placed into system size of actuator force matrix is increased. Actuator force matrix is found as follows:

$$[F_a] = \begin{bmatrix} 0.89 & 0.89 \\ 0.45 & -0.45 \end{bmatrix} \tag{E-18}$$

E.2 STATE SPACE TRANSFORMATION

Similar to FEM modal state transformation is done for two configuration.

E.2.1 Configuration 1: One Actuator

Let nodal displacement and velocities are states of the stytem. Then,

$$\begin{aligned} x_i &= q_i \qquad i = 1 \cdots n \\ \dot{x}_i &= x_{i+n} \end{aligned} \tag{E-19}$$

$$[M]\{\ddot{q}\} + [K]\{q\} = [F_a]\{U\} \tag{E-20}$$

$$\dot{x}_{i+n} = -[M]^{-1}[K]x_i + [M]^{-1}[F_a]\{U\}$$

$$[A] = \begin{bmatrix} 0 & [I]_{nxn} \\ -[M]^{-1}[K] & 0 \end{bmatrix}_{2nx2n} \tag{E-21}$$

$$[B] = \begin{bmatrix} 0 \\ [M]^{-1}[F_a] \end{bmatrix}_{2nxr} \tag{E-22}$$

$$[V] = [M]^{-1}[K] \ (1/s^2)$$

$$[V] = \begin{bmatrix} \dfrac{52.235\ 10^3(a_1 + a_2)}{0.10062\ 10^{-2}(a_1 + a_2) + 50.25} & \dfrac{26.117\ 10^3(a_2 - a_1)}{0.10062\ 10^{-2}(a_1 + a_2) + 50.25} \\ \dfrac{26.117\ 10^3(a_2 - a_1)}{0.10062\ 10^{-2}(a_1 + a_2) + 50.25} & \dfrac{13.059\ 10^3(a_1 + a_2)}{0.10062\ 10^{-2}(a_1 + a_2) + 50.25} \end{bmatrix} \tag{E-23}$$

$$[A]=\begin{bmatrix} 0 & 0 & \vdots & 1 & 0 \\ 0 & 0 & \vdots & 0 & 1 \\ \cdots & \cdots & \vdots & \cdots & \cdots \\ \dfrac{52235(a_1+a_2)}{0.0010062(a_1+a_2)+50.25} & \dfrac{26117(a_2-a_1)}{0.0010062(a_1+a_2)+50.25} & \vdots & 0 & 0 \\ \dfrac{26117(a_2-a_1)}{0.0010062(a_1+a_2)+50.25} & \dfrac{13059(a_1+a_2)}{0.0010062(a_1+a_2)+50.25} & \vdots & 0 & 0 \end{bmatrix} \quad \text{(E-24)}$$

$$\{B\}=\begin{bmatrix} 0 \\ 0 \\ \cdots \\ \dfrac{0.89}{0.0010062(a_1+a_2)+50.25} \\ \dfrac{0.45}{0.0010062(a_1+a_2)+50.25} \end{bmatrix} \quad \text{(E-25)}$$

E.2.2 Configuration 2: Two Actuator

$$[V]=[M]^{-1}[K]\ (1/s^2)$$

$$[V]=\begin{bmatrix} \dfrac{52235(a_1+a_2)}{0.0010062(a_1+a_2)+50.5} & \dfrac{26117\ (a_2-a_1)}{0.0010062(a_1+a_2)+50.5} \\ \dfrac{26117(a_2-a_1)}{0.0010062(a_1+a_2)+50.5} & \dfrac{13059(a_1+a_2)}{0.0010062(a_1+a_2)+50.5} \end{bmatrix} \quad \text{(E-26)}$$

$$[A]=\begin{bmatrix} 0 & 0 & \vdots & 1 & 0 \\ 0 & 0 & \vdots & 0 & 1 \\ \cdots & \cdots & \vdots & \cdots & \cdots \\ \dfrac{52235(a_1+a_2)}{0.0010062(a_1+a_2)+50.5} & \dfrac{26117(a_2-a_1)}{0.0010062(a_1+a_2)+50.5} & \vdots & 0 & 0 \\ \dfrac{26117(a_2-a_1)}{0.0010062(a_1+a_2)+50.5} & \dfrac{13059(a_1+a_2)}{0.0010062(a_1+a_2)+50.5} & \vdots & 0 & 0 \end{bmatrix} \quad \text{(E-27)}$$

$$\{B\} = \begin{bmatrix} 0 \\ 0 \\ \cdots \\ \dfrac{0.89}{0.0010062(a_1 + a_2) + 50.5} \\ \dfrac{0.45}{0.10062(a_1 + a_2) + 50.5} \end{bmatrix} \quad \text{(E-28)}$$

E.3 CALCULATION OF CONSTRAINTS

Two structural constraints are submitted in optimization problem as mentioned in Chapter 4.

E.3.1 Configuration 1: One Actuator

$$W_t = (m_t)_1 + (m_t)_2 = 0.0030187(a_1 + a_2)\ (kg) \quad \text{(E-29)}$$

$$\omega_{1,2} = \sqrt{eig(T)}$$

$$\omega_{1,2} = \sqrt{\frac{65.3\ 10^3(a_1 + a_2) \pm \sqrt{(39.2\ 10^3(a_1 + a_2))^2 + (52.2\ 10^3(a_2 - a_1))^2}}{2(0.0010062(a_1 + a_2) + 50.25)}} \quad \text{(E-30)}$$

$$\omega_l = \sqrt{\frac{65.3\ 10^3(a_1 + a_2) - \sqrt{(39.2\ 10^3(a_1 + a_2))^2 + (52.2\ 10^3.(a_2 - a_1))^2}}{2(0.0010062(a_1 + a_2) + 50.25)}} \quad \text{(E-31)}$$

E.3.2 Configuration 2: Two Actuator

$$W_t = (m_t)_1 + (m_t)_2 = 0.0030187(a_1 + a_2)\ (kg) \quad \text{(E-32)}$$

$$\omega_{1,2} = \sqrt{eig(T)}$$

$$\omega_{1,2} = \sqrt{\frac{65.3\ 10^3(a_1 + a_2) \pm \sqrt{(39.210^3(a_1 + a_2))^2 + (52.2\ 10^3(a_2 - a_1))^2}}{2(0.0010062(a_1 + a_2) + 50.5)}} \quad \text{(E-33)}$$

$$\omega_l = \sqrt{\frac{65.3\ 10^3(a_1 + a_2) - \sqrt{(39.2\ 10^3(a_1 + a_2))^2 + (52.2\ 10^3(a_2 - a_1))^2}}{2(0.0010062(a_1 + a_2) + 50.5)}} \quad \text{(E-34)}$$

APPENDIX F

OPTIMIZATION INPUTS OF PARABOLIC TRUSS EXAMPLE

Some important inputs of the parabolic shaped multi truss example are given.

F.1 NODAL COORDINATES

Nodal coordinates are taken similar to Liu and Begg [17].

Table F-1 Nodal Coordinates in spatial coordinates

	Nodal coordinates (m)	
Node number	X	Y
1	−30	0
2	−20	$5/9\,h_b$
3	−10	$8/9\,h_b$
4	0	h_b
5	0	h_t
6	−10	$8/9\,h_t$
7	−20	$5/9\,h_t$
8	10	$8/9\,h_b$
9	20	$5/9\,h_b$
10	30	0
11	20	$5/9\,h_t$
12	10	$1/9\,h_t$

F.2 DESIGN PARAMETER LINKING OF PARABOLIC SHAPE TRUSS

Structural design parameter linking scheme is used in this problem as shown in the Figure F-1. It is also shown in tabulated version in Table F-2.

Table F-2 Design parameter linking scheme

Linked variable 1	Linked variable 2	Used symbol of design parameter
a_1	a_{13}	a_1
a_2	a_{14}	a_2
a_3	a_{15}	a_3
a_4	a_{16}	a_4
a_5	a_{17}	a_5
a_6	a_{18}	a_6
a_7	a_{19}	a_7
a_8	a_{20}	a_8
a_9	a_{21}	a_9
a_{10}	a_{22}	a_{10}
a_{11}	a_{23}	a_{11}
a_{12}	a_{24}	a_{12}

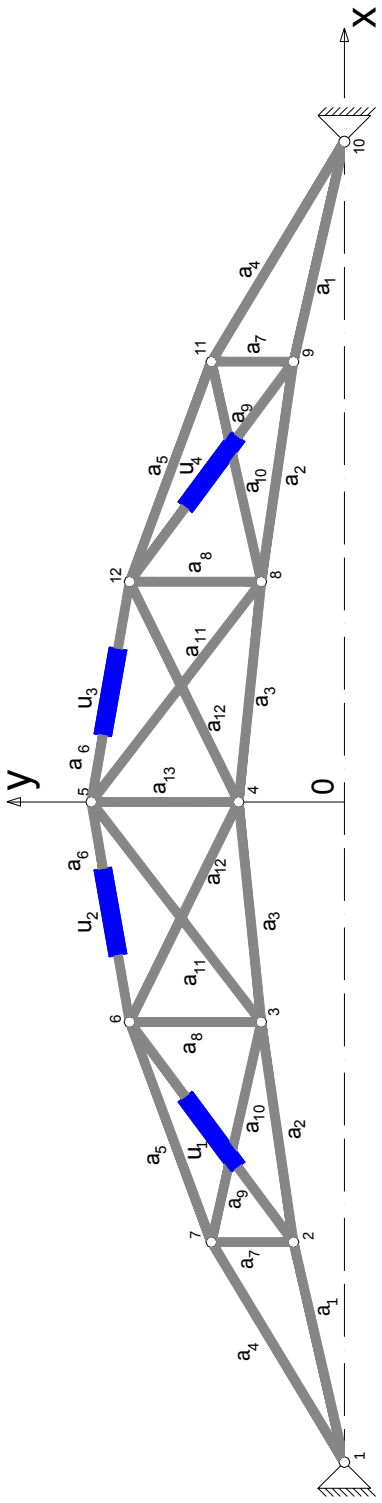

Figure F-1 Design parameter linking scheme

APPENDIX G

OPTIMIZATION RESULTS OF PARABOLIC SHAPE TRUSS

The iteration histories of the cross sectional areas of the bar elements are given for the single objective optimization, Case I of the parabolic shape truss.

G.1 SINGLE OBJECTIVE OPTIMIZATION USING QPI

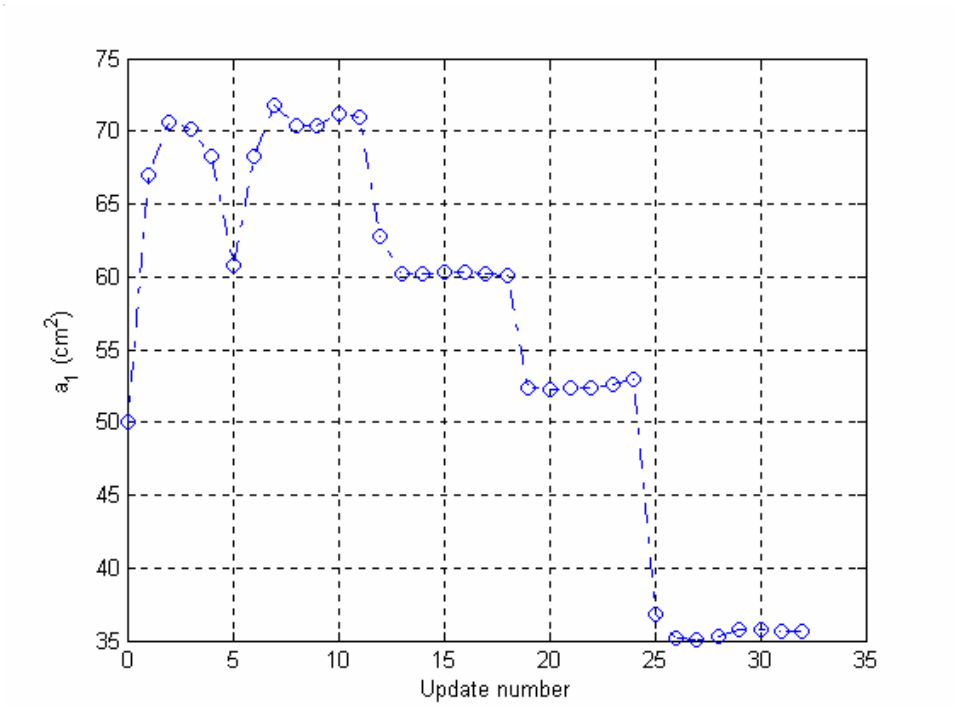

Figure G-1 Iteration history of cross sectional area of a bar element for single objective case, Case I

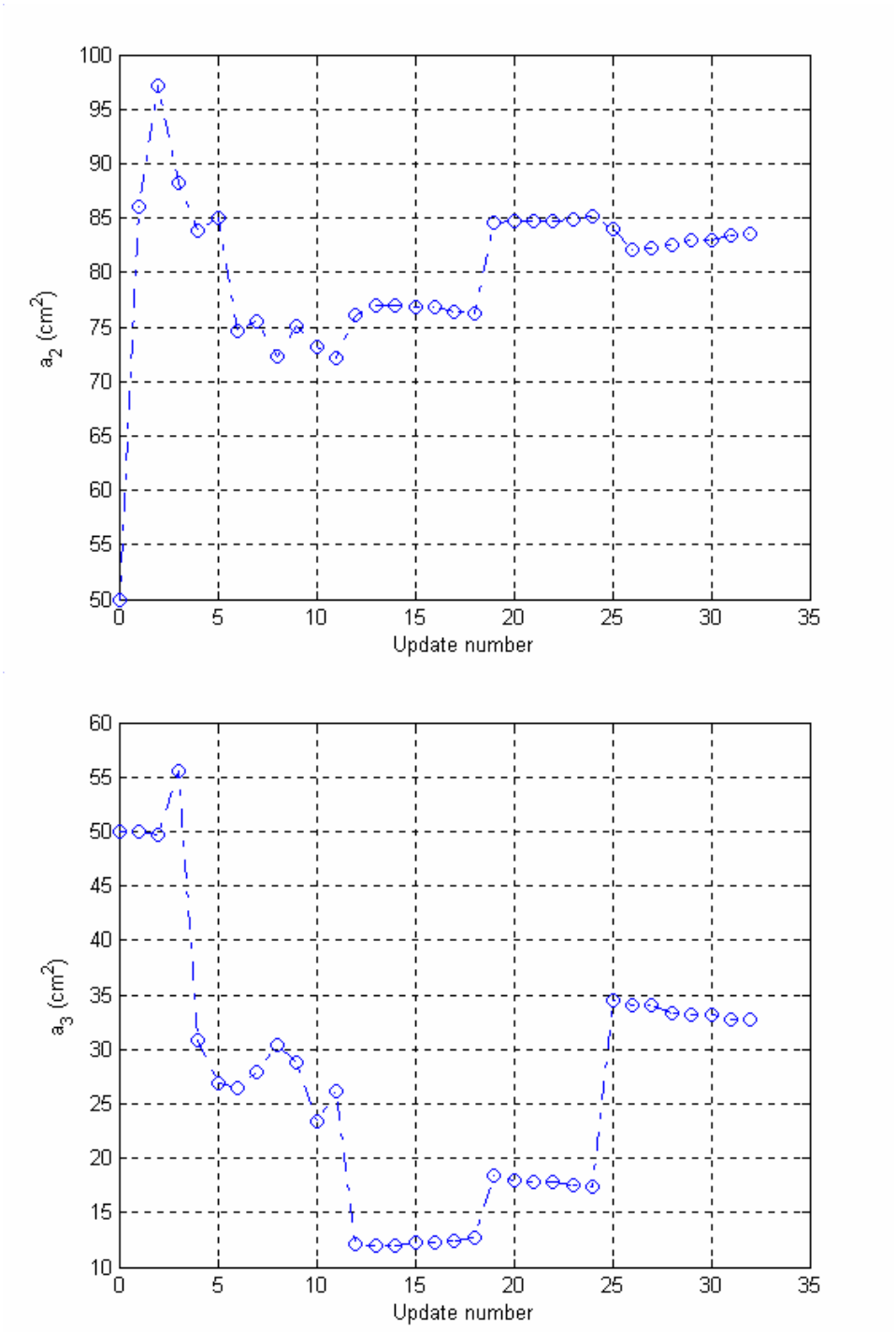

Figure G-1 Iteration history of cross sectional area of a bar element for single objective case, Case I (continued)

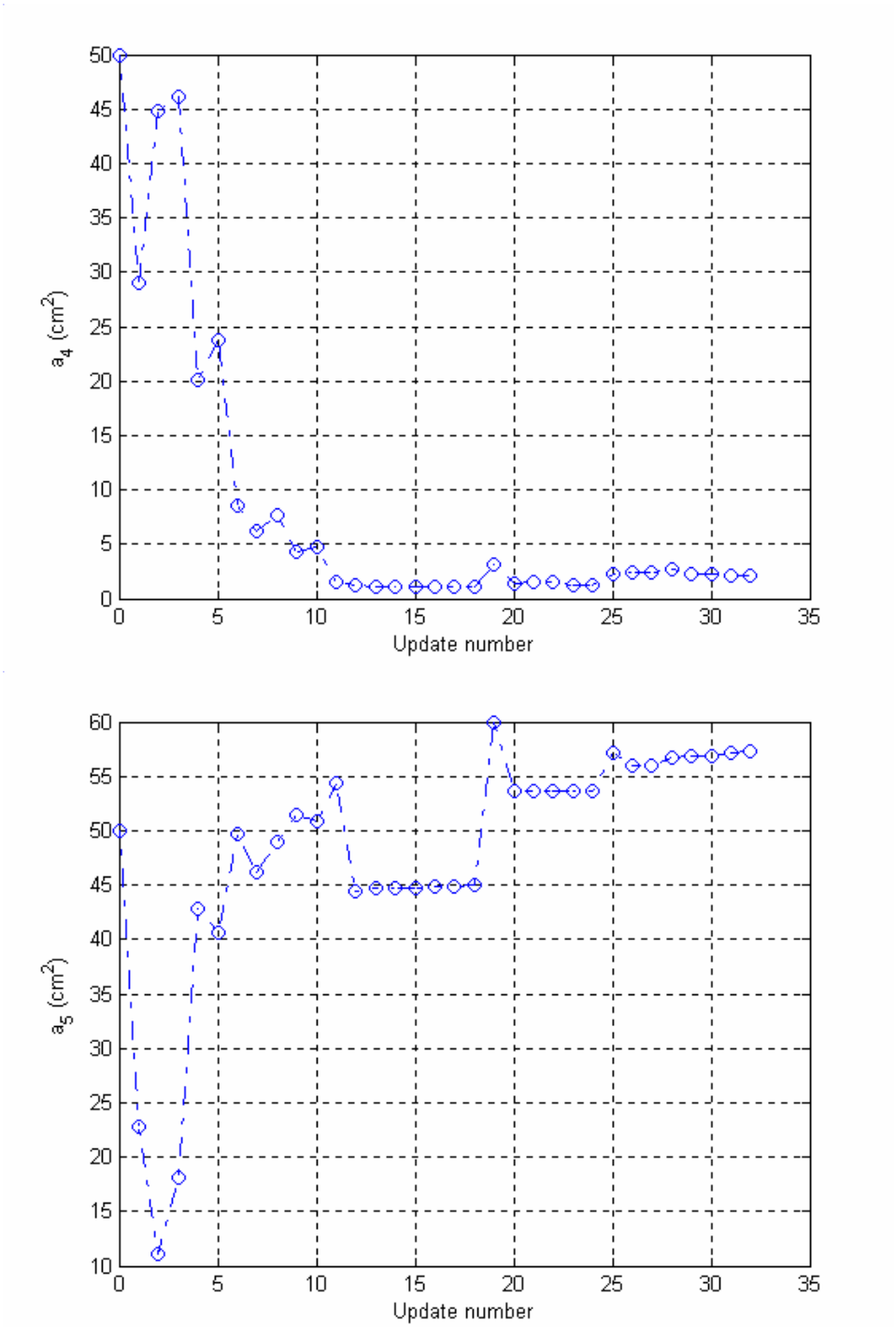

Figure G-1 Iteration history of cross sectional area of a bar element for single objective case, Case I (continued)

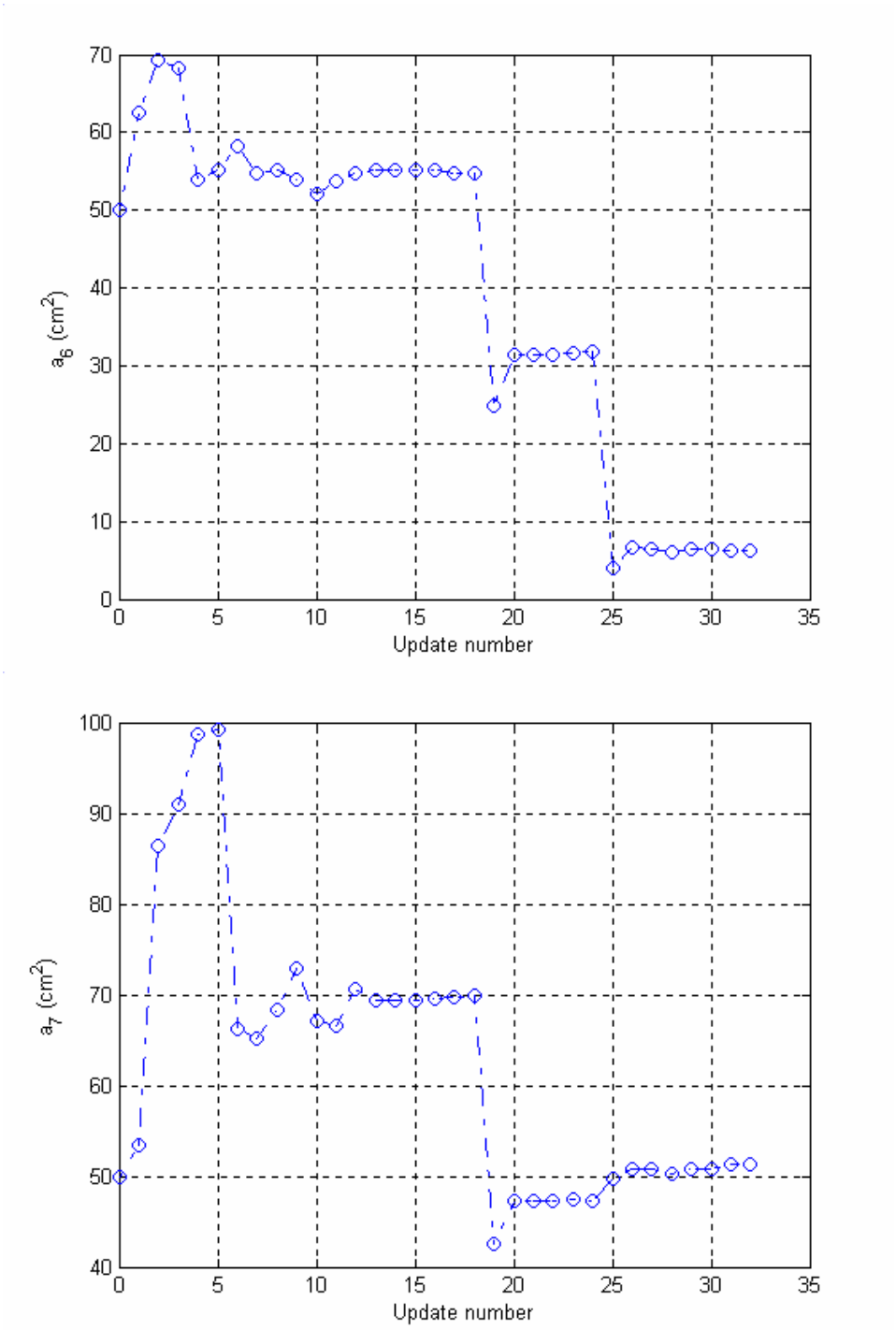

Figure G-1 Iteration history of cross sectional area of a bar element for single objective case, Case I (continued)

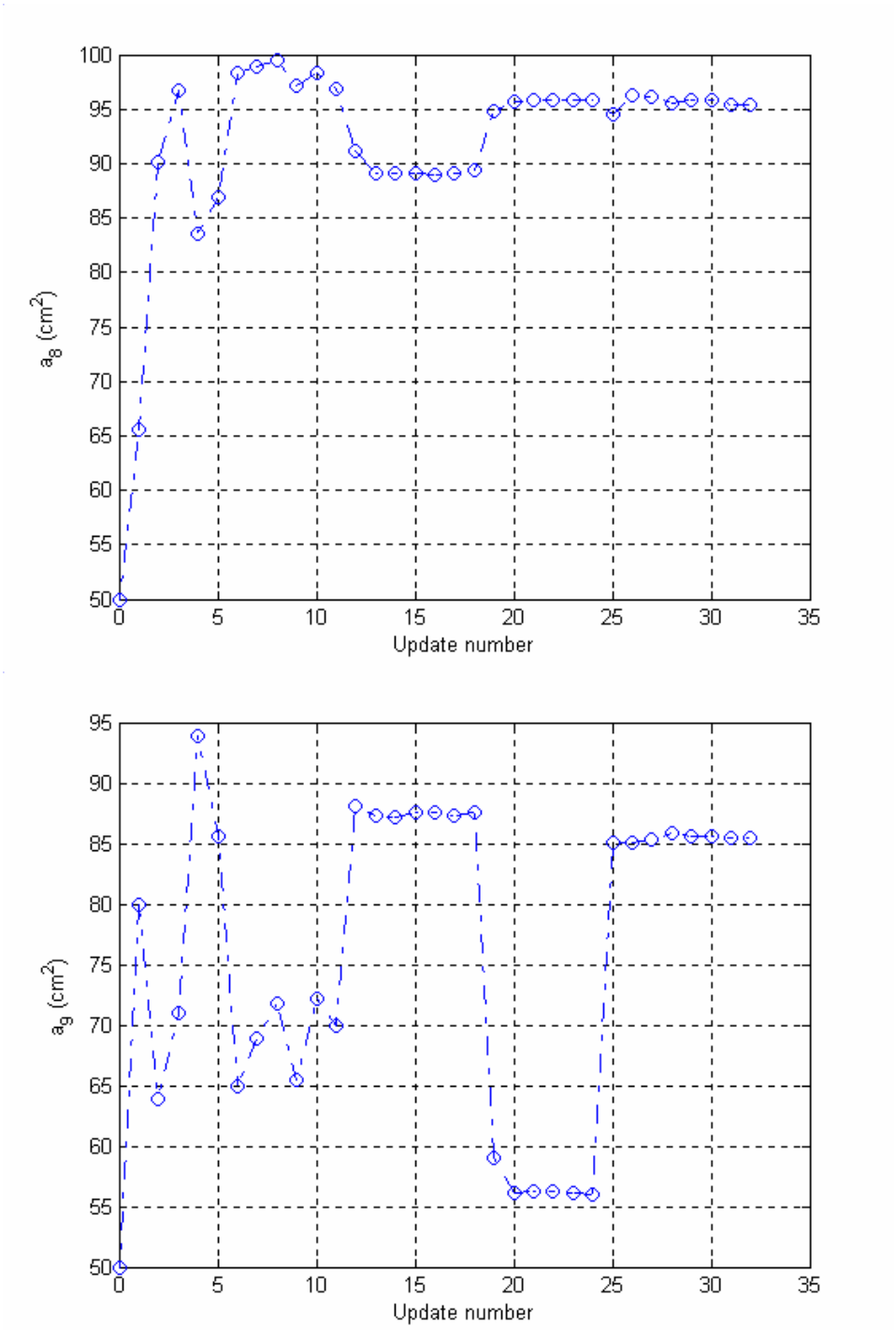

Figure G-1 Iteration history of cross sectional area of a bar element for single objective case, Case I (continued)

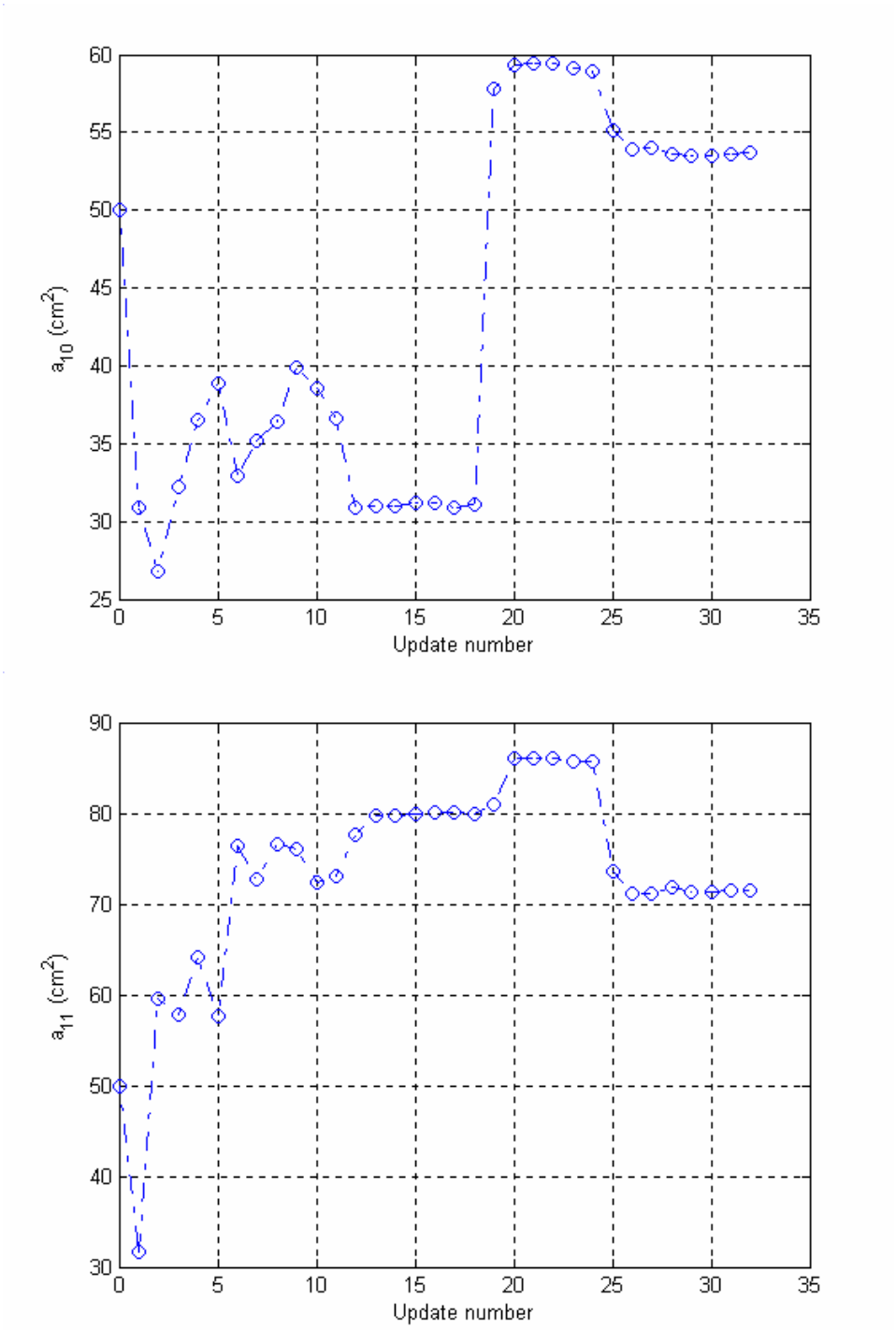

Figure G-1 Iteration history of cross sectional area of a bar element for single objective case, Case I (continued)

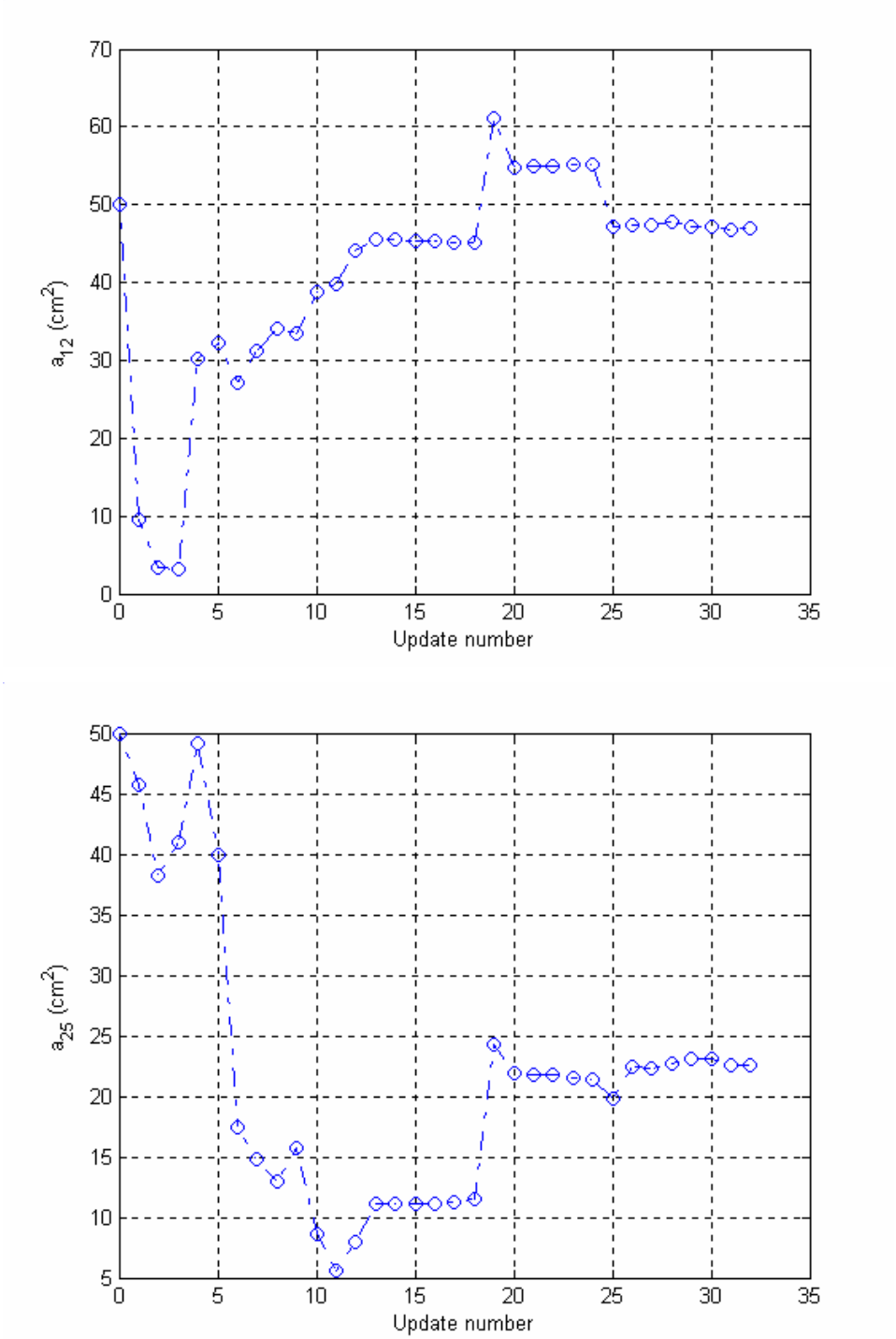

Figure G-1 Iteration history of cross sectional area of a bar element for single objective case, Case I (continued)